A STUDY ON ISOTHERM CHARACTERISTICS OF ADSORBENT-ADSORBATE PAIRS USED IN ADSORPTION HEAT PUMPS

A Thesis Submitted to
the Graduate School of Engineering and Sciences of
İzmir Institute of Technology
in Partial Fulfillment of the Requirements for the Degree of

MASTER OF SCIENCE

in Energy Engineering

by
Zeynep Elvan YILDIRIM

June 2011
İZMİR

We approve the thesis of **Zeynep Elvan YILDIRIM**

_____

Assoc. Prof. Dr. Moghtada MOBEDİ
Supervisor

_____

Prof. Dr. Semra ÜLKÜ
Co-Supervisor

_____

Assoc. Prof. Dr. Fehime ÖZKAN
Committee Member

_____

Assist. Prof. Dr. Ünver ÖZKOL
Committee Member

30 June 2011

_____

Assist. Prof. Dr. Gülden GÖKÇEN
Head of the Department of Energy Engineering

_____

Prof. Dr. Durmuş Ali DEMİR
Dean of the Graduate School of Engineering and Sciences

ACKNOWLEDGEMENTS

I would like to thank to my advisors, Assoc. Prof. Dr. Moghtada MOBEDİ and Prof. Dr. Semra ÜLKÜ for their supervision, guidance and support during this study. I am also thankful to Assoc. Prof. Dr. Fehime Özkan and Assist. Prof. Dr. Ünver Özkol for their valuable recommendations and contributions.

I would like to thank and indicate gratitude to Gamze Gediz İliş, Erdal Çoban, Dr. Güler Narin, Dr. Hasan Demir and Gizem Maraba for their helps and supports.

I would like to thank to BAP committee for the financial support on the study performed.

Lastly, I would like to thank to my dear family for their endless encouragement and support during my master thesis study.

ABSTRACT

A STUDY ON ISOTHERM CHARACTERISTICS OF ADSORBENT-ADSORBATE PAIRS USED IN ADSORPTION HEAT PUMPS

Adsorption heat pumps are promising systems due to their ability to recover heat at low temperature levels and to provide cooling and/or heating effects. It has advantages such as using renewable energy sources, being environmental friendly, having no vibration and lower operation costs.

In this study, the most common pairs used in adsorption heat pumps were reviewed and their thermophysical and adsorption behaviors were discussed. The adsorption equilibrium phenomena were explained in details. The different experimental methods for determination of adsorption equilibrium for pairs were explained and compared.

The change of heat of adsorption according to the varying adsorbed amount was studied numerically for two different equilibrium equations. It is found that, the heat of adsorption for pairs fitting Dubinin-Astakhov equation has a decrease with increasing adsorbed amount, while the heat of adsorption for pairs fitting Freundlich equation does not depend on adsorbed amount.

A numerical study was performed to investigate the performances and cooling capacities of three different adsorption chillers for six different pairs. The results showed that when S40 silica gels - water pair is used, the chiller cooled with low temperature source gives the highest performances.

In the experimental section of the present study, a volumetric setup was designed and constructed. Experiments were performed for a conventional pair of silica gel – water. It was observed that the maximum adsorption capacity of the experimented silica gel –water pair was 21% (kg water vapor /kg silica gel) at 35 °C, 19% (kg water vapor/kg silica gel) at 45 °C and 11% (kg water vapor /kg silica gel) at 60 °C.

ÖZET

ADSORPSİYONLU ISI POMPALARINDA KULLANILAN ADSORBENT-ADSORBAT ÇİFTLERİNİN İZOTERM KARAKTERİSTİKLERİ ÜZERİNE BİR ÇALIŞMA

Adsorpsiyonlu ısı pompaları düşük sıcaklıklardaki atık ısıları ve/veya yenilenebilir enerji kaynaklarını kullanabilme kabiliyetlerinden ötürü son günlerde oldukça önem kazanmıştır. Fosil kaynaklara bağımlı elektrik enerjisini kullanmadıkları, sarsıntısız ve uzun yıllar sorunsuz çalışabildikleri için oldukça büyük avantajları bulunmaktadır.

Bu çalışmada adsorpsiyonlu ısı pompalarında kullanılabilecek çiftler araştırılmış, ve bu çiftlerin termofiziksel özellikleri ve adsorpsiyon davranışları incelenmiştir. Adsorpsiyon kavramı ve adsorpsiyonda denge tayini için kullanılan deneysel metotlar detaylarıyla açıklanmış ve kıyaslanmıştır.

Çalışmanın deneysel kısmında, volumetrik metoda dayalı iki sistem dizayn edilmiş ve kurulmuştur. Deneyler adsorpsiyonlu ısı pompalarında sıklıkla kullanılan bir çift olan silika jel – su çifti ile gerçekleştirilmiş; sonuç olarak 35 °C'de maksimum %21 (kg su/kg silika jel), 45 °C'de maksimum %19 (kg su/kg silika jel) ve 60 °C'de maksimum %11 (kg su/kg silika jel) adsorplama kabiliyetine sahip olduğu bulunmuştur. Bu silika jel – su çiftinin Tip II izotermi ile uyumlu olduğu gözlenmiştir. Bu izoterm tipi su buharının mikropor gözenekli silika jele adsorpsiyonunda beklenebilecek bir davranıştır.

Dubinin-Astakhov ve Freundlich denklemlerini kullanan iki farklı çiftin, adsorplama miktarının değişimine bağlı adsorplama ısısının değişimi numerik bir çalışma ile incelenmiştir. Çalışmanın sonucunda, Dubinin-Astakhov denklemine uyum gösteren çiftlin adsorpsiyon ısılarının artan adsorplama miktarıyla azaldığı, ancak, Freundlich denklemine uyum gösteren çiftin adsorpsiyon ısılarının adsorplama miktarı değişiminden bağımsız olarak her noktada sabit kaldığı bulunmuştur.

Ayrıca, altı farklı çift için üç farklı chiller dizaynı kullanılarak, chiller performansı ve soğutma kapasitesi üzerine numerik bir çalışma gerçekleştirilmiştir. Sonuç olarak, altı farklı çiftten S40 silika jel – su çiftini kullanan ve düşük sıcaklık kaynağı ile soğutulan chillerin en yüksek performans ve soğutma kapasitesine sahip olduğu bulunmuştur.

TABLE OF CONTENTS

LIST OF FIGURES

Figure **Page**

LIST OF TABLES

Table **Page**

LIST OF SYMBOLS

c	knee shape constant
C_∞	equilibrium concentration, kg/m^3
COP	coefficient of performance
c_p	specific heat, kJ/kgK
D	Diffusivity, m^2/s
DB	dry bulb
E	diffusional activation energy, J/mol
h	enthalpy, kJ/kg
H_{ads}	heat of adsorption kJ/kg
K_0	Henry's constant
m	mass, kg
$\dot{m}$	mass flow rate, kg/s
n	amount of adsorbate, mol adsorbate/kg adsorbent
P	pressure, Pa
P_{sat}	saturation pressure, Pa
Q	heat transferred, kJ
q	adsorbed amount, kg adsorbate/kg adsorbent
q*	adsorbed amount at equilibrium, kg adsorbate/kg adsorbent
q_0	equilibrium adsorption coefficient, kg/kg
Q_{ab}	heat of isosteric heating process, kJ
Q_{bc}	heat of isobaric desorption process, kJ
Q_{cd}	heat of isosteric cooling process, kJ
Q_{da}	heat of isobaric adsorption process, kJ
q_m	monolayer coverage, kg adsorbate/kg adsorbent
r	particle radius, mm
R	gas constant, $kJm^3/kmolK$
T	temperature, °C
t	Toth's constant
W	work done, kJ
WB	wet bulb
ρ	density, kg/m^3

Subscripts

C	cooling
cond	condenser
eff	effective
ev	evaporator
fg	evaporation
H	high
i	in
i	number of elements
L	low
l	liquid
max	maximum
min	minimum
o	out
R	refrigeration
s	solid
sat	saturation
∞	infinite

CHAPTER 1

INTRODUCTION

Air - conditioning is a requirement for human to provide the comfort conditions. Heating and cooling systems are used for both human comfort and industrial applications. Several types of air - conditioning devices are produced by manufacturers. Heat pumps are preferred air - conditioning equipment because of their high thermal performances.

Heat pumps can be divided into two groups as mechanical and thermal heat pumps according to third energy source. The mechanical energy is used in mechanical heat pump as the third energy source, while the thermal driven heat pump operates with thermal energy sources.

Mechanical heat pump is widely used in the recent years due to its advantages such as high thermal efficiency and packed structure. However, it is found out that the refrigerants used in mechanical heat pump plays an important role in the depletion of the ozone layer and global warming. Mechanical heat pump operates with electrical power generally produced from fossil fuels. The growing need of energy forces researchers and manufacturers to investigate on environmental friendly devices with high energy performance that can operate with renewable energy resources.

Thermal driven heat pump has the advantage of using not only the renewable thermal sources such as solar and geothermal energy, but also the waste heat of industrial processes. It does not contain hazardous materials. Thermally driven heat pump can be classified into three groups as absorption, chemical and adsorption heat pumps. The absorption and adsorption heat pumps were studied since 1970s.

An absorption heat pump basically consists of an evaporator, a condenser, an expansion valve, a generator and an absorber. The compressor of a mechanical heat pump is replaced by an absorber in this system. Absorption heat pump working fluid is a solution of two liquids with high and low boiling points. The most common pairs used in an absorption heat pump are ammonia - water and water - lithium bromide, as the refrigerant - absorbent pairs.

Mechanical and absorption heat pumps are commonly studied, however research in the other category of heat pumps which are chemical heat pumps has gained momentum in recent years. Chemical heat pumps provide heat storage capacity and high heat of reaction when compared to the absorption heat pumps. They use reversible reactions between a gas and a salt that is part of a porous solid material inside a reactor (Wongsuwan 2001; Mbaye 1998).

The life time of absorption and chemical heat pumps are shorter than adsorption heat pump due to the problem of salt corrosion and using chemicals. Moreover, the absorbent used in absorption system should be changed in every 4 to 5 years. In adsorption heat pump, the system does not require changing of the adsorbent-adsorbate pairs for a long period of time. The applicability of adsorption heat pumps and the availability of materials used for adsorption process which are mostly environmental-friendly leaded the studies to progress on that area. The first studies on adsorption heat pumps took start up with Close and Duncle in 1977 and the first construction was performed by Tchernev in 1978 (Ülkü 1986).

An adsorption heat pump consists of an adsorbent bed, an evaporator, a condenser and an expansion valve. The adsorbent bed is filled with the adsorbent and the working fluid is used within the cycle. Basically, adsorption heat pump operates by cycling adsorbate between adsorber, condenser and evaporator (Demir 2008). In the adsorption heat pump cycle, adsorption phenomena play the same role of mechanical power, so that the working fluid can be circulated in the cycle without any mechanical power.

The processes occurred in a cycle of and adsorption heat pump can be summarized as; evaporation, adsorption, desorption and condensation processes. A basic adsorption cycle consists of four thermodynamic steps as isosteric heating, isobaric desorption, isosteric cooling and isobaric adsorption.

Adsorption is an adhesion processes in which fluid (adsorbate) is transferred from the fluid phase to the surface of rigid particles (adsorbent). Adsorption may occur in two ways as chemical adsorption (chemisorption) and physical adsorption (physisorption). Physisorption is a reversible process, while chemisorption is irreversible. Physisorption is caused by Van der Waals forces and chemical adsorption or chemisorption involves valence forces. In adsorption heat pumps, the adsorption and desorption processes have to be reversible to provide the repetition of cycle. Therefore, the interaction between adsorbent and adsorbate must be a physical adsorption type.

The removal of adhered adsorbates from the surface adsorbent is called as desorption process. Adsorption is an exothermic process, while desorption is endothermic.

Since adsorption is a phenomena occurring between two phases (pair) and adsorption/desorption process occurs in adsorption heat pump; the properties of pair is an important issue. Each adsorption pair has specific characteristic properties. The behavior of adsorbents, adsorbates and interaction between these two should be investigated in order to select the right pair for cycle.

The aim of study this study is to give brief explanations on adsorption phenomena and working principle of adsorption heat pump and review on adsorbent-adsorbate pairs used in adsorption heat pumps by researchers in recent years. In theoretical part of the study, the structure and thermophysical properties of those pairs are investigated and presented. A special attention is paid on the adsorption equilibria of different adsorbent-adsorbate pairs. Different equilibrium equations are reviewed and classified. In experimental part of the study, two experimental set up were designed and manufactured in order to find out adsorption equilibria of conventional silica gel – water pair.

The performed studies on adsorption heat pumps were reviewed in literature and presented in Chapter 2. The methods used for determination of adsorption equilibrium are categorized and presented also in Chapter 2. The experimental studies on determination of equilibrium of common pairs performed by researchers are reviewed and presented in this chapter.

In Chapters 3 and 4 the working principle of adsorption heat pump, adsorption phenomena and properties of common adsorbents, adsorbates and pairs are given in details. The adsorption characteristics of pairs, equilibrium states and equations are explained in Chapter 5. Additionally the definition for heat of adsorption is presented. The change in heat of adsorption of a pair with varying adsorbed amount is studied numerically in Chapter 5.

A numerical study on the adsorption chiller performances is performed within the study. The change of performance of an adsorption chiller is investigated, based on the effect of used pair. The COP of the adsorption chiller depending on the pair used and the type of chiller is studied and solved numerically. The description of the designed chillers, the equilibrium equations of pairs used and the numerical results are presented in Chapter 6 in details.

The experimental part of this study is performed with two constructed experimental setups. The methodology of experiments was compatible with literature studies; unfortunately, the impediments faced during experiments prevented the persistence of experiments in first constructed setup. The design and equipments of setup was changed, therefore the procedure was changed. The improved setup, its components and experimental procedure is explained in details in Chapter 7.

Chapter 8 includes results and discussion for the experiments performed in both first and second setups. The adsorption behavior of silica gel - water pair and isotherm characteristic were discussed based on the experimental results. Chapter 9 gives the conclusions of studies performed. The evaluations and the comments made about the study are presented in this chapter.

CHAPTER 2

LITERATURE SURVEY

In this chapter, the pairs used in adsorption heat pumps are surveyed in the studies presented in literature. Furthermore, the methods for determination of adsorption equilibrium of these pairs are also investigated and categorized.

2.1. Literature Survey on Employed Pairs

The structural and thermophysical properties of various adsorbents and adsorbates commonly used in adsorption heat pumps are going to be explained briefly within next chapter. The pair interactions and behaviors are also going to be mentioned. The adsorption heat pumps, adsorption chillers or ice making adsorption devices studied since 1982 are surveyed in this section. The pair used in the study, the aim of the device and their performance are listed below in Table 2.1.

Table 2.1. Literature survey on employed adsorbent-adsorbate pairs

Year	Researcher	Pair Used	Aim	Product	COP
1982	Dupont et al.	zeolite 13X - water	Ice making	7 kg/day	0.04 - 0.14
1984	Grenier et al.	zeolite 13X - water	Cooling	-	0.086
1986	Ülkü	natural zeolite – water	Heating	-	0.34
1986	Pons and Guilleminot	active carbon – methanol	Ice making	6 kg/day	≈ 0.12
1987	Exell et al.	active carbon – methanol	Ice making	4 kg/day	≈ 0.1
1987	Ülkü	natural zeolite – water	Heating	-	0.4
1987	Pons and Grenier	zeolite – water	Ice making	-	≈ 0.1
1987	Kluppel and Gurgel	silica gel – water	Cooling	-	0.077
1989	Ülkü and Mobedi	active carbon – methanol	Comparison	-	-
		active carbon – ammonia			
		zeolite – water			
1993	Critoph	active carbon - ammonia	Ice making	3 kg/day	0.04
1993	Philip et al.	zeolite 13X - water	Ice making	-	-
1994	Headley et al.	active carbon - methanol	Ice making	1 kg/day	0.02
1996	Critoph	active carbon - ammonia	Ice making	-	0.3

(cont. on next page)

Table 2.1 (cont.).

1998	Oertel and Fischer	silica gel - methanol	Cooling	-	≈ 0.3
1998	Wang et al.	active carbon – methanol	Ice making	14 kg/day	0.15 - 0.23
1999	Sumathy and Li	active carbon - methanol	Ice making	4-5 kg/day	0.1- 0.12
2000	Wang et al.	active carbon - methanol	Ice making	10 kg/day	0.04
2001	Li et al.	active carbon - methanol	Ice making	5-6 kg/day	0.12 - 0.14
2001	Wang et al.	active carbon - methanol	Cooling	-	0.15
2002	Li et al.	zeolite 13X - water	Cooling	-	0.4
2004	Restuccia	novel silica gel - water	Cooling	-	0.6
2004	Xia et al.	silica gel - water	2 stage Cooling	-	0.28
		silica gel - methanol			
2005	Wang et al.	active carbon - methanol	Cooling	-	0.087
2005	Wang	silica gel – water	Cooling	RC: 7.15 kW	0.38
2006	El-Sharkawy et al.	active carbon fiber - ethanol	Cooling	-	-
2006	Liu and Leong	silica gel - water	2 stage Cooling	SCP: ≈ 42.7 W/kg	1.35
		zeolite – water			
2006	Luo and Dai	silica gel – water	Cooling	CP: 4.5 kW	≈ 0.26
2007	Nunez et al.	silica gel - water	Cooling	-	0.4 - 0.6
2008	Daou et al.	novel silica gel – water	Cooling	SCP: ≈ 60 W/kg	≈ 0.2
2008	Demir	silica gel – water	Heating - Cooling	SCP: ≈ 0.3 W/kg	≈ 0.54
2008	Elnekave	zeolite – water	Cooling	P: ≈ 2000 W/kg	≈ 0.14
2008	El-Sharkawy	active carbon – methanol	Cooling	SCE: 420 kJ/kg	-
2008	Kubota et al.	silica gel – water	Cooling	CP: 3.12 kW	≈ 0.30
2008	Liu and Leong	zeolite – water	Cooling	SCP: 50 W/kg	≈ 0.45
2009	Saha et al.	silica gel - water	Cooling	CP: 11 kW	0.3
		novel silica gel – water	Comparison	CP: 14 kW	0.4
2009	San and Hsu	novel silica gel – water	Cooling	-	≈ 0.35
2009	Wang and Zhang	silica gel – water	Cooling	SCP: 70 kW/kg	≈ 0.47
2009	Xia et al.	silica gel – water	Cooling	SCP: 90 W/kg	≈ 0.40
2010	Grisel et al.	silica gel – water	Cooling	PD: 17 kW/ m^3	≈ 0.62
2011	Hassan et al.	active carbon – methanol	Cooling	CP: 2.326 kW	0.211

Near 2000s, the studies on silica gel – water pair came into prominence and the devices were aimed chilling medium or water. Oertel and Fischer (Sumathy et al. 2003) have studied a rarely encountered pair which is silica gel – methanol. The COP of adsorption cooling device was found as 0.3. Since the availability and applicability

of water is more possible than methanol, the silica gel – methanol studies were rarely handled.

Among all the reviewed studies, the highest COP value was achieved by Grisel et al. in 2010 which is 0.62 (Grisel et al. 2010). The silica gel – water pair was used in the developed adsorption chiller.

2.2. Methods for Determination of Isotherms

The adsorbed mass per unit mass of adsorbent is the characteristic equilibrium quantity for a porous solid. This characteristic quantity must be investigated for the studied pair. This characteristic state and adsorption equilibrium behavior of the pair can be determined by different experimental methods.

As a result of literature survey, there were found methods used to identify the adsorption equilibrium for a specified pair; such as volumetric, gravimetric and calorimetric methods. In this section, these most common methods are going to be defined, briefly.

2.2.1. Volumetric Method

Volumetric method, which is also called as manometry, is the oldest method known so far. The first adsorption experiment using volumetric method was performed by C. W. Scheele in 1777, and the studies were proceeded by W. Ostwald in 1905 and J. Langmuir in 1912 (Gregg and Sing 1982).

Figure 2.1 illustrates the schematic view of equipment generally present in the volumetric method. The volumetric method adsorption instrument basically consists of a gas storage vessel and an adsorption container connected by a proper tube and a valve. The temperature of both vessels should be completely controlled by using devices such as water or oil bath. The vessels and tubes should be insulated well in order to prevent any temperature instability. The pressure and temperature measuring devices are placed to proper points.

For the studies with pressures under atmospheric pressure, a vacuum pump is used and connected to the system. All vessels and tubes should be manufactured of non-corrosion materials and inside surfaces should be polished. For vacuum systems

the glass would be a better choice than metallic materials. Sealing materials should be chosen according to the adsorptive gases used and the ranges of temperature and pressure of operation.

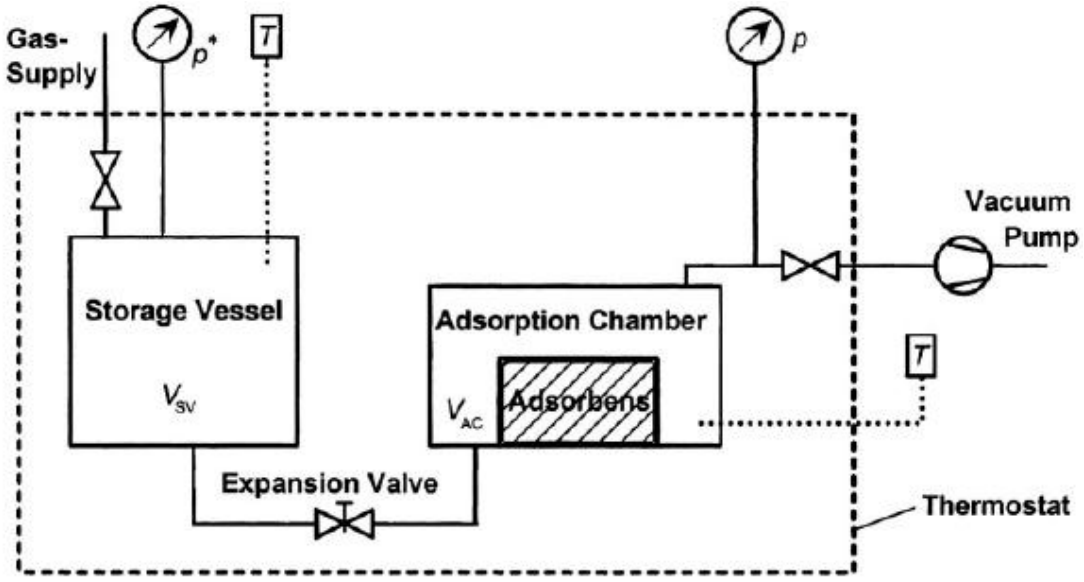

Figure 2.1. Schematic view of volumetric method instruments
(Source: Keller and Staudt 2005)

The volumetric gas adsorption experimental procedure can be summarized simply as;

- evacuation of adsorbent sample vessel,
- expansion of adsorptive to the adsorbent vessel,
- adsorption of a portion of gas introduced to the adsorbent,
- calculation of adsorbed amount by mass balance.

The experimental procedure in volumetric method can be explained as follows. A certain amount of gas is placed in the storage vessel (vapor vessel) and the adsorption container is evacuated. Upon opening the expansion valve, the gas expands to the adsorption container where it is partly adsorbed on the surface of the adsorbent. This process may last milliseconds, minutes, hours or even several days. After thermodynamic equilibrium, such as temperature and pressure inside the vessel has been realized, these data can be taken as a basis to calculate the mass of the gas adsorbed on the adsorbent. Adsorbed amount calculations of volumetric adsorption experiments are mainly performed using pressure differences (Keller and Staudt 2005).

2.2.2. Gravimetric Method

Gravimetric measurements are used both to characterize the porous media and to measure the adsorption equilibrium. The measurement is carried out with the regard of change in weight of adsorbent. The equilibrium adsorbed amount may decrease with respect to temperature and pressure. Hence, the sensitivity of the measuring device should be high in order to detect the difference. Automated instruments including microbalances are available for various purposes such as water vapor adsorption and thermo-gravimetry.

Gravimetric measurements of a pure gas onto an adsorbent may be performed by single or two beam balanced devices. Two beam microbalance devices (schematic view is illustrated in Figure (2.2) consist of two containers which are adsorbent and ballast vessels. These two containers are at balance with each other before the adsorption process. During the adsorption, since the adsorbent is filling with adsorbate, the weight of the first container is increased while the ballast container remains constant. The difference between the weights of two containers contributes the adsorbed amount.

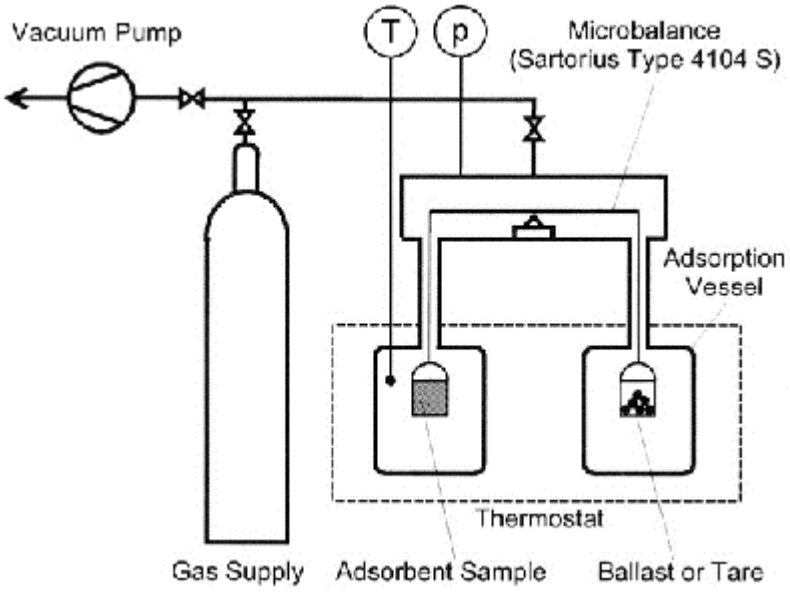

Figure 2.2. Schematic view of a two beam balance gravimetric instrument (Source: Keller and Staudt 2005)

Single beam balance gravimetry devices differ from two beam balance with including only one container which adsorbent is placed. The adsorption of corrosive

gases like NH_3, H_2S or NO_x onto porous materials can be determined by this device. The measurement arises with a magnetic field formed by an electromagnetic instrument placed onto the wall of adsorption chamber. The weight difference in the adsorption chamber is sensed by the magnetic field and the equilibrium is determined by this way (Keller and Staudt 2005). Magnetic suspension balance devices need a great sensitivity in the usage of instrument For example, the incline of the floor where the instrument is placed and any possible vibrations should be taken into consideration.

2.2.3. Calorimetric Method

Gas adsorption calorimetry is a method for measurements of both heats and isotherms of adsorption or desorption processes. Thus, calorimeters can be used for determination of thermal equilibrium and mass equilibrium conditions. Types of calorimeters may be simply classified into four groups as adiabatic calorimeters, diathermal-conduction calorimeters, diathermal-compensation calorimeters and isoperibol calorimeters.

In the adiabatic adsorption calorimeter, the heat evolved on adsorption increases the temperature of the sample and container. The flow of heat is prevented to flow by a peripheral shield control of temperature. Thus the shield is maintained at the same temperature with the sample container. The temperature rise due to heat of adsorption is measured by a resistance thermometer attached to the sample container. This type of calorimeter can be useful for close adsorption systems at low temperatures (Rouquerol et al. 1999).

The diathermal-conduction adsorption calorimeter has two main types as phase-change adsorption calorimeter and heat-flow adsorption microcalorimeter. However, it is not used nowadays; the temperature of adsorption calorimeter is imposed by the temperature of phase change in the first type. The most important type of isothermal calorimeter in current use is based on the principle of the heat flow meter, firstly improved by Tian and Calvet, and so called as heat-flow adsorption microcalorimeter. The Tian-Calvet calorimeter consists of up to 1000 thermocouples (thermopile) between the adsorbent container and the thermostat and the thermopile measures the heat flux between these two boundaries. This type of calorimeter is useful for open adsorption systems (Rouquerol et al. 1999).

The diathermal-compensation and isoperibol adsorption calorimeters are now unused because of their complexity, stability and uncertainty problems.

In these four types of calorimeters, there are three main operational procedures to obtain the adsorption amount, thus the equilibrium conditions. Two of them are gravimetric and volumetric methods which are already mentioned in previous sections. The third one is gas-flow procedure in which the quantity of flow-rate of gas in the entrance and exit of the adsorbent container is measured and the adsorbed amount is obtained.

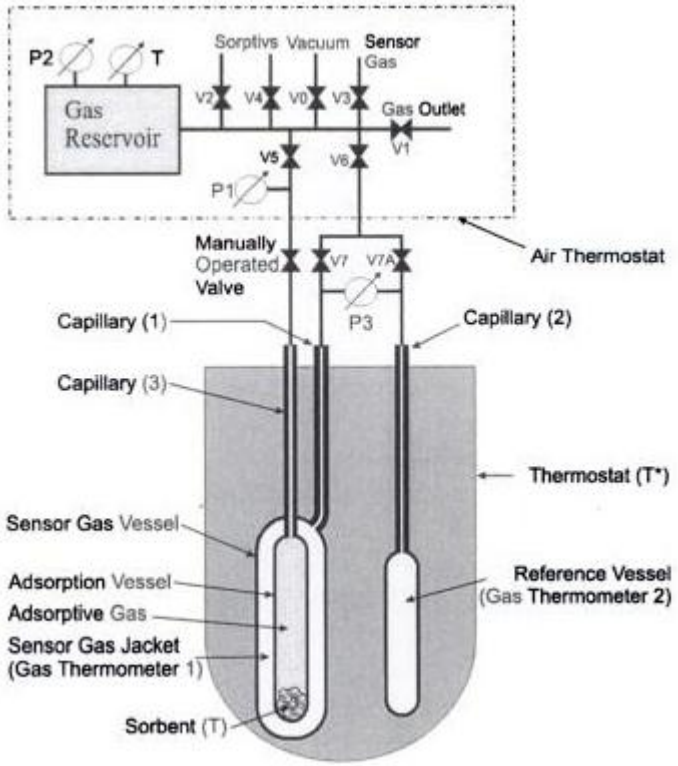

Figure 2.3. Schematic view of a sensor gas calorimeter
(Source: Keller and Staudt 2005)

With the improvements in determining the adsorption equilibrium, W. Langer adduced a new calorimeter for measurements of heats and isotherms of adsorption. This device is called as sensor gas calorimeter (SGC), since a reference gas which differs from the adsorptive and has no interaction with adsorption pair (i. e. He or N_2) is surrounding the adsorption container. A schematic view of a SGC is illustrated in Figure 2.3. As seen in figure, valves and pressure measuring devices involving the reference gas are distinct from the adsorption chamber side. The heat evolved by the

adsorption process is sensed by the reference gas; hence, the heat of adsorption and adsorbed amount is determined by the reference gas (Keller and Staudt 2005).

2.2.4. Level Sensor Method

In this method, the liquid level in the condenser/evaporator is measured by the level sensor, and this information, together with the value of the useful area of the adsorbate tank and the density of the refrigerant, is used to calculate the adsorption or desorption quantity. The precision in the measurement increases with the mass of adsorbent, because the amount desorbed/adsorbed, and thus, the variation of the liquid level inside tank also varies (Wang et al. 2009). A test rig with level sensor method is used by Dellero et al. and the schematic view of the device shown in Figure 2.4.

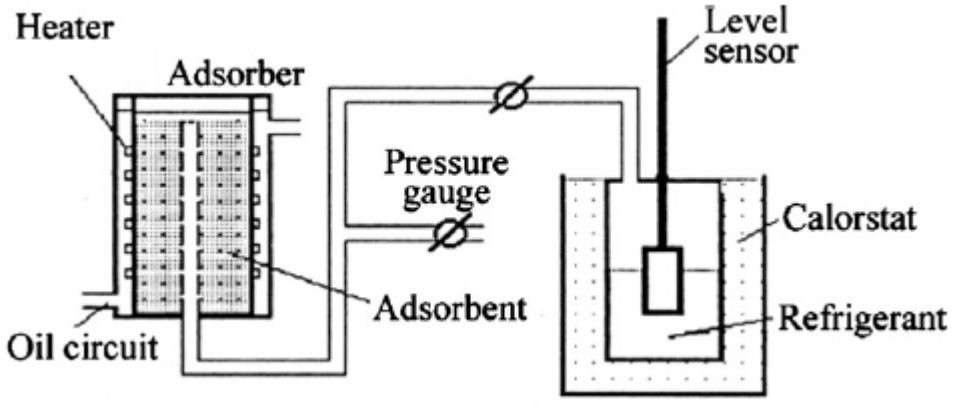

Figure 2.4. Schematic view of a level sensor adsorption device
(Source: Dellero et al. 1999)

2.3. The Performed Studies on Equilibrium Determination

The methods for determination of adsorption equilibrium can be classified as volumetric, gravimetric, calorimetric and level sensor methods, as mentioned above. The pairs experimentally studied and the methods employed in the presented literature studies will be discussed in this section. The procedure of investigations and results of studies are going to be presented. Although several studies based on volumetric method were available in literature, only a study based on calorimetric method was found.

2.3.1. Calorimetric Study

An experimental study on adsorption kinetics and isotherm characteristics was performed by Li et al. (Li et al. 2007). The aim of the study was to estimate the effect of pore size on adsorption characteristics. Three types of silica gels (type A, B and C), manufactured by Qingdao Haiyang Chemicals, were investigated. The experimental studies were carried out by nitrogen gas in order to examine the physical properties and by water vapor in air in order to examine the adsorption kinetics and isotherm characteristics. The physical properties of silica gel were measured by the Micromeritics ASAP 2010 instrument, operates based on volumetric method. Type A silica gel was found to have microporous structure while type B and C silica gels were mesoporous. For the water vapor adsorption, experiments were carried out under atmospheric conditions by an instrument (see Fig. 2.5) constructed by the researchers using gravimetric method.

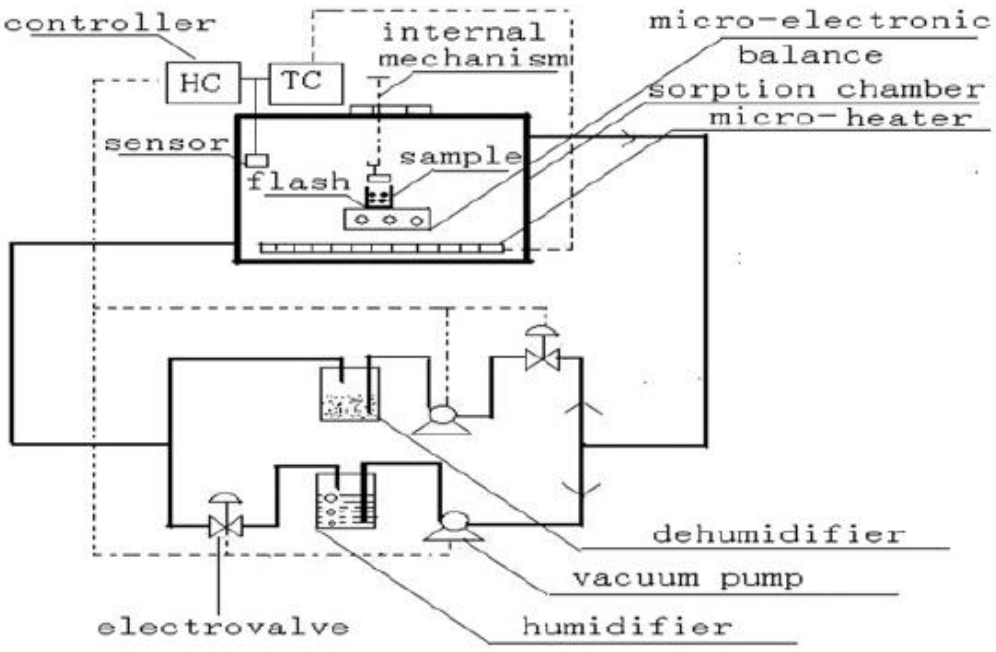

Figure 2.5. Experimental apparatus used in the study of Li et al.
(Source: Li et al. 2007)

As seen from Figure 2.5, the air with varying relative humidity was introduced to silica gels and the change in the mass was recorded by time. In the study, type A silica gel was found to have a Type I isotherm, while type B and C silica gels had Type

V isotherm according to the IUPAC classification. The experimental data of the study for type A silica gel was fitted to Langmuir and Freundlich models. Type A silica gel was found to have a longer adsorption time than type B and C silica gels, while the maximum adsorption capacity for type A was greater than others. The relative humidity of air was also a parameter for adsorption rate; the greater relative humidity quantity refers to a shorter adsorption time.

2.3.2. Volumetric Studies

An experimental study was performed on investigation of silica gel – water pair for isotherm characteristics by Ng et al. (Ng et al. 2001). The investigation was done on three types of silica gel which are Fuji Davison of types A, 3A and RD. The constant-volume variable-pressure (CVVP) instrument was used to measure the characteristic properties (see Fig. 2.6). The regeneration tests were also applied to the pairs since the desorption time is crucial. The results of study indicated that type 3A and RD silica gels were found to be better than type A silica gel due to shorter regeneration time. Between 70 and 90 °C, 75% regeneration could be achieved for type 3A and RD silica gels. The all types were found to be fitted with the Henry's equation. The coefficients of mathematical isotherm equations were found based on the experimental results. They also found that at a temperature range between 60 and 70 °C, type A silica gel was found to have better potential for cooling capacity; while at temperatures higher than 70 °C, types 3A and RD silica gels had a better cooling capacity.

An experimental study on investigation of silica gel – water adsorption was performed by Chua et al. (Chua et al. 2002). The studied adsorbents were Fuji Davison type A and RD silica gels. The thermophysical properties of silica gel types were also examined besides the isotherm characteristics. The physical properties such as surface area, pore size and pore volume were measured by Micromeritics ASAP 2010 instrument; the resulted quantities for both types were listed in the study. The thermophysical properties for both types were found to be similar to each other, while thermal conductivity of type RD was found greater than of type 3A. The adsorption experiments were performed with a CVVP apparatus (see Fig. 2.7) constructed by the researchers. The studied temperature and pressure ranges were 25-65 °C and 500-7000

Pa, respectively. Toth's equation was the best fitted to the experimental data to express the isotherm behavior. Constants of the correlation for both types were computed and presented in the study. The isosteric heat of adsorption value was found smaller than those found in literature, such as nearly 2700 kJ/kg. For the experiments at a temperature of 30 °C; type RD silica gel was found to have a maximum adsorption capacity of 0.45, while type A silica gel had a maximum adsorption capacity of 0.40.

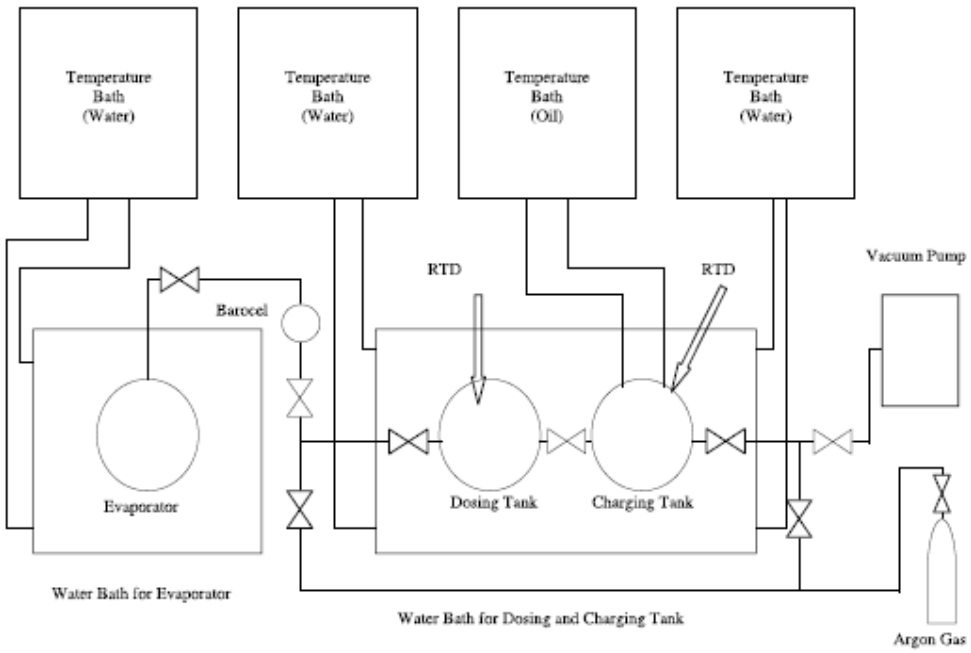

Figure 2.6. Experimental apparatus used in the study of Ng et al.
(Source: Ng et al. 2001)

Zeolites are classified in two groups as natural and artificial zeolites. Both can be used as adsorbent for adsorption heat pumps. Experimental studies using volumetric method on zeolites were also reported in literature.

For instance, Özkan and Ülkü (Özkan and Ülkü 2005) experimentally studied the effect of HCl treatment on water vapor adsorption characteristics of natural zeolite. They used infrared and water vapor adsorption data, in the characterization of the CLI (clinoptilolite) and its HCl treated forms. They performed water adsorption experiments using volumetric apparatus (Omnisorp 100cx). They reported that clinoptilolite rich natural zeolite gives Type I isotherm, while a slight increase in adsorption at high relative pressure was observed. They also resulted that HCL treatment was not effective in the amount of adsorption and isotherm type.

Solmuş et al. (Solmuş et al. 2010) experimentally studied on the adsorption characteristics of a natural zeolite mined in Turkey. Maximum adsorption capacity and isosteric heat of adsorption for natural zeolite in the ranges of 40–150 °C temperature and 0.87–7.38 kPa pressure were investigated. An experimental apparatus was designed and constructed by researchers as seen in Figure 2.8. Since the system was a constant volume variable pressure apparatus, the adsorbed amount was determined by pressure change in the adsorbent vessel. The maximum adsorption capacity of natural zeolite was found to be nearly 0.12 (kg water/kg dry adsorbent) for low temperatures. The calculated isosteric heat of adsorption was found to vary from 2500 to 3800 kJ/kg water for adsorption capacities ranging from 0.12 to 0.02 kg water/kg dry adsorbent.

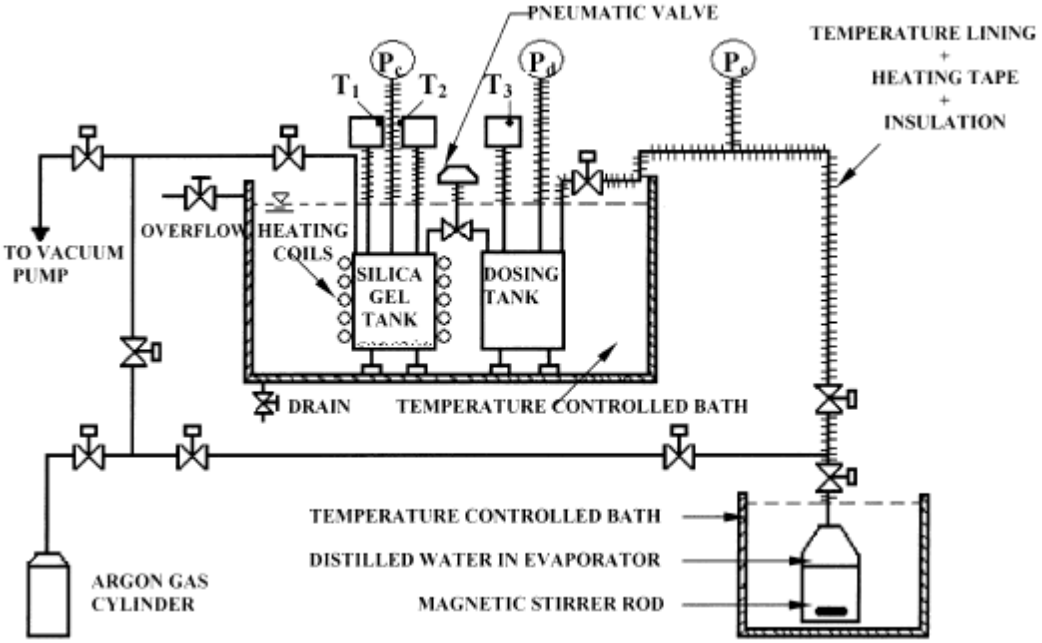

Figure 2.7. Experimental apparatus used in the study of Chua et al.
(Source: Chua et al. 2002)

They also compared the cyclic adsorption capacity of the most common pairs such as natural zeolite – water, active carbon – methanol, silica gel – water and zeolite 13X – water. They resulted that; the adsorbed amount change during the cycle of the investigated working pairs increases with increasing evaporator and regeneration temperatures and with decreasing condenser temperature. The activated carbon – methanol working pair was found to be the best among all pairs in terms of cyclic adsorption capacity change (Δq_{cycle}). Required regeneration temperatures were lower

for activated carbon – methanol and silica gel – water since Δq_{cycle} of these pairs increases slightly for increases in regeneration temperature above 140 °C.

The studies on adsorption characteristics of new generation materials are progressing in order to improve the performance of adsorption devices.

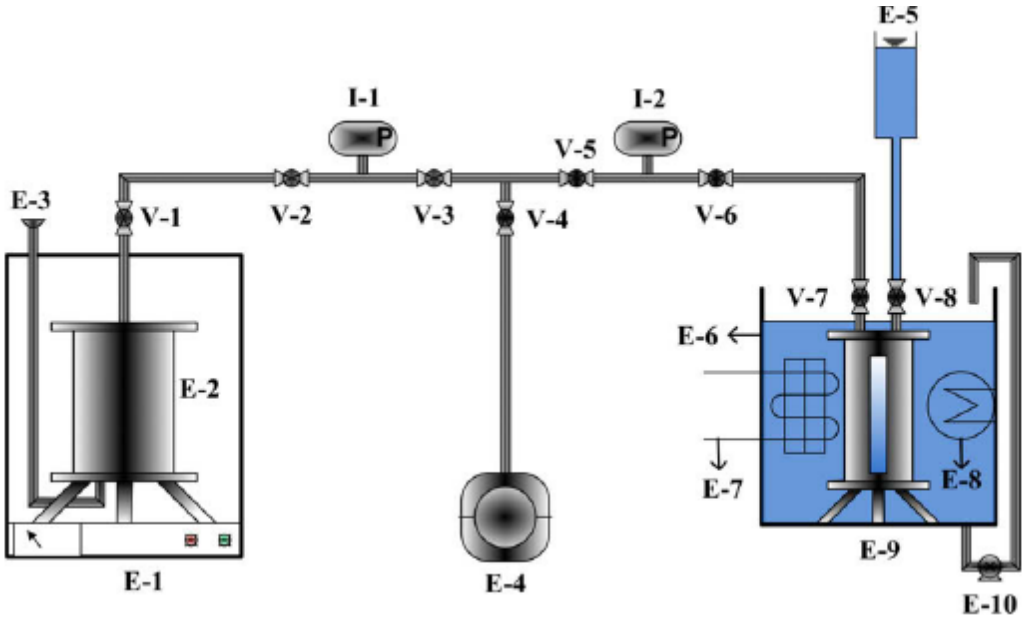

Figure 2.8. Experimental apparatus used in the study of Solmuş et al. (Source: Solmuş et al. 2010)
(E-1 oven; E-2 zeolite canister; E-3 thermocouple output; E-4 vacuum pump; E-5 feed water; E-6 water bath; E-7 V–C cooling system; E-8 electrical heater; E-9 evaporator/condenser; E-10 circulation pump)

For example, Dawoud and Aristov (Dawoud and Aristov 2003) performed an experimental study on comparison of water vapor adsorption characteristics of five different adsorbents including two novel materials. The microporous silica gel, mesoporous silica gel, SWS-1A, SWS-1L and alumina A1 were tested and the supplier was Borescov Institute of Catalysis. The testing device was a CVVP apparatus (see Fig. 2.9) constructed by the researchers. The adsorption kinetics and isotherm behavior were studied. SWSs were found to have a greater maximum adsorption capacity such as twice of others. However, the adsorption rate was smaller for impregnated adsorbents compared to the microporous and mesoporous silica gels.

Aristov et al. (Aristov et al. 2002) also performed an experimental study on selective water sorbents (SWSs). The water adsorption amount was measured by CHAN C2000 thermal balance device for a temperature and pressure range with 20-50 °C and 0.8-13 kPa respectively. SWS-1L (mesoporous silica gel with 33.7% $CaCl_2$),

SWS-2L (mesoporous silica gel with 32% LiBr), SWS-1L (mesoporous silica gel with 57% LiBr), and SWS-1L (microporous silica gel with 21.7% $CaCl_2$) were the examined sorbent samples. As the result, the impregnated adsorbents were found to have an adsorption capacity near to 0.75 kg water/kg dry adsorbent which was a very high quantity when compared with adsorbents known so far. As a comparison between these four new generation materials, SWS-1L was found to have a greater capacity than others. They also denoted that, a better performance of the heat pumping systems was observed in comparison with the pure adsorbents and impregnation materials were highly competitive with the common working materials like silica gel, zeolite and active carbon.

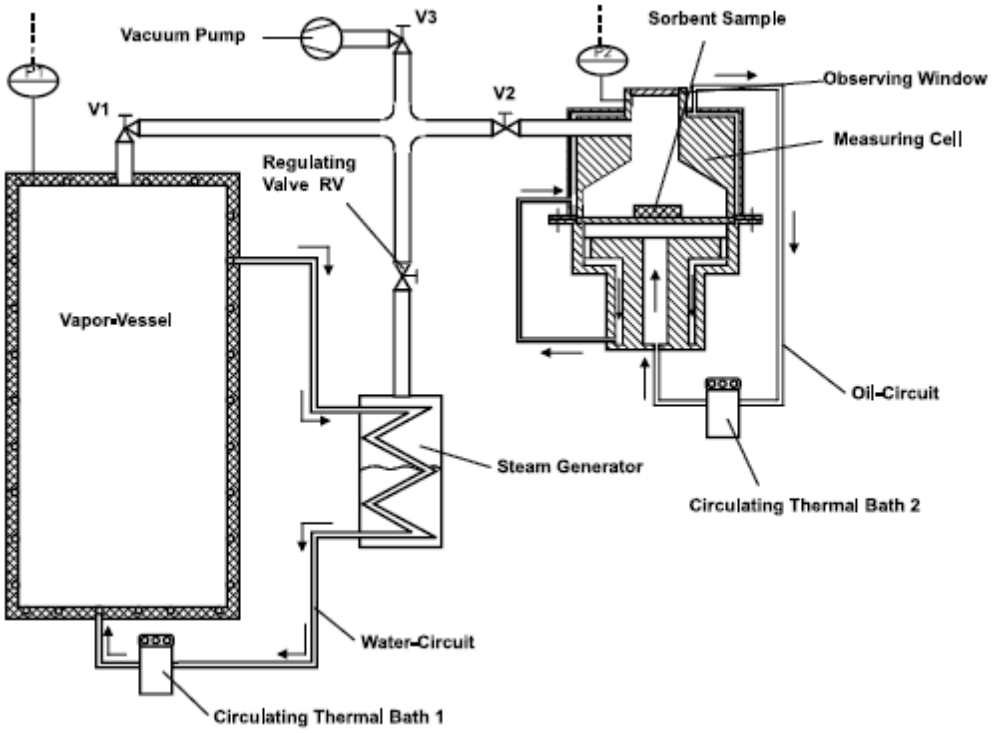

Figure 2.9. Experimental apparatus used in the study of Dawoud and Aristov (Source: Dawoud and Aristov 2003)

Saha et al. (Saha et al. 2009) performed an experimental study on R-134a adsorption onto active carbon. R-134a was an unfamiliar adsorbate for adsorption heat pumps systems; hence the study was interesting among other determination studies. They constructed a volumetric test rig as shown in Figure 2.10. The study was performed in the temperature range of 5 to 70 °C and pressure range up to 12 bars. The

experimental data have found to be fitted with the Dubinin–Astakhov isotherm equation. The maximum adsorption capacity for R-134a onto active carbon was found to be 2.1 kg/kg.

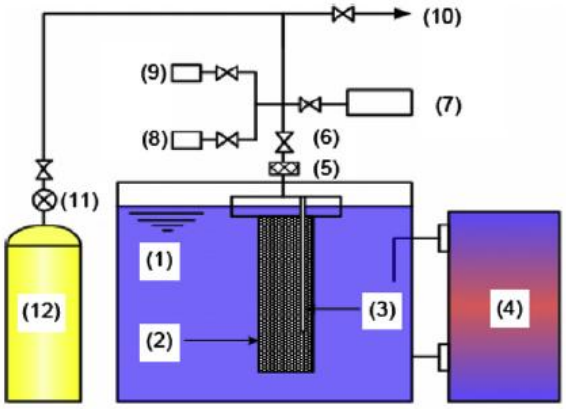

Figure 2.10. Experimental apparatus used in the study of Saha et al.
(Source: Saha et al. 2009)
(1: water bath, 2: adsorption cell, 3: thermocouple, 4: water circulator, 5: fine mesh, 6: valve, 7: mass flow controller, 8: vacuum gauge, 9: pressure transducer, 12: R-134a tank)

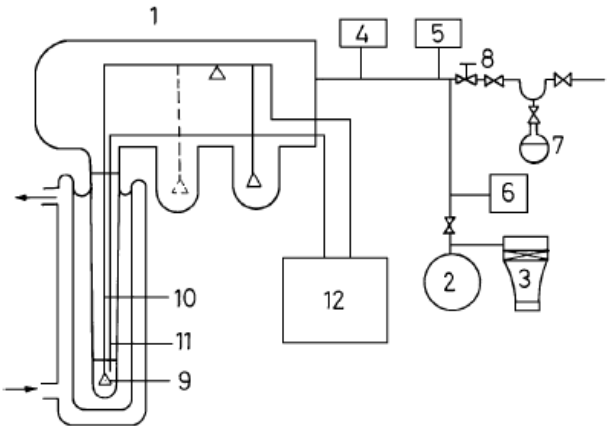

Figure 2.11. Experimental apparatus used in the study of Ülkü et al.
(Source: Ülkü et al. 1998)
(1-Cahn 2000, 2-Edwards vacuum pump 3-Edwards Diffstak 250, 4-MKS 0–2 mbar pressure gauge, 5-Penning gauge, 6-EMV 251 pressure gauge, 7-water reservoir, 8-BRY needle valve, 9-wool sample, 10-nicrome wire, 11-thermocouple, 12-recorder)

Ülkü et al. (Ülkü et al. 1998) experimentally studied adsorption of water vapor on wool. The adsorption and desorption isotherms of water vapor for wool were investigated using both volumetric and gravimetric methods. Coulter Omnisorp 100CX instrument and Cahn 2000 electronic microbalance (see Fig. 2.11) were the

instruments used in experiments for volumetric and gravimetric methods, respectively. Adsorption isotherm was found to be fitted with B.E.T. model. Hysteresis (path difference) on desorption was observed. The average effective diffusion coefficient of water in wool was found as $8.4x10^{-14}$ m^2/s at 25 °C temperature. The isotherm plots of performed experiments for water adsorption onto wool are given in Figure 2.12. Nearly 20 % maximum adsorption capacity was achieved as it can be seen in figure.

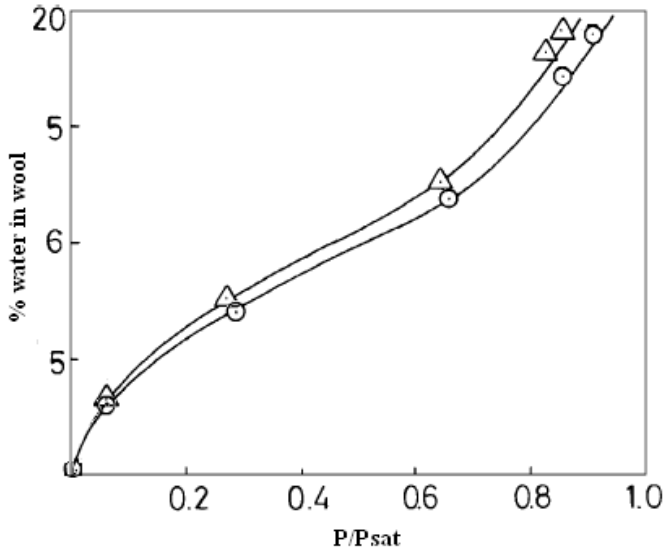

Figure 2.12. Adsorption isotherm result of water vapor adsorption on wool at 15 °C (Δ) and 25 °C (o) (Source: Ülkü et al. 1998)

CHAPTER 3

ADSORPTION HEAT PUMP

Heating and cooling systems are widely used in industry and comfort applications. Improvement of these systems is an important research area due to the growing need of comfort conditions. Decrease in the fossil energy sources also leads improvements in this area. Attentions on the renewable energy and usage of low cost energy sources are increasing day by day. Heat pumps are one of the most common devices used for that purpose in heating and cooling systems. They are preferred because of their high COPs. Heat pumps are classified as mechanical and thermal driven heat pumps. Thermal driven heat pump can be grouped into three different types as absorption, chemical and adsorption heat pumps.

In this section, the components and working principle of the heat pumps are going to be expressed in details.

3.1. Heat Pumps

The heat pump is a device which transfers heat from low to high temperature source. Heat transfer from low to high temperature source is only possible by a third energy source, according to the second law of thermodynamics. Figure 3.1 depicts heat pump and operating energy sources.

The measure of performance of a heat pump is expressed in terms of the Coefficient of Performance, COP. The COP relation for both heating and cooling processes can be defined as follows:

$$COP_R = \frac{Q_L}{W_i} \ or \ COP_R = \frac{Q_L}{Q_i} \tag{3.1}$$

$$COP_H = \frac{Q_H}{W_i} \ or \ COP_H = \frac{Q_H}{Q_i} \tag{3.2}$$

Q_L denotes the heat taken from the low temperature heat reservoir, while Q_H refers to the heat transferred to the high temperature one. If the third energy source is

thermal energy, the transferred energy is represented by Q_i. If the third energy source is mechanical, the transferred energy is expressed by W_i.

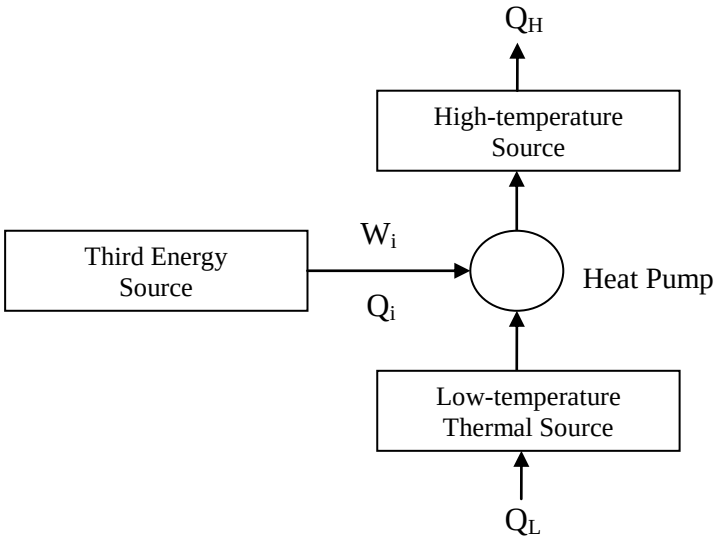

Figure 3.1. Heat pump principle

3.2. Classification of Heat Pumps

Heat pumps can be divided into two groups according to the employed third energy source. If the third energy source is mechanical, the heat pump is called as mechanical heat pump. If the third energy source is thermal energy, then the heat pump is called as thermal driven heat hump. Thermal driven heat pump can be divided into three groups as absorption, chemical and adsorption heat pumps. In thermal heat pumps, a reversible or irreversible reaction, whose energy can be stored, occurs. For example, a chemical heat pump uses reactions between a gas and a salt that is part of a porous solid material inside a reactor (Wongsuwan 2001; Mbaye 1998). Brief information on the mechanical and absorption heat pump systems are given while a detailed discussion on adsorption heat pump is presented within further sections.

3.2.1. Mechanical Heat Pump

Heat pumps are classified in two groups (mechanical and thermal) as mentioned before. A mechanical heat pump consists of an expansion valve, a compressor, an evaporator and a condenser. Figure 3.2 depicts a mechanical heat pump

and its components. The working fluid, refrigerant, flows through four components. Points 1, 2, 3 and 4 in the figure are the state points for the entrance and exit of components.

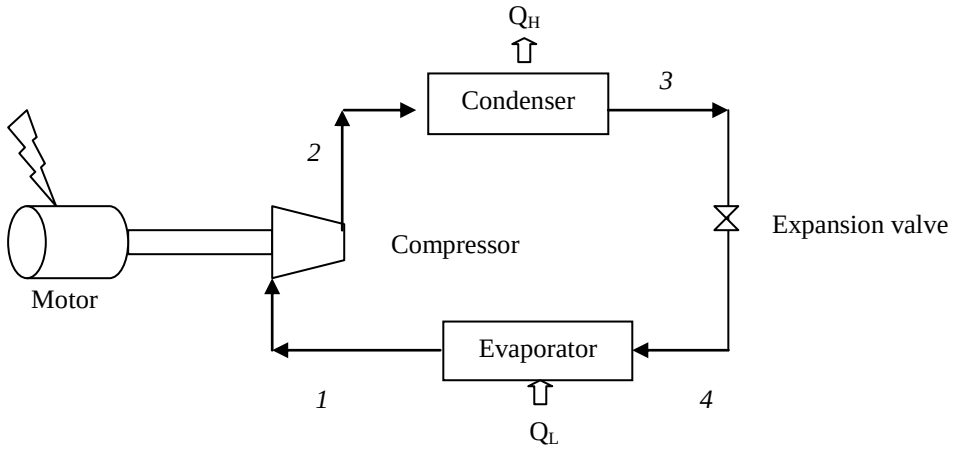

Figure 3.2. Mechanical heat pump cycle and its components

The refrigerant is evaporated in the evaporator while it takes heat from its environment (Q_L). Then, it is pressurized and its temperature is increased in the compressor with the work done. The vapor with high pressure and temperature release heat to environment (Q_H) and is condensed in the condenser. Its pressure is decreased to the evaporator pressure in the expansion valve. The cycle is completed with the expansion process and it is repeated in this order.

The heats of evaporation and condensation achieved in a mechanical heat pump can be calculated by following equations:

$$Q_{ev} = \dot{m}(h_4 - h_1) \tag{3.3}$$

$$Q_{cond} = \dot{m}(h_2 - h_3) \tag{3.4}$$

$$W = \dot{m}(h_3 - h_2) \tag{3.5}$$

In the equations, $\dot{m}$ expresses mass flow rate of refrigerant and h defines the enthalpy at the entrance or exit of each process.

The Coefficient of Performance relations for both cooling and heating processes are:

$$COP_R = \frac{Q_{ev}}{W} \tag{3.6}$$

$$COP_H = \frac{Q_{cond}}{W} \tag{3.7}$$

where, Q_{ev}, Q_{cond} and W are cooling and heating capacities and work done by compressor, respectively.

3.2.2. Absorption Heat Pump

The thermally driven heat pumps may involve adsorption or absorption processes. Absorption is a physical or chemical phenomenon which refers to the solution (or intimate contact) of gas with a liquid. In accordance to the principle of absorption, absorption heat pump working fluid is a solution of two liquids having a high and a low boiling point. Most commonly used working fluids for absorption heat pumps are ammonia-water, lithium chloride-water and lithium bromide-water. Ammonia, lithium chloride and lithium bromide serve as the refrigerant where water serves as the transport medium. A schematic view of an absorption heat pump is presented in Figure 3.3. The working fluid (solution) is heated with high pressure and temperature in the generator. The fluid with low boiling point is vaporized and then transferred to the condenser. It releases heat to the environment (Q_{cond}) while it is condensed. The pressure of condensed fluid is decreased in the expansion valve and it is transferred to the evaporator. It gains heat from the environment (Q_{evap}) during vaporization. The vaporized fluid is absorbed onto the high boiling point fluid transferred from generator to absorber. The solution is pumped to the generator back and the cycle is completed.

The COP values for both heating and refrigeration processes of absorption heat pump are defined with the following relations (Çengel and Boles 2002):

$$COP_H = \frac{Q_{cond}}{Q_{gen} + W_{pump}} \tag{3.8}$$

$$COP_R = \frac{Q_{ev}}{Q_{gen} + W_{pump}} \tag{3.9}$$

where, Q_{ev}, Q_{cond}, Q_{gen} and W are cooling and heating capacities, absorption heat taken from environment by generator and work done by compressor, respectively.

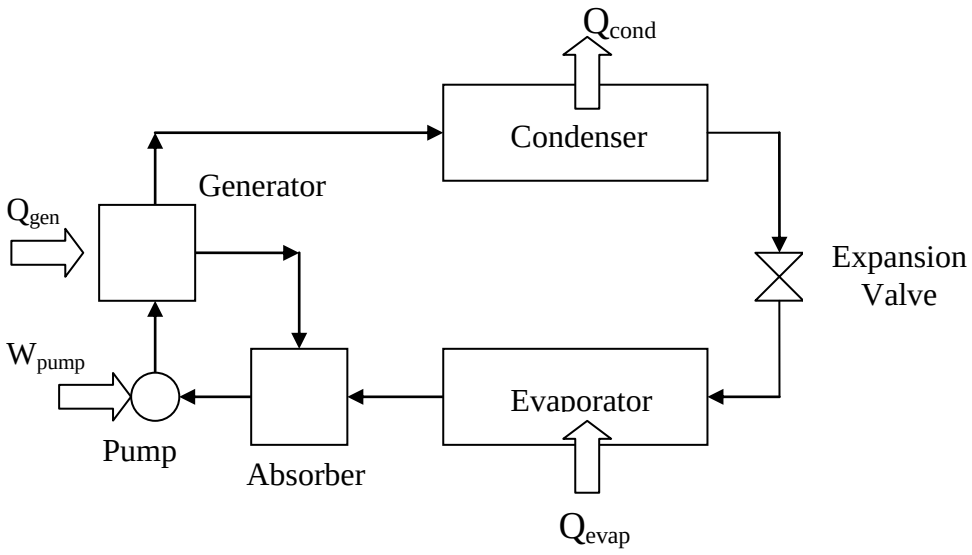

Figure 3.3. Absorption heat pump cycle and its components

3.2.3. Adsorption Heat Pump

Adsorption heat pump cycles were firstly defined by Faraday in 1848, while the commercial studies in this area activated in 1920s (Demir et al. 2008). The interest in adsorption heat pump increased after 1970s due to the oil crisis (Wang and Oliveira 2006). Later, adsorption heat pump gained more interest because of ecological problems related to the use of CFC and HCFC refrigerants which deplete the ozone layer and contribute to the greenhouse effect. Adsorption heat pump can recover heat at low temperature levels and provide a cooling/heating effect. It can be a useful equipment to increase the performance of thermal systems in industry. Adsorption heat pump has advantages such as the use of waste heat or solar energy, being environmental friendly, having no vibration and lower operation costs when it is compared with mechanical vapor compression systems (Ülkü 1986).

A basic adsorption heat pump consists of four main components as; an adsorbent bed, which is a container filled with an adsorbent (such as zeolite, active carbon, silica gel, etc.), a condenser, an evaporator, and an expansion valve. Basically, adsorption heat pump operates by cycling adsorbate through these four components. In

the adsorption heat pump cycle, adsorbent bed plays the same role of mechanical power, so that the working fluid can be circulated in the cycle without any compressor.

The adsorption heat pump is a promising thermal energy storage device with storing the latent and sensible heat. The thermal energy can be stored in the adsorbent during desorption stage at high temperature level from any source (solar energy, waste heat, geothermal energy, etc.) and it is possible to use it during adsorption period (Demir 2008).

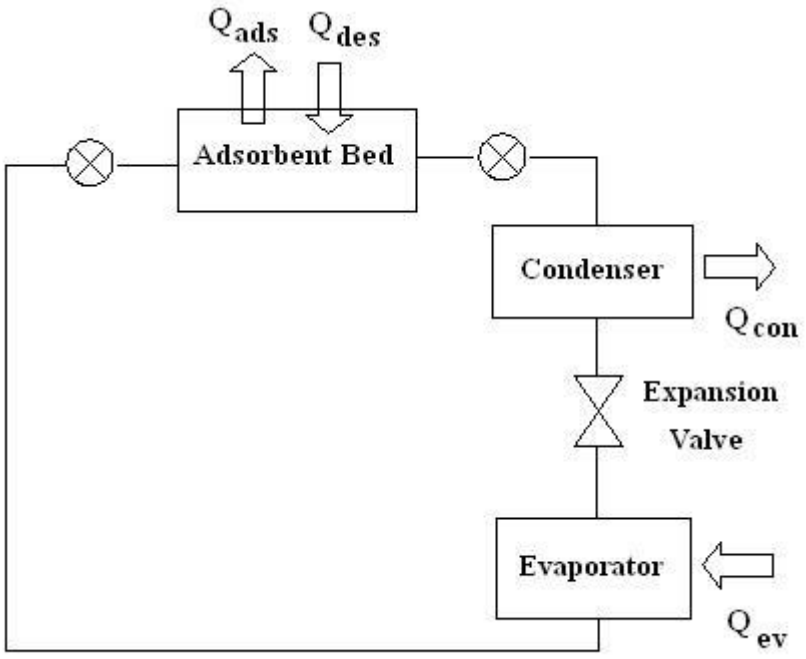

Figure 3.4. Adsorption Heat Pump Cycle

3.2.3.1. Working Principle of Adsorption Heat Pump

The schematical view of an adsorption heat pump is illustrated in Figure 3.4. Two valves placed on the both sides of the adsorbent bed are necessary to fulfill the adsorption and desorption processes of a basic adsorption air-conditioning system. Adsorbent bed is constructed according to the corresponding design parameters and filled with the proper adsorbent of selected pair. The adsorbate of pair is placed into the evaporator. After the construction of the whole system, the system is vacuumed and all the valves within the system are fully closed.

The cycle might be started with desorption process. At the beginning of the desorption process, the valve between adsorbent bed, which was saturated with the

adsorbate beforehand, and condenser is opened, as a result the adsorbate desorbed from adsorbent bed is condensed in the condenser. During condensation the fluid loses heat and rejects it to the environment (Q_{con}). After condensation, the fluid flows through expansion valve and expands. Evaporator evaporates the fluid to the vapor state. During evaporation fluid gains heat and ejects it from the environment (Q_{evap}). After evaporation, fluid flows towards adsorption bed in order to be adsorbed onto the adsorbent particles. The valve between adsorbent bed and evaporator is closed during evaporation and the valve between the bed and condenser is closed. Since the adsorption is exothermic process, heat of adsorption is released during the process. The adsorption is completed and no more adsorbate can be adsorbed by the adsorbent when the level of fluid in the evaporator is constant. At the end of adsorption process, the cycle is completed. The following cycle initiates with the desorption of the fluid, again, while the heat of desorption is ejected from the environment to the system (Wang et al. 2009).

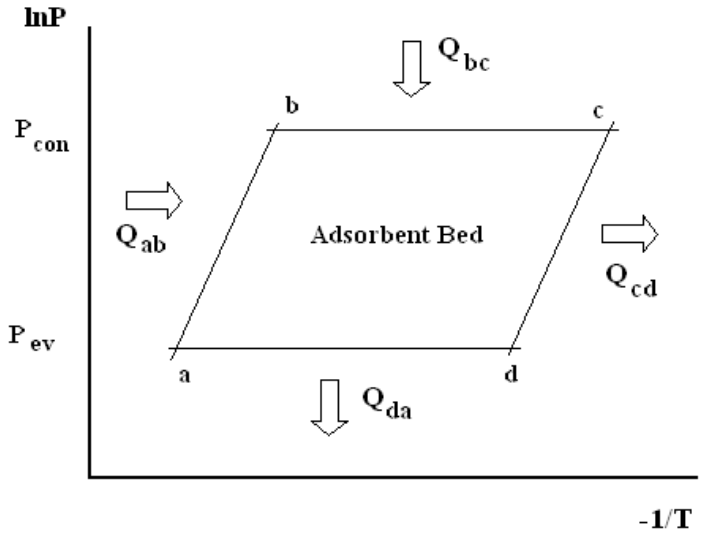

Figure 3.5. The ideal adsorption heat pump cycle (Clapeyron Diagram)

A basic adsorption cycle consists of four thermodynamic steps, which can be presented by Clapeyron diagram, as shown in Figure 3.5. The cycle begins with isosteric heating (a-b) process. The valves between the adsorbent bed and the condenser and evaporator are closed. The temperature of adsorbent bed is increased from T_a to T_b by heating the adsorbent bed without desorption. The amount of heat

which should be transferred to the adsorbent bed to increase temperature of the bed from T_a to T_b is calculated by the following equation:

$$Q_{ab} = m_s c_{ps}(T_b - T_a) + m_s q_{\max} c_{pl}(T_b - T_a) \tag{3.10}$$

After the isosteric heating of the adsorbent bed, the heating process is continued. The next process is isobaric desorption process. The valve between the adsorbent bed and condenser is opened. Desorption process is started and water vapor is condensed in the condenser, while the pressure of the cycle remains constant. The amount of heat drawn from the environment can be calculated by the following relation:

$$Q_{bc} = m_s c_{ps}(T_c - T_b) + m_l(\frac{q_b + q_c}{2}) c_{pl}(T_c - T_b) + m_s(q_{\max} - q_{\min})\Delta H_{ads} \tag{3.11}$$

The third term of equation, here, denotes the heat of adsorption. Since the heat of adsorption is a function of adsorbed amount, the difference between maximum and minimum adsorbed amounts is taken into account.

The next process is isosteric cooling. The valve between the condenser and adsorbent bed is closed and the temperature of adsorbent bed (T_c), which is the maximum temperature of the cycle, is decreased to T_d. During this process both the pressure and temperature of the adsorbent bed are decreased to the evaporator conditions. The amount of heat for isosteric cooling process is evaluated by the following equation:

$$Q_{cd} = m_s c_{ps}(T_c - T_d) + m_s q_{\max} c_{pl}(T_c - T_d) \tag{3.12}$$

The cycle is completed by the last process which is isobaric adsorption process. The valve between the adsorbent bed and evaporator is opened and adsorbate is evaporated. During adsorption of the adsorbate in the adsorbent, heat is released due to heat of adsorption. This generated heat should be removed from the adsorbent bed and the bed temperature should be decreased to T_a. The amount of heat released to environment for isobaric adsorption process is given by equation 3.13 (Demir 2008):

$$Q_{da} = m_s c_{ps}(T_d - T_a) + m_l(\frac{q_d + q_a}{2}) c_{pl}(T_d - T_a) + m_s(q_{\max} - q_{\min})\Delta H_{ads} \tag{3.13}$$

The performances of the adsorption air-conditioning devices are defined by COPs. The cooling and heating COPs of an adsorption heat pump can be determined by equations 3.14 and 3.15 (Demir 2008):

$$COP_H = \frac{Q_{cond} + Q_{cd} + Q_{da}}{Q_{ab} + Q_{bc}} \tag{3.14}$$

$$COP_R = \frac{Q_{evap}}{Q_{ab} + Q_{bc}} \tag{3.15}$$

3.2.4. Multi-bed Adsorption Heat Pump

An adsorption heat pump with a single bed is named as intermittent adsorption heat pump, since it can not provide heating or cooling effect continuously. Condenser is not used while adsorbate is evaporating and flowing through the adsorbent bed. Multi-bed adsorption heat pump is a solution for the primary problem of an intermittent adsorption heat pump. The continuous heating or cooling processes can be achieved with addition of another adsorption bed to the system. For a two bed adsorption heat pump; as soon as the adsorption is completed in the first bed, the valve between bed and evaporator is closed and heating process takes start. At the same time the valve between the second bed and evaporator is open and adsorption begins in the second bed. Thus, continuous evaporation and condensation processes are achieved. The schematical view of two bed adsorption chiller used by Wang and Chua (Wang and Chua 2007) in their experimental study can be a good example for illustration of these systems (see Fig. 3.6).

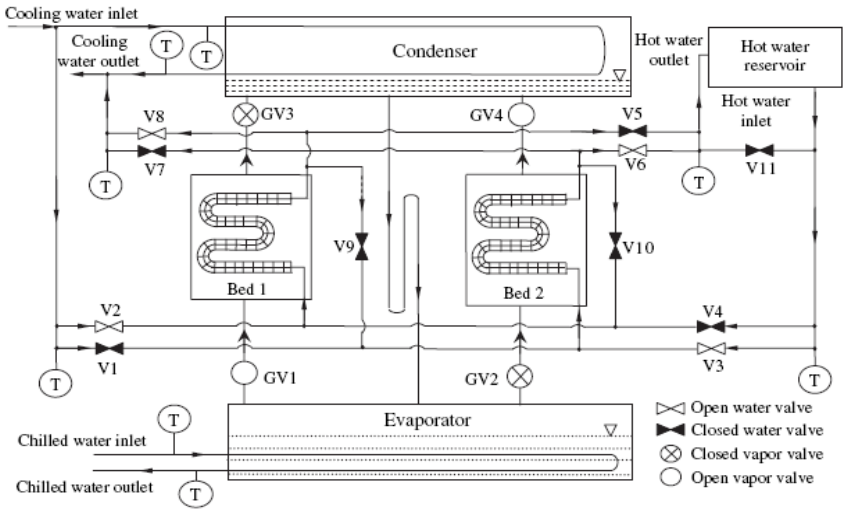

Figure 3.6. Schematic view of a two-bed adsorption cooling system (Source: Wang and Chua 2007)

3.2.5. Comparison Among Heat Pumps

As it was mentioned before, heat pumps are classified as mechanical and thermal heat pumps. Thermal heat pumps are also classified as absorption, chemical and adsorption heat pumps. The selection of these three devices may be decided according to their advantages and disadvantages. The advantage and disadvantages of these pumps are given in this section.

Advantages of mechanical heat pump are:

1. having a compact construction,
2. having low cost,
3. well known working principle.

Disadvantages of mechanical heat pump are:

1. using hazardous refrigerants,
2. being noisy,
3. need of periodic maintenance.

The absorption heat pump which is a type of thermal heat pump and it has such advantages:

1. the use of primary and thermal energy sources,
2. continuous working principle,
3. using no hazardous materials,

4. well known working principle.

Disadvantages of this device are:

1. need of high third heat source temperature,
2. the large size of device (prevents applicability),
3. using corrosive materials which may damage the system with time.

The advantage of adsorption heat pump system can be listed as:

1. using waste, solar or geothermal heat sources directly,
2. ability to use low temperature heat source according to the pair used,
3. having no moving components, thus vibration and noise are prevented,
4. using non-hazardous fluids such as water and methanol,
5. Since the adsorbents and adsorbates can be used for years, the maintenance need is minimum,
6. It can store energy and use it when required.

It has disadvantages such as:

1. providing non-continuous heating or cooling in case of using single bed,
2. working under vacuum conditions; therefore the leakage prevention needs high technology,
3. having not very common commercial production.

CHAPTER 4

COMMON ADSORBENT-ADSORBATE PAIRS USED IN ADSORPTION HEAT PUMPS

4.1. Adsorption

The first scientific and quantitative work on adsorption was performed as early as 1773, by Schele and Fontana. Its use for cooling and heating applications was started in 1848 by Michael Faraday (Zhong and Critoph 2005). Adsorption is a surface phenomenon occurring at the interface of two phases, a solid and a fluid, in which cohesive forces including Van der Waals forces and hydrogen bonding are included. Solid, and the fluid adsorbed on the solid surface are called as adsorbent and adsorbate, respectively.

Adsorption is different from absorption. In absorption, a substance diffuses into a liquid or solid to form a solution; while adsorption is an adhesion process of a fluid onto surface of a solid. Figure 4.1 shows the adhesion of fluid particles onto the surface of solid phase. The concepts as adsorbate, adsorptive and adsorbates are shown. They will be explained in details in next sections. The term sorption encompasses both adsorption and desorption processes. The desorption is the reverse process of adsorption.

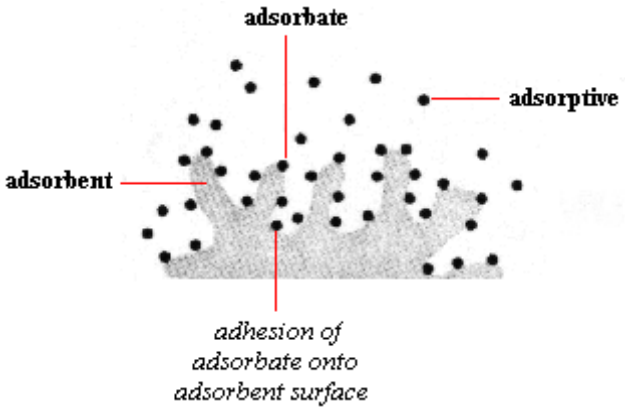

Figure 4.1. Illustration of adsorption phenomena

Adsorption is present in many natural physical, biological, and chemical systems, and is widely used in industrial applications such as dehumidification and water purification. Adsorption is a sorption processes in which certain adsorbates are selectively transferred from the fluid phase to the surface of insoluble, rigid particles suspended in a vessel or packed in a column.

Similar to surface tension, adsorption is a consequence of surface energy. In a bulk material, all the bonding requirements (ionic, covalent, or metallic) of the constituent atoms of the material are filled by other atoms in the material. However, atoms on the surface of the adsorbent are not wholly surrounded by other adsorbent atoms and therefore can attract adsorbates. The exact nature of the bonding depends on the details of the species involved, but the adsorption process is generally classified as a physical process referred to as physical adsorption, or physisorption, caused by Van der Waals forces, or a chemical process referred to as chemical adsorption or chemisorption, involving valency forces (Srivastava and Eames 1998). Chemical and physical adsorption can be distinguished by following properties;

- Physisorption is generally reversible process but chemisorption is irreversible process.
- Physisorption may occur as multilayer adsorption, chemisorption only takes place as monolayer adsorption.
- Physisorption occurs with polarization of adsorbate molecules. In chemisorption, there is bond formation between adsorbate and surface of adsorbent.
- Physisorption is always exothermic and evolved energy is not much larger than the energy of condensation of adsorptive. The energy of chemisorption is nearly the same as the energy in chemical reaction (Rouquerol et al. 1999).

The adsorption behavior such as maximum capacity, isotherm type and heat of adsorption depends on the properties of adsorbent and adsorbate and the interaction with each other. Maximum capacity can be defined as the possibility of maximum adsorbed adsorbate amount onto the corresponding adsorbent. Therefore it is a concept which is concerned to the interaction between adsorbent and adsorbate. Isotherm type is the definition of adsorption equilibrium in terms of plots at constant temperatures.

Since, adsorption is an exothermic process, there is a term called as heat of adsorption. It is the heat evolved by the pair during the adsorption process.

4.2. Adsorbents

Adsorbents are the substances which are usually porous in nature and have high surface area. They can adsorb the adsorbate onto their surfaces by intermolecular forces. In order to decide the adsorbent being used, the properties of the adsorbent should be well known. The thermophysical requirements for an adsorbent in order to be used in an adsorption heat pump and their explanations can be listed as:

- good compatibility with adsorbate,
- high surface area: as the surface area gets larger, adsorption surface increases,
- high adsorption capacity: depends on the interaction with adsorbate,
- quick response of adsorption capacity to temperature change: the change of temperature during the operation of adsorption heat pump is an important parameter,
- high thermal conductivity: the heat transferred along the bed depend on the conductivity of adsorbent,
- high mass diffusivity: the diffusion of adsorbate through the pores of adsorbent should be high in order to achieve high power within the system,
- thermal stability: the durability of material is important due to long life usage of the system.

Additionally, structural properties of adsorbent such as nature of material and pore dimensions are the noteworthy parameter that should be taken into consideration.

Adsorbents can be classified into three groups by their structures, by the size of the pores inside and by the nature of their surfaces.

1. By nature of their structure:
    - Amorphous adsorbents: They have a specific surface area in the range of 200-1000 m^2/g, generally. Pore size distribution might be very wide.

- Crystalline adsorbents: The dimensions of the micropores are determined by the crystal framework. The crystals are generally quite small and they are aggregated with a suitable binder.

2. By the size of their pores:
   - Microporous: adsorbents with pores having diameter smaller than 20 Å.
   - Mesoporous: adsorbents with pores having diameter between 20 Å and 500 Å.
   - Macroporous: adsorbents with pores having diameter larger than 500 Å.

Figure 4.2 and 4.3 show the macro-, meso- and micro- dimensions of a porous particle in order to illustrate the dimensions of pores.

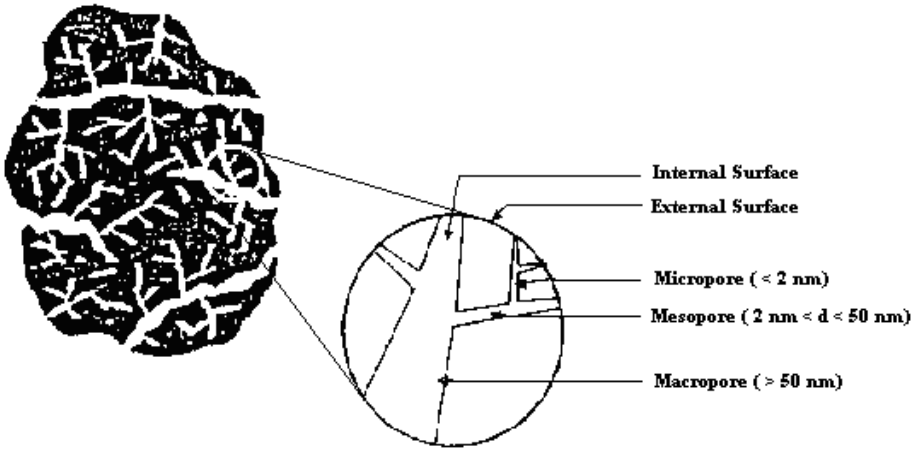

Figure 4.2. Schematical view of pore dimensions

3. By the nature of their surfaces
   - Polar or hydrophilic: Water which is a polar molecule is very strongly adsorbed due to electrostatic forces onto these adsorbents.
   - Non-polar of hydrophobic: Water is weakly adsorbed on any non-polar surfaces.

The most common adsorbents used in adsorption heat pumps are zeolite, silica gel, active carbon and activated alumina. The physical structures and behaviors of adsorbents and adsorbates are crucial in selection of the proper working pair.

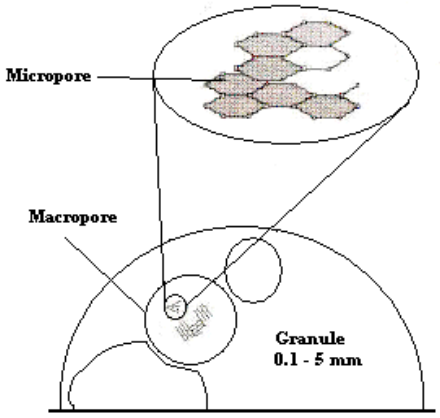

Figure 4.3. Illustration of a porous structure

4.2.1. Properties of Common Adsorbents

4.2.1.1. Silica Gel

Silica gel ($SiO_2.xH_2O$) is a type of amorphous synthetic silica compound. It is a rigid, continuous net of colloidal silica, connected to very small grains of hydrated SiO_4. Structure of silica gel is given as an illustration in Figure 4.4. The hydroxyl in the structure is the adsorption center because it has a polar structure and can form hydrogen bonds with polar oxides, such as water and alcohol. The adsorption ability of silica gel increases with the increasing polarity. One hydroxyl can adsorb one molecule of water (Wang et al. 2009).

Silica gel retains chemically bonded traces of water (about 5%). If it is overheated (over 150 °C) and loses this water, its adsorption capacity is lost. Therefore, it is generally used in temperature applications under 130 °C. The removal of adsorbate from the surface of silica gel occurs at respectively lower temperatures such as 110-120 °C. Since desorption temperature of silica gel is not high, the maximum temperature of the bed that should be reached is relatively low. This is the most advantageous property of silica gel in order to use in an adsorption heat pump due to ability of using low temperature heat sources such as waste heat, solar and geothermal energy. Therefore, the decrease in cycle time occurs and higher COP values can be achieved in the adsorption heat pump device.

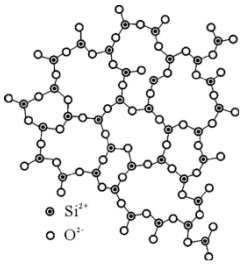

Figure 4.4. Bonding structure of silica gel

Silica gel is available in various pore sizes. It has an average pore diameter of 30 Å. Its average surface area is around 600 m^2/g. It nearly has 0.180 W/mK of thermal conductivity.

Since the adsorption performance of silica gel depends mainly on its surface area and pore distribution, types of silica gel which are classified according to their pore sizes, should be investigated. The most commonly used silica gel types are Type A, Type B, Type 3A and Type RD. Some structural properties, such as specific surface area, pore size, pore volume, average pore diameter, apparent density, pH, mesh size and water content, and also thermo-physical properties such as specific heat capacity, thermal conductivity of common silica gel types are listed in Table 4.1 (Ng et al. 2001; Chua et al. 2002). Due to its high surface area and higher thermal conductivity, Type RD silica gel seems as the better one along these four types.

Table 4.1. Structural and thermophysical properties of silica gel types

	Type A	**Type B**	**Type 3A**	**Type RD**
Specific Surface Area (m^2/g)	650	550	606	720
Porous Volume (ml/g)	0.3	0.6	0.45	0.35
Pore Size (nm)	0.8-5	0.7-5	-	0.8-7.5
Micropore Volume (%)	57	-	-	49
Mesopore Volume (%)	43	-	-	51
Average Pore Diameter (nm)	2.2	5.2	3.1	2.1
Apperant Density (kg/m^3)	730	-	770	800
pH	5	-	3.9	4
Water Content (wt. %)	<2.0	-	0.87	-
Specific Heat Capacity (kJ/kg K)	0.921	-	0.921	0.921
Thermal Conductivity (W/m K)	0.174	-	0.174	0.198
Mesh Size	10-40	-	60-200	10-20
Isotherm Type	II	V	II	I

The surface characteristics and the pore structure of types are the determining factors which affect the adsorption equilibrium. Type A and type RD silica gels are the most preferred types and they have many physical similarities. Although type RD

silica gel has a slightly higher thermal conductivity than the type A silica gel, the most significant difference between these two types of silica gel is their maximum adsorption capacity features. Type RD silica gel had been commonly employed for the adsorption chiller as the adsorbent by the chiller manufacturers. Chua et al. experimentally studied the isotherm characteristics of Fuji Davison type A and type RD silica gels. The experimental results were also compared by manufacturer's data. Type RD silica gel could achieve around 45% of water uptake at 30°C, while type A could adsorb around 40% at that temperature.

Li et al. experimentally studied the isotherm characteristics of silica gel types. Silica gels used in this study were purchased from Qingdao Haiyang Chemical Co., Ltd and Special Silica Gel Factory (Qingdao,China). They resulted that, the isotherm of the water vapor on the A-type silica gel with an average pore diameter of 2 nm was of type I, which can be well described by the Langmuir model. The isotherm of the water vapor on the B-type and the C-type mesoporous silica gels with average pore diameters of 5.28 nm and 10.65 nm, respectively, were of type V (Li et al. 2007).

4.2.1.2. Zeolite

Zeolites are crystalline hydrated alumina silicates of group 1 and group 2 elements. Crystalline structures are composed of tetrahedral units, at the center of silicon (Si) atom which is surrounded with four oxygen atoms. Molecular structures of different zeolites can be shown as in Fig. 4.5. In the figure, a is the chain of fibrous zeolites; b is the singly connected 4-ring chain; c is the doubly connected 4-ring chain; d is the 6-ring (single); e is the 6-ring (double) and f is the 4-4-1-1 heulandite unit.

In each drawing, the balls represent tetrahedra (SiO_4^{4-} or AlO_4^{5-}) and the bars represent oxygen atoms shared by the tetrahedral structure (Gottardi and Galli 1985).

Zeolites are also known as molecular sieves. The term molecular sieve refers to a particular property of these materials, i.e., the ability to selectively sort molecules based primarily on a size exclusion process. This is due to a very regular pore structure of molecular dimensions. The maximum size of the molecular or ionic species that can enter the pores of a zeolite is controlled by the dimensions of the channels. These are conventionally defined by the ring size of the aperture, where, for example, the term "8-ring" refers to a closed loop that is built from 8 tetrahedrally coordinated silicon (or

aluminum) atoms and 8 oxygen atoms. These rings are not always perfectly symmetrical due to a variety of effects, including strain induced by the bonding between units that are needed to produce the overall structure, or coordination of some of the oxygen atoms of the rings to cations within the structure.

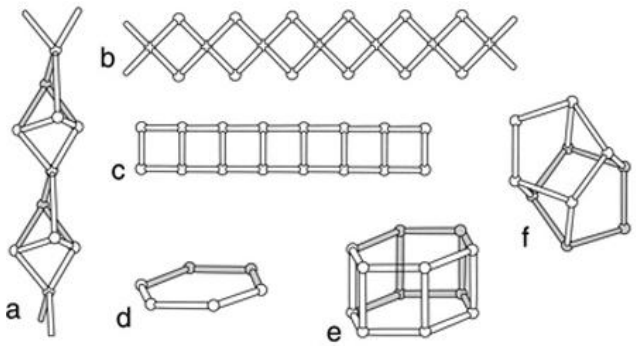

Figure 4.5. The structural units defining different zeolite types
(Source: Gottardi and Galli 1985)

Zeolite molecular sieves are mostly microporous adsorbents and the pore sizes are uniform throughout the particle. The regularity of their pore size structure makes them especially convenient for adsorption applications. They have high surface area such as 800-1000 m^2/g. They can adsorb polar and non-polar molecules if appropriate conditions are provided; and they can adsorb water vapor with high heats of adsorption even at very low concentrations (Ülkü 1991).

Table 4.2. Structural and thermophysical properties of zeolite types

	4A	**5A**	**13X**	**Natural Zeolite**
Specific Surface Area (m^2/g)	-	~ 600	~ 700	-
Porous Volume (ml/g)	-	-	-	-
Pore Size (Å)	10-15	12	8	4
Micropore Volume (%)	67	82	-	-
Mesopore Volume (%)	33	28	-	-
Average Pore Diameter (nm)	-	-	-	-
Apperant Density (kg/m^3)	-	-	-	650-850
Water Content (wt. %)	5	5	-	-
Specific Heat Capacity (kJ/kg)	1.07	1.07	1.07	-
Thermal Conductivity (W/m K)	-	-	-	0.155
Isotherm Type	I	I	I	I

Commercial zeolites are classified as natural and synthetic zeolites. The main usage of natural zeolite as adsorbent are as drying agents, deodorants, adsorbents for

air separation, ion exchangers for water purification especially for removing ammonium ion and heavy metal ions and for water softening, soil upgrading etc.

The artificial zeolites 3A, 4A, 5A, 10X and 13X are the main types used for adsorption refrigeration. The 4A type zeolite contains Na^+ ion and it permits molecules smaller then 4Å to enter through the blank sites. If K^+ ion is replaced instead of Na^+ ion, the effective site size becomes 3Å. Under these conditions, molecules which are greater than H_2O and NH_3 molecules are not able to penetrate through the pores. This type is called as 3A (KA) zeolite. If Ca^{+2} ion is replaced instead of Na^+ ions, in this case the site gets larger and it has a pore diameter around 5Å. This type is called as 5A (CaA) zeolite. Type X zeolites has much larger open sites and usually called as 13X (Suzuki 1990). Zeolite 13X is used mostly in case of its high adsorption capacity and average heat of adsorption which is about 4400 kJ/kg when it is used with water. The zeolites are usually employed in adsorption air conditioner systems with a heat source between 200-300 °C. Some thermophysical properties for several zeolite types are given in Table 4.2 (Demir et al. 2006; Tamainot-Telto et al. 2009). Type 13X zeolite is the most common zeolite used along these four types in adsorption heat pump studies.

4.2.1.3. Active Carbon

Activated carbons are produced through the activation of carbonaceous materials such as coal, wood, coconut shell, fossil oil, bone, peat and high polymers.. The activated carbon is composed of multiple carboatomic rings. The original carbonaceous material and applied activation process determines the functional groups on the surface of activated carbon and the adsorption performance is influenced by the functional groups that are connected to the carboatomic ring. Arene group connected to the ring increases adsorption, while sulfonic group decreases it.

Activation method and technology also determines adsorbent's tridisperse porous texture (macroporous, microporous, mesoporous structure). However, activated carbons mostly have microporous structure. This adsorbent is available in various forms such as powdered, granular, molecular sieves and carbon fibers. The structure of activated carbon is near to the structure of graphite. The structure of active carbon is illustrated in Figures 4.6 and 4.7.

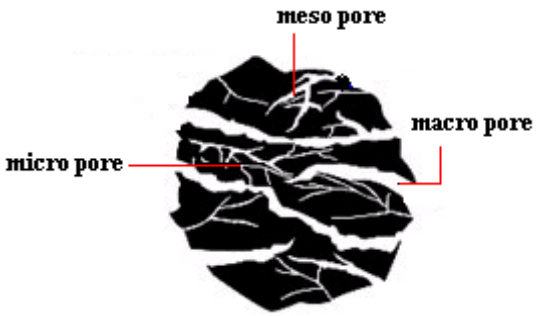

Figure 4.6. Schematic structure of active carbon

Its surface feature distinguishes the activated carbon from other adsorbents. The whole surface of activated carbon is covered by an oxide matrix and by some inorganic materials (Zhong and Critoph 2005). The other unique surface property of activated carbon, in contrast to the other major adsorbents, is that its surface is nonpolar or only slightly polar as a result of the surface oxide groups and inorganic impurities. The average specific surface area of activated carbon is approximately 1000 m^2/g. The heat of adsorption of activated carbon pairs is lower than others.

Figure 4.7. Structure of active carbon (SEM visualization)

Because of its large, accessible internal surface and large pore volume, active carbon adsorbs more non-polar and weakly polar organic molecules than other adsorbents do. For example, the amount of methane adsorbed by activated carbon at 1 atm and room temperature is approximately twice that adsorbed by an equal weight of molecular sieve 5A. The heat of adsorption, or bond strength, is generally lower on activated carbon than on other adsorbents.

Although active carbon has a nonpolar structure; it is not a hydrophobic adsorbent. The sorption of water vapor on activated carbon follows a Type V with a sigmoidal or S-shaped curve.

Table 4.3. Structural and thermophysical properties of active carbon types

	Active Carbon	**Granular Carbon**	**A. C. Fibers**	**Monolithic Carbon**
Specific Surface Area (m^2/g)	ACX21: 3000 (Yaping and Li 1996)	700 – 1500 (Hamamoto et al. 2006)	~ 250 (Hamamoto et al. 2006)	-
BET Surface Area	-	-	895 (Tamainot-Telto et al. 2009) ACF15: 900 ACF20: 1610 ACF25: 2420 (Cal et al. 1994)	-
Porous Volume (ml/g)	1.5 (Yaping and Li 1996)	-	ACF15: 0.330 ACF20: 0.628 ACF25: 0.655 (Cal et al. 1994)	-
Pore Size (Å)	-	-	9.8 (Tamainot-Telto et al. 2009)	-
Micropore Volume (cm3/g)	-	-	0.43 (Tamainot-Telto et al. 2009)	-
Average Pore Diameter (nm)	1.2 – 4.0 (Hamamoto et al. 2006)	1.2 -3.5 (Hamamoto et al. 2006)	ACFA20: 2.160 ACFA15: 2.175 (El-Sharkawy et al. 2006)	--
Density (kg/m^3)	450 (Yang 2003) 2000 (Hassan et al. 2011)	366 – 500 (Tamainot-Telto et al. 2009) 466 - 500 (Zhong and Critoph 2005)	104-384 (Tamainot-Telto et al. 2009)	773 - 750 (Zhong and Critoph 2005) LM127: 750 LM128: 715 (Tamainot-Telto and Critoph 2001)
Specific Heat (kJ/kgK)	920 (Yang 2003) 711 (Hassan et al. 2011)	6500 (Demir et al. 2006)	-	8000 (Tamainot-Telto and Critoph 2001)
Thermal Conductivity (W/m K)	1.6 (Hassan et al. 2011)	0.1 (Zhong and Critoph 2005) 0.16 (Tamainot-Telto and Critoph 2001)	ACF15: 0.104 (Cal et al. 1994)	0.27-0.34 (Zhong and Critoph 2005) 0.40 (Demir et al. 2006) LM 127: 0.44 LM128: 0.35 (Tamainot-Telto and Critoph 2001)
Isotherm Type	I	I	I	-

Active carbon fiber (ACF) is a type of active carbon with a higher adsorption capacity. Synthetic fibers such as polyacrylonitrile (PAN), coal tar (pitch), phenolic

resin and viscose rayon are carbonized at high temperature in inert atmosphere and activated carbon fiber is prepared by careful activation (Hamamoto et al. 2006). These carbon fibers have high tensile strength, high elasticity and contain considerable more graphite than activated carbon because a mesophase is usually formed during the carbonization process of the fibers. Adsorption rate of the fiber is also faster than that of the granule. This is attributed that outer surface area, which is 0.5 m^2/g, of the fiber is higher than that of the granule. Figure 4.8 illustrates the porous structure difference between these two active carbon types. The outer surface area of the grain is 0.01 m^2/g. The micro pores are exposed on the surface of a fiber. Therefore, refrigerant vapor reaches at the adsorbent site easily.

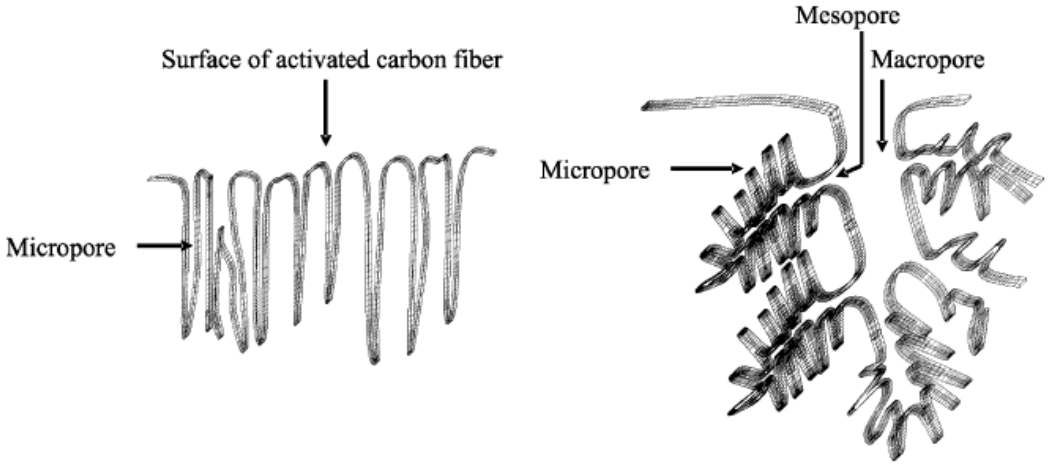

a) active carbon fiber b) granular active carbon

Figure 4.8. Schematic views of active carbon fiber and granular activated carbon (Source: Hamamoto et al. 2006)

Some structural and thermo-physical properties for four different types of active carbons are given in Table 4.3. Each type of active carbon has better properties for different cases. For example monolithic carbon has higher specific capacity than other types, while ACX21 has much higher specific surface are than others. The selection of right active carbon has to be done according to the parameters and requirements of the adsorption heat pump.

4.2.1.4. New Working Materials

The adsorption behavior properties of pairs lead the differences in performance of adsorption conditioning devices, as mentioned before. As soon as the properties are improved, the performance of these devices would be increased. The discovery of new microporous materials for the use in adsorption heat pump processes is now promising research topic in order to achieve more efficient adsorption processes and have higher efficiencies in adsorption air-conditioners. Exciting improvements and numerous publications on these studies were presented in literature.

The new type porous materials are produced with the improvements of conventional adsorbents. In example, a family of new composite sorbents has been developed. These materials are called selective water sorbents (SWSs). They are two-phase systems which consist of a porous host material with pores (silica gel) and salt compounds ($CaCl_2$, LiBr, etc.) impregnated to its pores (Aristov et al. 2002; Aristov and Gordeeva 2009). The salt interacts with adsorbate to increase the adsorption capacity. Since SWS is a silica gel based matrix, it is commonly paired with water in reported literature studies.

The production of these novel materials is assessed by impregnation process. The impregnation process starts with the preparation of an aqueous solution of salt. The solution was kept under ambient temperature for two hours and stirred up for facilitating and accelerating the dissolution process, and preventing crystallization. The process continues with the immersion of the host matrix in that solution and kept in for twelve hours in order to let salt to penetrate into the pores of adsorbent. The last step is the drying process. The silica gel + solution material is dried under an average temperature of 80 °C; the water is removed throughout the matrix. The preparation of ‘a salt in a porous matrix’ is completed by that way (Daou et al. 2008).

The impregnated adsorbents (SWS’s) are named according to their host matrices and salts; in example SWS-1L is the name of calcium chloride (1) impregnated to mesoporous silica gel (L). SWS-2L is the name of lithium bromide (2) impregnated to mesoporous silica gel (L) and SWS-1S is the name of calcium chloride (1) impregnated to microporous silica gel (L).The researchers experimentally studied the performance of SWS’s. Aristov et al. resulted that composite materials based on $CaCl_2$ and LiBr as the impregnated salts and on microporous and mesoporous silica

gels as the host materials were able to adsorb up to 75% by weight. Figure 4.9 shows the comparison of isobar plots of conventional silica gels and SWSs which were experimentally performed by Aristov et al. (Aristov et al. 2002). As it can be seen clearly, at the same pressure and temperature, impregnated materials have higher adsorption capacities than the conventional ones. SWS-2L has the biggest adsorption capacity along three selective sorbents. The regeneration temperature was found to be between 70 and 120 °C. Thus, SWS materials were applicable for low temperature heat sources. The disadvantage for these materials was found as the low diffusion rate. As soon as the rate is decreased, the complete adsorption time is increased so that the cycle time for refrigeration is increasing.

Another novel adsorbent studied on is a zeolite based material which is named as functional adsorbent material (FAM). FAM-Z01 is a molecular sieve having one-dimensional structure with 0.73 nm windows and its framework consists of AlO_4, PO_4 and FeO_4 tetrahedrons, where Al and P atoms are partially substituted by Fe atoms. FAM-Z01 was synthesized from iron-containing aluminophosphate gels in the presence of organic amines under the hydrothermal condition.

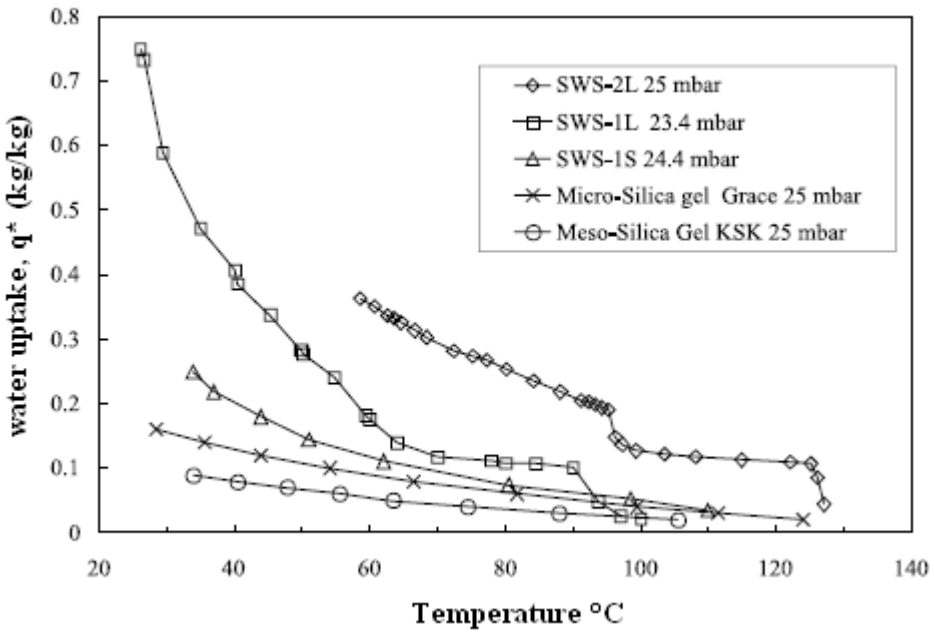

Figure 4.9. Comparison of 25 mbar isobars of different adsorbents
(Source: Aristov et al. 2002)

FAM-Z02 is a novel molecular sieve having three-dimensional structure. The structure has large ellipsoidal cages. Small guest molecules, such as water, can diffuse into the cages through 0.38 nm windows. FAM-Z02 framework consists of AlO_4, PO_4 and SiO_4 tetrahedrons, where Al and P atoms are partially substituted by Si atoms.

Water vapor adsorption isotherms and physical properties of FAM-Z01 and FAM-Z02 were studied experimentally by Kakiuchi et al. (Kakiuchi et al. 2004) and the adsorbents were found to have different behaviors than other conventional adsorbents. Figure 4.10 and Table 4.4 give the isotherm graph and some physical properties of their experimental results, respectively. As seen in Figure 4.10, at low relative pressure ranges, FAMs can adsorb high amounts of water vapor compared to conventional silica gel and active carbons. Water vapor adsorption isotherm of FAMZ01 gives type V isotherm, while FAMZ02 is near to type I isotherm. The knee shape for both adsorbents is sharper than conventional adsorbent isotherms. From the table, it can be seen that thermophysical properties of FAMZ02 are mostly higher than FAMZ01's; therefore a higher adsorption capacity was achieved by FAMZ02 as seen from its isotherm plot.

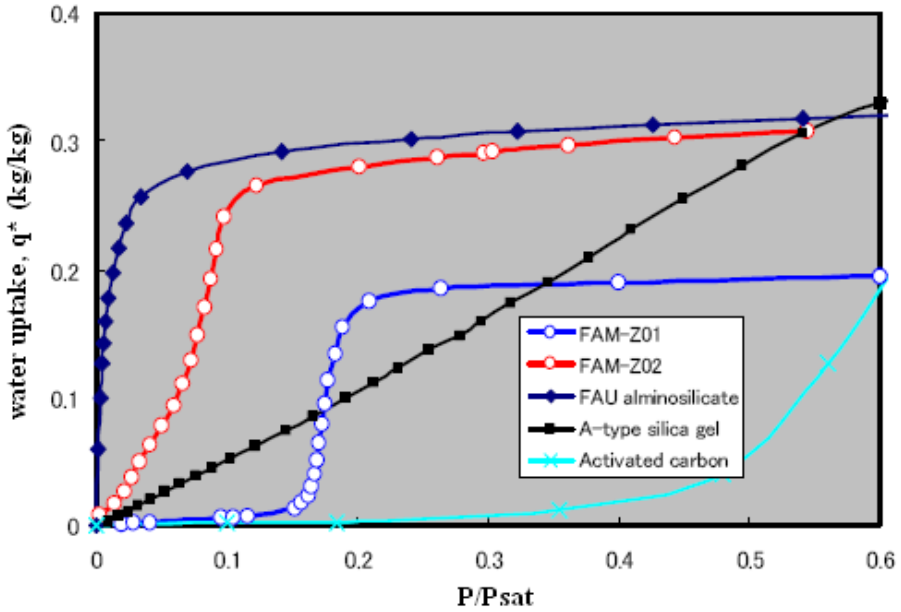

Figure 4.10. Comparison of 25 °C isotherm of FAMZ01 and FAMZ02 (Source: Kakiuchi et al. 2004)

Metal-Organic Frameworks (MOFs) are also new studied materials emerging class of microporous materials possessing unique features such as huge surface areas, large pore volumes. With improvements on studies, extremely high surface areas up to

5000 m^2/g have now been reported for several MOFs. According to the elements inside, MOFs may be named as MIL100, MIL101 etc. As the result of experimental studies, MIL101 was found to have an impressive water loading of 103 % at 40 °C and 5.6 kPa, which is the largest water adsorption capacity reported so far (Henninger et al. 2011). Table 4.5 shows the water adsorption capacity and heat of adsorption data for several MOF types. As seen, the minimum water vapor adsorption is for any type of MOF is even near to 60 %. Adsorption capacity values are extremely higher than the water adsorption capacities of conventional adsorbents (Bauer et al. 2009).

AIPO adsorbents are also novel materials which are the improved forms of zeolite molecular sieves. They were found to provide promising sorption properties among typical boundary conditions of adsorption refrigerators. The structures of AlPO zeolites are formed by altering $(AlO_4)^-$ and $(PO_4)^+$ tetrahedrons resulting hydro-philic properties. S-shaped water sorption isotherms and low desorption temperatures have been measured for different types of AlPO. Presence of aluminum in the adsorbent increases the thermal conductivity of the material and it possesses higher power due to lower cyclic times.

Table 4.4. Thermophysical properties of FAMZ011 and FAMZ02

		FAMZ01	**FAMZ02**
Bulk Density	g/ml	0.6-0.7	0.6-0.7
Particle size	Mm	100-2000	100-2000
Thermal conductivity	W/mK	0.113 (303 K) 0.123 (343 K)	0.117 (303 K) 0.128 (363 K)
Heat of adsorption (H_20, 298 K)	kJ/mol	56.0	58.3
	kJ/g H_20	3.11	3.24
Specific heat	J/gK	0.805 (303 K) 0.896 (343 K)	0.822 (303 K) 0.942 (363 K)

Incorporation of silicon atoms into an AlPO framework forms another novel material which is called as SAPO. High adsorption capacities at specific operating conditions have been measured for different AlPO and SAPO structures (Bauer et al. 2009). Figure 4.11 shows the isotherm graph for experimental results of study performed by Bauer et al. (Bauer et al. 2009). Maximum adsorption capacities of 0.07–0.20 g adsorbed water per gram AlPO(Al) or SAPO(Al) composite adsorbent are reached varying according to the layer thicknesses.

Table 4.5. Adsorption capacity and heat of adsorption for water vapor adsorption on different MOFs (Source: Henninger et al. 2011)

	Relative Pressure	**Adsorption Capacity (kg/kg)**	**Heat of Adsorption (kJ/mol)**
MIL-101 (Cr)	0.921	1.01	46.6
MIL-101	0.9	1.03	45.13
MIL-100 (Al)	0.899	0.568	-
MIL-100 (Fe)	0.9	0.651	48.83

In this section, the studies on novel materials and the adsorption behaviors of materials were summarized. The usage of these novel materials in adsorption heat pumps will be applicable as soon as the experimental studies are performed on this area.

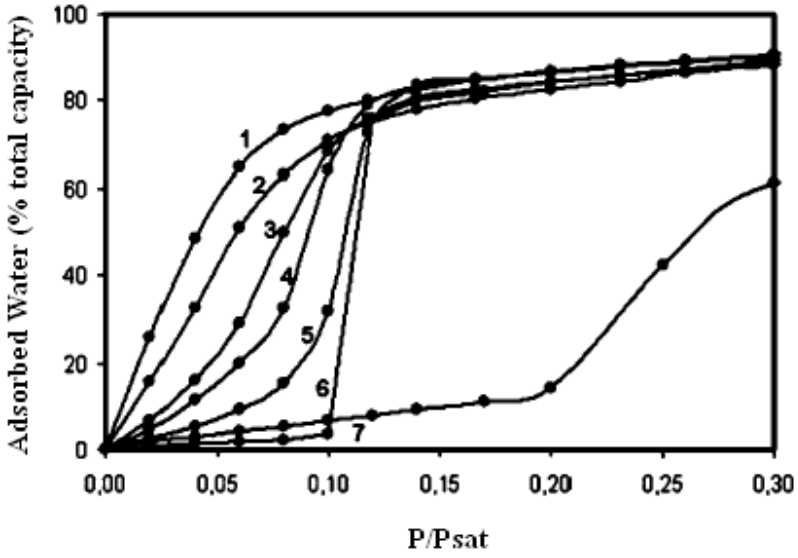

Figure 4.11. Experimental water adsorption isotherm results for different AlPO(Al) and SAPO(Al) composite adsorbents [1-4: SAPO-34, 5: SAPO-18, AIPO-18, AIPO-5] (Source: Bauer et al. 2009)

4.3. Adsorbates

Adsorbable substance in the fluid phase is called as adsorptive. Adsorptive tends to diffuse into the pores of the adsorbent. The substance in the adsorbed state is called adsorbate. The commonly used adsorbates for adsorption heat pumps are water, methanol, ethanol and ammonia. The thermophysical properties of a proper adsorbate which should be considered are (Sumathy et al. 2003):

- latent heat,
- freezing and boiling point,
- saturation vapor pressure,
- viscosity,
- non-toxicity, non-flammability and non-corruption,
- good thermal stability.

Some thermophysical properties of adsorbates such as boiling point, latent heat of vaporization and density, for adsorption systems are shown in Table 4.6.

Table 4.6. Some thermophysical properties of common adsorbates
(Source: Perry and Green 2008)

a

Adsorbate	**Chemical Formula**	**Normal Boiling Point (°C)**	**Normal Freezing Point**	**Molecular Weight**
Water	H_2O	100	0	18.01
Ammonia	NH_3	-34	-78	17.03
Methanol	CH_3OH	65	-97	32.04
Ethanol	C_2H_5OH	79	-114	46.07
R-134a	$C_2F_4H_2$	-26.3	-103.3	102.03
Diethyl ether	$C_4H_{10}O$	34.6	-116.3	74.12

b

Adsorbate	**Latent Heat of Vaporization (kJ/kg)**	**Density ρ (kg/m^3)**	**Specific Heat (kJ/kgK)**	**Thermal Conductivity (W/mK)**
Water	2258	958	4.186	0.609
Ammonia	1368	681	4.391	0.507
Methanol	1102	791	1.917	0.202
Ethanol	842	789	2.442	0.171
R-134a	215	4.25	-	-
Diethyl ether	-	558	1.611	-

Adsorbates with boiling point below -10 °C at 1 atm are positive pressure refrigerants, whereas the other ones are vacuum refrigerants. Ammonia is an example of positive pressure refrigerant. Methanol is normally used in association with activated carbons or activated carbon fibers. Water could be considered as a perfect refrigerant, except for its low saturation pressure and for the impossibility to produce temperatures below 0 °C. Water is normally employed in pair with silica gel or zeolite

(Wang et al. 2009). Ethanol is commonly employed with active carbon as the adsorbent, however after 2000s; it was also seen as paired off with silica gel, in literature. R-134a and diethyl ether are also newly studied fluids. They were used with active carbon, by Saha and Al-Ghouti (Saha et al. 2009; Al-Ghouti et al. 2010); however, R1-134a is a non-environmental friendly and diethyl ether is a corrosive fluid. Besides, for these two adsorbates, adsorption equilibrium properties were not reported yet.

The saturation pressure quantities for varying temperatures of these common adsorbates are used in the equilibrium determination relations. The saturation pressure equations and equation constants are given in Section 5.3.10 for the common adsorbates used in adsorption heat pumps.

4.4. Required Properties

The selection of appropriate adsorbent-adsorbate pair is vitally important for an adsorption heat pump system. Main requirements for an adsorbate are having high latent heat, non-corrosivity, non-toxicity and, good thermal and chemical stability within the working temperature and pressure ranges. On the other hand, adsorbents should have high adsorption capacity, high thermal conductivity and diffusivity, and also thermal stability.

After decision on adsorbent and adsorbates, the behavior of pair and interaction between them due to adsorption should be investigated. The adsorption and desorption temperatures and maximum adsorption capacity as well as evaporation and condensation temperatures, hysterisis upon thermal cycling, cyclic repeatability, heat of adsorption, diffusion rate of adsorbate in adsorbent particle and isotherm type should be the considering features for selection of a proper adsorbent-adsorbate pair (Gregg and Sing 1982).

In adsorption heat pumps, both the adsorption and desorption processes are used so that the process should be reversible to provide repetition of the same cycle. Therefore, the interaction between adsorbent and adsorbate must be a physical type adsorption. Silica gel-water, zeolite-water, active carbon-methanol, active carbon-ammonia and activated alumina-water are the common adsorbent-adsorbate pairs used in adsorption heat pump systems (Srivastava and Eames 1998).

4.5. Common Pairs used in Adsorption Heat Pumps

Gas adsorption systems normally do not only differ in their adsorption capacity, but also in their kinetic behavior, in example, spontaneity of uptake or release of gas upon increase or decrease of adsorptive gas pressure (Keller and Staudt 2005). The structures and properties of common adsorbents and adsorbates are presented in details in previous section. The investigation of affinity of adsorbent and adsorbate is an important issue due to its usage in an adsorption heat pump.

Table 4.7. Thermophysical properties of some common adsorbent-adsorbate pairs

Adsorbent – adsorbate	**Maximum adsorption capacity (kg/kg)**	**Average heat of adsorption (kJ/kg)**	**Adsorbent specific heat (kj/kg)**	**Energy density (kj/kg)**	**Temp. range (°C)**
Silica gel – water	0.37	2560	0.88	1000	30-150
Silica Gel – water	0.20	2500	1.045	600	20-130
Activated alumina – water	0.19	2480	1.00	660	30-250
Zeolite 4A – water	0.22	4400	1.05	1250	30-350
Zeolite 5A – water	0.22	4180	1.05	1200	30-350
Zeolite 10A – water	0.20	4000	-	897	50-250
Zeolite MgA – water	0.29	3400	1.06	800	60-250
Zeolite 13X – water	0.27	-	0.84	930	20-300
Zeolite 13X – water	0.27	3400	1.06	1200	30-350
Zeolite 13X – water	0.30	4400	0.92	1290	30-350
Zeolite 4A – methanol	0.16	2300	1.07	-	-
Zeolite 5A – methanol	0.17	2300	1.07	-	-
Zeolite 13X – methanol	0.20	2400	1.07	-	-
Activate carbon - methanol	0.32	1400	0.9	590	20-140

The most common pairs used in adsorption heat pumps are silica gel – water, zeolite – water, active carbon – methanol, active carbon – ammonia and active carbon – ethanol. The detailed information about these common pair behaviors will be given in this section. Some thermophysical properties for common adsorbent -adsorbate pairs used in solar adsorption heat pumps will be given in Table 4.7 (Gregg and Sing 1982; Ülkü and Mobedi 1989).

As an overview of Table 4.7, it could be seen that the maximum adsorption capacity among all pairs is achieved by active carbon-methanol pair. Zeolite-water pair has high heat of adsorption quantities. The working temperature range is small for silica gel-water pair due to structure of silica gel. The properties for the pair vary according to the type of adsorbent selected. Even the same type of an adsorbent may vary according to the manufacturer. As seen, silica gel-water and zeolite 13X-water pairs are presented with different thermophysical properties in the table. This is due to the change on structure of adsorbent in case they are produced by different manufacturers. Detailed information about pairs is given separately in further sections.

4.5.1. Silica Gel – Water

Since early 1980s, the work on silica gel – water systems have been popular and a lot of study was carried out. Silica gel-water is a low temperature working pair, which can be driven by about 75 °C heat source. For adsorption based air-conditioning systems the isotherm of silica gel is more advantageous, allowing one to operate the process in a wide rage of pressure ($0.1 < P/P_{sat} < 0.6$) with fairly large amounts of water vapor to be either adsorbed or desorbed upon pressure increase or decrease in this region (Keller and Staudt 2005). Silica gel-water refrigeration system is better to be applied in the air-conditioning with large circulation flow rate of chilled water, where a higher evaporating temperature can be used (Sumathy et al. 2003).

The average heat of adsorption for this pair is about 2500 kJ/kg and the desorption temperature is lower than other pairs. The maximum adsorption of water vapor onto pure silica gel is about 25% kg water/kg silica gel for atmospheric pressures.

As the disadvantage of the pair, it does not work at temperatures below 0 °C (Wang et al. 2009) and it can not be used in ice-making adsorption refrigerators.

4.5.2. Zeolite – Water

Zeolite – water pair is preferable for its high adsorption capacity. The average value of adsorption heat for zeolite – water pair is higher than that of silica gel – water pair, and is about 2700-4200kJ/kg. Natural zeolites with a heat of adsorption of 2800 kJ/kg were found to be more suitable for cooling systems than synthetic zeolites having a heat of adsorption of 4200kJ/kg (BenAmar et al. 1996). This is due to the fact that with lower heat of adsorption, the adsorbent bed can be cooled more effectively.

Zeolite is an adsorbent which is stable at high temperatures. Hence, zeolite – water pair can be used to recover heat at temperature above 200°C. At the same time, it is a disadvantage due to need of high temperature heating sources for desorption. The disadvantage of the pair is similar to the disadvantage of the silica gel – water pair and it can not work at evaporation temperatures below 0 °C. The pair should be used at vacuum conditions; therefore the systems constructed for using zeolite–water pair requires great attention to prevent leakage.

4.5.3. Active Carbon – Methanol

Active carbon – methanol pair is the most common pair used in solar adsorption applications because of its high cyclic adsorption capacity. The pair possesses a high vapor pressure in the adsorbent bed. A higher vapor pressure would result a larger overall heat transfer coefficient. As soon as the heat transfer coefficient increases, cycle time decreases. The desorption temperature of this pair is low. It leads a lower heat source for desorption process, so that the renewable energy sources are applicable. It has been reported in literature that maximum COP for the devices using activated carbon is achieved when it is paired off with methanol. Over 150°C, activated carbon would catalyze methanol to decompose into dimethyl ether, thus the working temperature range of active carbon-methanol pair is small.

Active carbon fiber – methanol pair has an adsorption capacity reaching up to 0.55 kg of methanol/kg of ACF. Disadvantages of active carbon-methanol systems are need of high vacuum in the system, the use of methanol which can act as a corrosive fluid through the system and active carbon has a very low thermal conductivity which is near to thermal conductivity of insulation materials (Sumathy et al. 2003).

4.5.4. Active Carbon – Ammonia

Active carbon – ammonia pair works at high pressure such as 1.6 MPa, unlike other pairs. Systems using this pair should be designed according to high pressures. Working at high pressure has an advantage as shortening the adsorption time due to increasing heat and mass transfer. The reported maximum adsorption capacity is around 0.4 kg ammonia/kg active carbon. This pair was not preferable previously, because of toxicity of ammonia and its irritant smell. Even at low concentrations, ammonia is a corrosive chemical. But recently, activated carbon – ammonia is a promising pair due to the high cooling capacity of ammonia, high heat and mass transfer performance and suitability for high temperature heat sources (Sumathy et al. 2003).

4.5.5 Active Carbon – Ethanol

The high adsorption capacity of the active carbon – ethanol pair makes it possible to use as the working pair in adsorption cooling systems. It has an adsorption capacity near to 45 % kg ethanol/kg active carbon for 40 °C temperature. Isosteric heat of adsorption for the pair is approximately 1100 kJ/kg. The desorption temperature is relatively higher than silica gel – water pair while it is considerably lower than zeolite – water pair. Active carbon-ethanol pair operates under low pressure like others except active carbon – ammonia pair. The working pressure range is between 0.01 and 40 kPa. The systems using this pair should also be designed for the low pressure operation conditions.

CHAPTER 5

EQUILIBRIUM EQUATIONS AND DIAGRAMS FOR ADSORBENT-ADSORBATE PAIRS

5.1. Adsorption Equilibria

The amount of vapor taken up by the adsorbent at specified temperature and pressure is described as adsorption equilibria. Equilibrium in adsorption process depends on the nature of the adsorbent like surface characteristic and pore structure, the nature of the adsorbate and the working temperature and the pressure ranges.

Adsorption equilibria between adsorbents and adsorbates can be estimated by various theoretical and empirical approaches. Experimental adsorption equilibria can be represented by equilibrium equations and plots.

The plot of amount adsorbed as a function of pressure at constant temperature represents the adsorption isotherm. The adsorbed amount is a function of pressure at constant temperature as it can be seen in Figure 5.1 (a),

$$q = f(P)_T \tag{5.1}$$

An isotherm is the most common plot type that is used to define the adsorption equilibrium. On the other hand, the plot of adsorbed amount as a function of temperature at constant pressure illustrates the adsorption isobar as in Figure 5.1 (b),

$$q = f(T)_P \tag{5.2}$$

Adsorption isoster is the plot of pressure as a function of temperature (see Fig. 5.1 (c)). When the adsorbed amount is constant, the pressure is a function of temperature,

$$P = f(T)_w \tag{5.3}$$

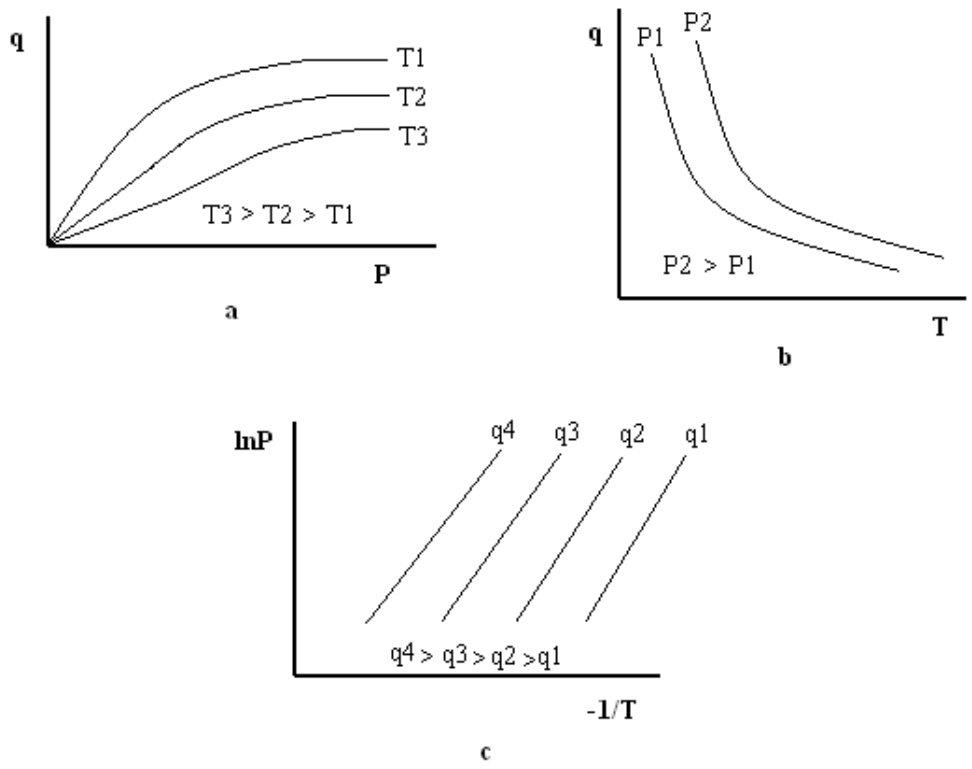

Figure 5.1. Graphical representation types of adsorption equilibrium
a) isotherm, b) isobar, c) isoster

5.2. Isotherm Types

The most common method of presenting equilibrium data is the adsorption isotherm plot. Although adsorption isotherms with various shapes have been reported in literature, there exist six basic types. The six IUPAC (International Union of Pure and Applied Chemistry) standard adsorption isotherms are shown in Figure 5.2. There exist five basic types which are defined by S. Brunauer, P. H. Emmett, E. Teller (BET), L. S. Deming and W. S. Deming (Suzuki 1990). Type VI isotherm is proposed further by S. W. Sing in 1982. It is a rarely encountered one which may also be named as the stepped isotherm (Gregg and Sing 1982). It occurs with layer by layer adsorption on a highly uniform surface.

Adsorption isotherm types, in principle, may yield valuable information about the surface area and pore structure of the adsorbent. Five basic isotherm types with their common properties will be explained in details in next sections.

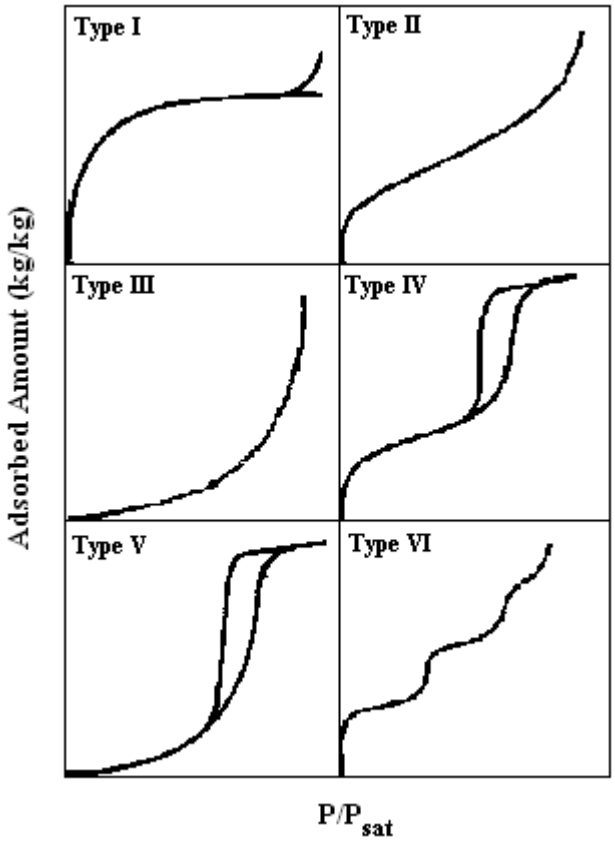

Figure 5.2. Schematic representation of IUPAC isotherm classifications

5.2.1. Type I Isotherm

The Type I isotherm structure is generally valid for adsorbents in which micropore structure is dominant through its pores. If an adsorbent contains micropore (pores with diameters smaller than 20 Å, as mentioned in Chapter 3), the potential fields from neighboring walls will overlap and the interaction energy of the solid with the gas molecule will be correspondingly enhanced. Thus, the interaction will be stronger enough to completely fill the pores at low relative pressure. As a result, the adsorbate concentration in an adsorbent particle with Type I isotherm increases rapidly at low relative pressures; however after a specified relative pressure the adsorbate concentration does not vary and becomes almost constant. The main reason for asymptotic behavior of adsorbate concentration at high relative pressure is that the adsorbent pores and adsorbate molecules have approximately the same sizes. The adsorbate concentration remains constant over a certain relative pressure value, since

the pores are so narrow that they cannot accommodate more than a single molecular layer on the walls, as seen from figure of Type Isotherm I (see Fig. 5.2).

Most common adsorbents which obey Type Isotherm I are molecular sieve zeolites, active carbon and a few types of silica gel. Type I isotherms exhibit no hysteresis generally. Hysterisis for a pair can be defined as following different isotherm paths for adsorption and desorption processes.

5.2.2. Type II Isotherm

Type II isotherm is a type of gas adsorption by non-porous adsorbents. The adsorbate is capable of filling the surface of adsorbent by a monolayer. The distribution of single molecules on the wall is defined as the monolayer adsorption.

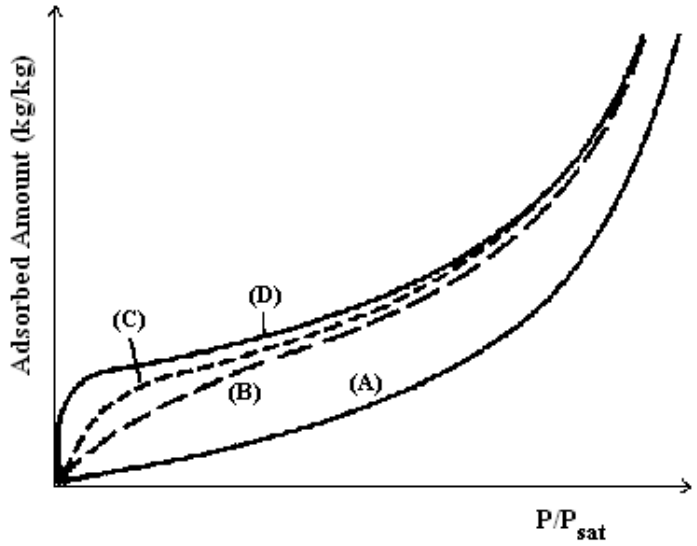

Figure 5.3. Type II isotherm (A: c=1, B: c=11, C: c=100, D: c=10000)

Type II isotherm has a knee shape at low relative pressures and a plateau in the middle and rise again at high relative pressures. The shape of the knee depends on the value of c, which can be defined as the following equation:

$$c = e^{\frac{\Delta H}{RT}} \tag{5.4}$$

Here; ΔH, R and T denote the net heat of adsorption, gas constant and temperature, respectively. It can be seen from Figure 5.3 that as c is increasing knee shape is becoming sharper (Gregg and Sing 1982).

5.2.3. Type III and V Isotherms

Figure 5.4 depicts type III and type V isotherms. These isotherms do not exhibit knee shape on the curve like other isotherms. This is an indicative of weak adsorbent-adsorbate interactions. Both are characterized by convexity towards y-axis. Type III isotherm keeps the convexity until the high relative pressures, while type V isotherm has an inflection point at very high values. After bending over, the adsorbed amount remains nearly constant; however there may be a final upward sweep which is attributable to adsorption in macropores.

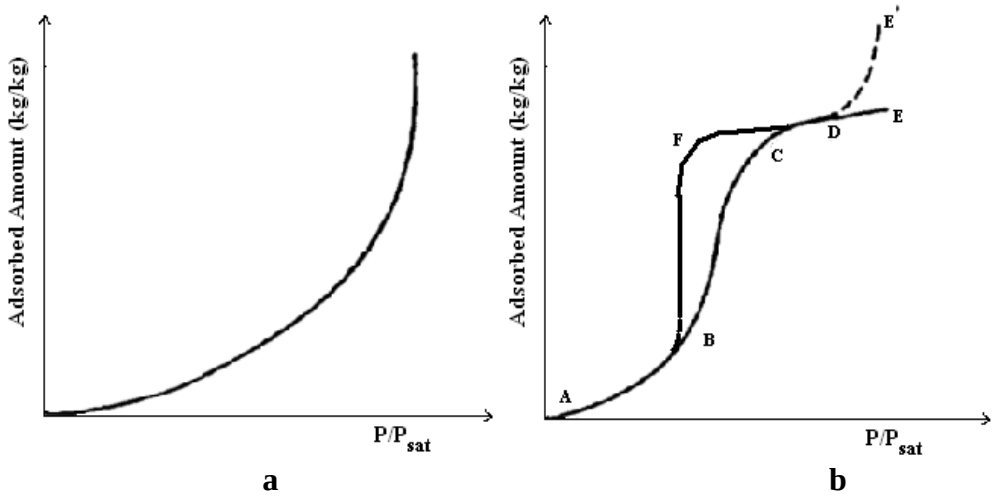

Figure 5.4. Type III (a) and Type V (b) isotherms

For both isotherms, the weak interaction between the adsorbent and adsorbate will cause small uptake at low relative pressures. But once an adsorbate molecule is adsorbed, the forces between adsorbate molecules will cause more adsorption of further molecules. A multilayer adsorption is expected in adsorbent-adsorbate pair with Type III and V isotherms. This increase leads to the convexity of the isotherm. Type III isotherm may be given by non-porous or macroporous adsorbents and Type V isotherm is given by mesoporous or macroporous adsorbents. These isotherms may

also originate through the adsorption of polar adsorbate molecules. Since water has a polar structure, it may give such type of isotherm as an adsorbate with having weak interaction between adsorbent. As seen in Figure 5.4.b, Type V isotherm features a hysteresis loop generated by the capillary condensation of the adsorbate in the mesopores of the solid. Hysteresis loop is generated when desorption behavior of the pair is different than the behavior of adsorption. The lower branch (ABC) represents the adsorption, while the upper branch (AFC) represents the desorption process of the pair.

5.2.4. Type IV Isotherm

Type IV isotherm also features a hysteresis loop. The lower branch represents the adsorption, while the upper branch represents the desorption process of the pair.

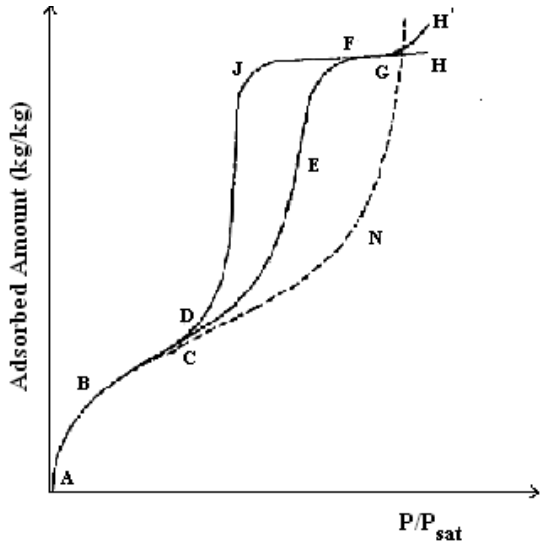

Figure 5.5. Type IV isotherm

In Figure 5.5, both type IV and type II isotherms are plotted, in order to compare these two isotherms. Points ABCNG is the plot of Type II. Points ABDEG shows the adsorption process of the pair, while points ABDJF shows the desorption process of the pair for type IV. Type IV isotherm plot may show a variation at very high relative pressures for different pairs, such points H and H'.

5.3. Adsorption Equilibrium Equations

Adsorption quantity which depends on pressure and temperature may also be defined by equations as mentioned before. There are several models defined to fit experimental data and utilize the behavior of the adsorption pair in literature. The most common equilibrium equations are Freundlich, Dubinin-Astakhov, Langmuir, Henry's and Toth's relations. The proposed relation defines the behavior of the adsorption pair. The coefficients of the equations are estimated according to the experimental studies of the related pairs. In this section, the most common equations and their coefficients which are estimated in literature by the experimental studies will be given. As will be seen, the equations content various coefficients which are different not only for different working pairs, but also for the same working pair having different brand and type of the adsorbent.

5.3.1. Freundlich Equation

Considering the literature studies on pairs used in adsorption heat pumps, Freundlich equation is the most common equation used for silica gel – water pair. The relation is as follows:

$$q^*=k\left(\frac{P}{P_{sat}}\right)^{\frac{1}{n}} \tag{5.5}$$

Here q* denotes the equilibrium adsorbed amount, P is pressure and P_{sat} is the saturation pressure at a specific temperature in kPa, k and n are dimensionless equation constants. Table 5.1 includes the coefficients of Freundlich equation for pairs with different types of silica gel used in adsorption heat pumps.

The different coefficients for Freundlich equations which are experimentally estimated in literature are plotted on the same diagram. Figure 5.6 shows the Freundlich plots of different silica gel – water pairs. Three silica gel – water pairs (silica gel (Xia et al. 2008) –water type A silica gel – water, type RD silica gel – water) show Type I isotherm, while the silica gel – water pair studied by Afonso and Silveira (Afonso and Silveira 2005) shows Type III isotherm. That means, silica gel studied by

Xia et al., type A silica and type RD silica gels are adsorbents with dominant micropore structure. The other silica gel probably has a non-porous structure and it is capable of filling its pores by monolayer.

Table 5.1. Coefficients for Freundlich equation

Pair	Adsorbent Type	Temp. Range (°C)	Pressure Range (kPa)	k	n
Silica gel - water	- (08Xia et al. 2008)	25-90	0.3-20	0.444	1.346
Silica gel - water	- (05Afonso and Silveira 2005)	-	-	0.355	0.79
Silica gel - water	Type A, RD (06Liu and Leong 2006; 06Liu and Leong 2006; 09Saha et al. 2009)	-	-	0.346	1.6
Silica gel - water	Type RD (09Saha et al. 2009)	-	-	0.552	1.6

Type RD silica gel – water pair gives has the highest adsorption capacity. At P/Psat = 0.6 type A silica gel has an equilibrium adsorbed amount such as 0.2, the pair studied by Xia et al. has an equilibrium adsorbed amount such as 0.3; while type RD silica gel has a capacity which is almost 0.6.

Table 5.2. Coefficients for modified Freundlich equation

$\mathbf{A_0}$	-14.2904	$\mathbf{B_0}$	36.1487
$\mathbf{A_1}$	0.1546	$\mathbf{B_1}$	-0.382
$\mathbf{A_2}$	-0.00055498	$\mathbf{B_2}$	0.0013016
$\mathbf{A_3}$	0.000000675	$\mathbf{B_3}$	-0.000001415

The modified Freundlich equation may also be used for adsorption heat pump systems, especially for silica gel – water pair. The equation is given below as 5.5.

$$q^* = A(T)\left[\frac{P}{P_{sat}}\right]^{B(T_{sat})} \tag{5.5}$$

$$A(T_s) = A_0 + A_1 T + A_2 T^2 + A_3 T^3 \tag{5.6}$$

$$B(T_s) = B_0 + B_1 T + B_2 T^2 + B_3 T^3 \tag{5.7}$$

Where, A_0 to A_3 and B_0 to B_3 are coefficients of $A(T_s)$ and $B(T_s)$ equations respectively, which are functions of saturation temperature. P is pressure and P_{sat} is the saturation pressure at specified temperature in Pa; T is temperature in K. Table 5.2 includes the coefficients of modified Freundlich equation for silica gel – water pair (silica gel type is not mentioned) which are distinguished by the experimental study of Xia et al. (Xia et al. 2008).

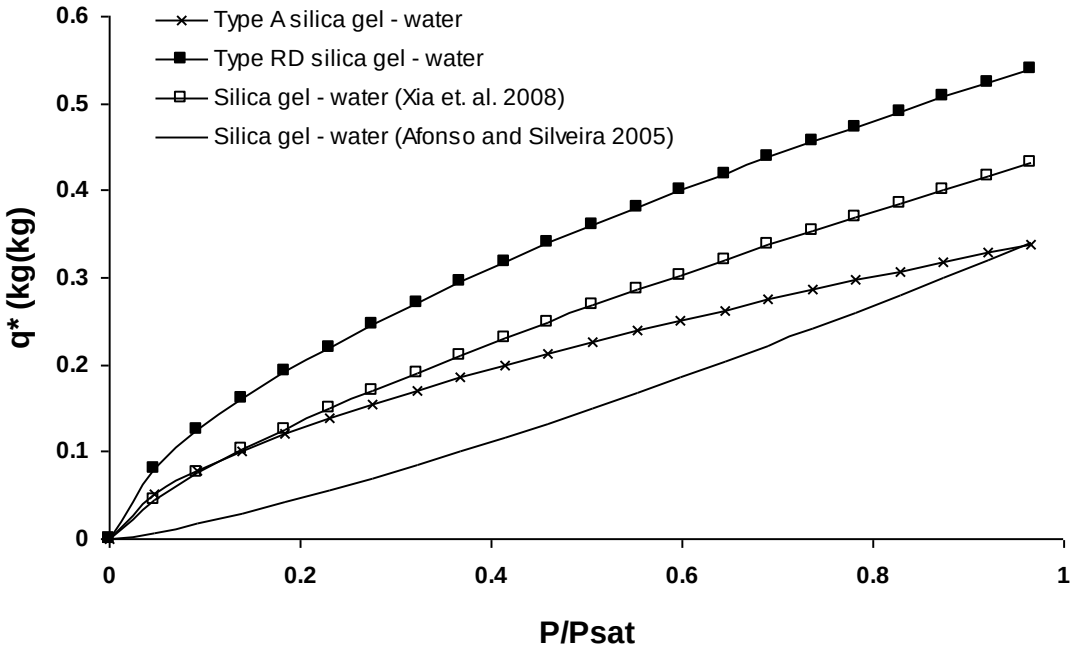

Figure 5.6. Graphical presentation of isotherms for different pairs at 30 °C, based on Freundlich equation

5.3.2. Dubinin – Astakhov Equation

Dubinin – Astakhov (DA) equation is commonly used in adsorption processes occurring in micropores of the adsorbent (Wang et al. 2009). Equation is given as;

$$q^* = q_0 \exp\left[-D\left(T\ln\frac{P_{sat}}{P}\right)^n\right] \tag{5.8}$$

where, q* denotes the equilibrium adsorbed amount, P is pressure and P_{sat} is the saturation pressure at T in kPa; q_0, D and n are dimensionless equation coefficients.

Table 5.3 gives the coefficients for Dubinin-Astakhov equation for different pairs used in adsorption heat pumps.

Table 5.3. Coefficients for Dubinin – Astakhov equation

Pair	Adsorbent Type	q_0	D	n
Silica gel - water	- (Afonso and Silveira 2005)	0.301	0.0226	1.08
Silica gel - water	S0 (Daou et al. 2008)	0.35	0.000006	1.7
Silica gel - water	S40 (Daou et al. 2008)	0.68	0.0000156	1.65
Silica gel - water	- (Xia et al. 2008)	0.348	0.449	1.609
Active carbon - methanol	AC 35 (Boubakri 1985)	0.407	0.000000322	2.195
Active carbon - ethanol	ACF A-20 (El-Sharkawy et al. 2006)	0.797	0.000001716	2
Active carbon – ethanol	ACF A-15 (El-Sharkawy et al. 2006)	0.570	0.000001067	2
Active carbon - ammonia	AX21 (BenAmar et al. 1996)	0.549	0.000001617	2

Three different types of silica gels with water as an adsorbate, and two different types of active carbons with ammonia and methanol as adsorbates were experimentally studied and found to be fitting DA equation, in literature. Here, these pairs were plotted and illustrated in Figure 5.8. As seen in the figure, the silica gel water pair, which is also plotted with Freundlich equation and commented on, is similar with Type III isotherm with Dubinin – Astakhov equation. That means this pair can be defined by both equations and it is resulted as the pair has Type III isotherm behavior. The adsorbed amount in silica gel begins to increase at very high relative pressure such as P/P_{sat} = 0.8. The other four pairs are similar to Type I isotherm which means that the adsorbent pores are mostly in micro dimensions. The highest adsorption capacity for these for pairs is belong to the S40 type silica gel – water pair which may reach up to 70 % adsorption at high relative pressures. They all show an asymptotic behavior. The adsorbed amount of type S0 silica gel – water and AC35 active carbon – methanol pairs remains nearly constant right after P/Psat = 0.3; while the increase in adsorbed amount of AX21 active carbon – ammonia and S40 silica gel – water pair is carried on up to P/P_{sat} = 0.8.

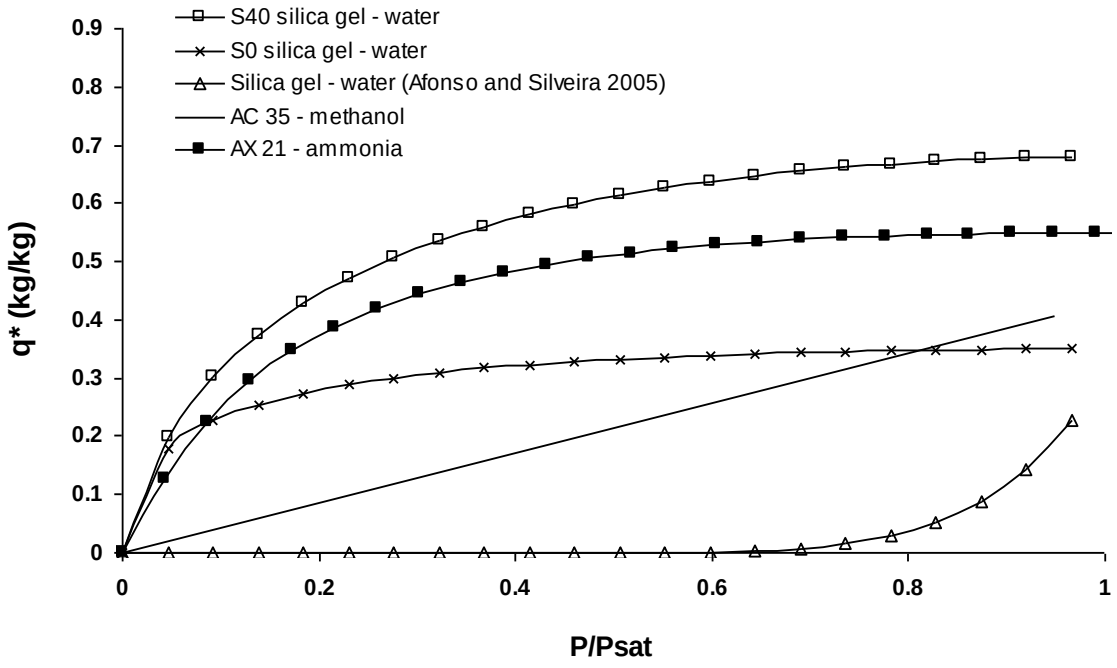

Figure 5.7. Graphical presentation of isotherms for different pairs at 30 °C, based on Dubinin -Astakhov equation

A modified type of Dubinin-Astakhov equation was defined to be fitted for active carbon – ethanol pair as:

$$q^* = q_0 \exp\left[-\left(\frac{RT\ln\frac{P_{sat}}{P}}{E}\right)^n\right] \tag{5.9}$$

The equation coefficients which are presented in literature are given in Table 5.4 for two different pairs.

Table 5.4. Coefficients for modified Dubinin – Astakhov equation

Pair	Adsorbent Type	q_0	E	n
Active carbon – R134a	- (Saha et al. 2009)	0.00164 (m^3/kg)	8460 (J/mol)	1.3
Active carbon – ethanol	Active carbon powder (Makimoto et al. 2011)	1.17 (kg/kg)	5184 (J/mol)	2.15

5.3.3. Dubinin - Radushkevich Equation

Dubinin – Astakhov equation is the modified form of Dubinin – Radushkevich equation and this equation is as follows:

$$q^{*}=q_{0}\exp\left[-k\left(\frac{T}{T_{sat}}-1\right)^{n}\right] \tag{5.10}$$

In the relation, q* denotes the equilibrium adsorbed amount, T is temperature and T_{sat} is the saturation temperature in K; q_0, k and n are dimensionless constants. Table 5.5 includes the coefficients of Dubinin-Radushkevich equation for active carbon – ammonia pair used in adsorption heat pumps (BenAmar et al. 1996).

Table 5.5. Coefficients for Dubinin – Radushkevich equation

Pair	**Adsorbent Type**	**Temp. Range (°C)**	**Press. Range (kPa)**	**q_0**	**k**	**n**
Active carbon – ammonia	- (Chahbani et al. 2004)	-	-	0.270	4.3772	1.1935
Active carbon – ammonia	LM128 (Tamainot-Telto et al. 2009)	-	-	0.333	3.696	0.99
Active carbon – ammonia	LM127 (Tamainot-Telto et al. 2009)	-	-	0.362	3.657	0.94
Zeolite – water	ROTA Natural zeolite	40-150	0.87-7.38	0.122	5.052	1.4

5.3.4. Langmuir Equation

Langmuir equation is a conventional relation for determination of pair adsorption. The equation is as following for Langmuir approach:

$$q_{langmuir}=\frac{C_{\infty}q_{m}b}{bC_{\infty}+1} \tag{5.11}$$

Where, C_{∞} can be calculated with the ideal gas relation at equilibrium pressure. The b is Langmuir constant and q_m is monolayer coverage. The monolayer coverage

and Langmuir constant can be found by plotting $C_\infty/q_{langmuir}$ versus C_∞ graph. Demir (Demir 2008) found Langmuir constant and monolayer coverage for silica gel – water pair by the result of his experimental study as 42.97 and 5.675, respectively.

5.3.5. Three-term Langmuir Equation

Three-term Langmuir equation (eqn. 4.10) is used to define the isotherm of zeolite NaX and 13X – water pairs, commonly. By substituting the equations 5.13 to 5.16 into equation 5.12 the isotherm is distinguished for different temperatures.

$$q^*=\frac{q_{s1}b_1P}{1+b_1P}+\frac{q_{s2}b_2P}{1+b_2P}+\frac{q_{s3}b_3P}{1+b_3P} \tag{5.12}$$

$$q_{s1}=\sum_{i=0}^{3}\frac{a_i}{T^i} \tag{5.13}$$

$$q_{s2}=\sum_{i=0}^{3}\frac{c_i}{T^i} \tag{5.14}$$

$$q_{s3}=0.276-(q_{s1}+q_{si}) \tag{5.15}$$

$$b_i=b_{0i}\exp\left(\frac{E_i}{T}\right)(i=1,2,3) \tag{5.16}$$

Here, q* denotes equilibrium adsorbed amount; P is pressure in Pa; T is temperature in K; q, a, b, c and E's are dimensionless coefficients of related equations. The coefficient values for zeolite NaX – water and zeolite 13X – water pairs are given in Table 5.6 (BenAmar et al. 1996; Makni et al. 2011).

Table 5.6. Coefficients for three-term Langmuir equation

	13X – water	**NaX – water**		**13X – water**	**NaX – water**
$\mathbf{a_0}$	0.152	0.07	$\mathbf{c_0}$	-0.896	-0.687
$\mathbf{a_1}$	-155.36	-119.9	$\mathbf{c_1}$	843.85	-775.7
$\mathbf{a_2}$	63700	63690	$\mathbf{c_2}$	-254000	-254200
$\mathbf{a_3}$	-8450000	-8450000	$\mathbf{c_3}$	27800000	27750000
$\mathbf{b_{01}}$	1.508E-10	1.508E-10	$\mathbf{E_1}$	7726.58	7726.58
$\mathbf{b_{02}}$	5.417E-10	5.417E-10	$\mathbf{E_2}$	6074.71	6074.71
$\mathbf{b_{03}}$	1.707E-10	1.707E-10	$\mathbf{E_3}$	5392.17	5392.17

5.3.6. Henry's Equation

Henry's equation is commonly used in the analysis of adsorption heat pump for the silica gel – water pair. The equation is a function of temperature and pressure and it distinguishes from others with including the isosteric heat of adsorption quantity as a variable. The equation is given as;

$$q^* = K_0 \exp\left[\Delta H_{ads}/(RT)\right]P \tag{5.17}$$

Here, q* denotes equilibrium adsorbed amount in kg/kg; P is pressure in Pa; T is temperature in K; R is gas constant in kJ/kgK; ΔH_{ads} is isosteric heat of adsorption in kJ/kg; K_0 is a constant in Pa^{-1}. Coefficients of Henry's equation for three types of silica gel when it is paired with water are given in Table 5.7. Furthermore the isotherm plots for these constants are given in Figure 5.8 (Ng et al. 2001).

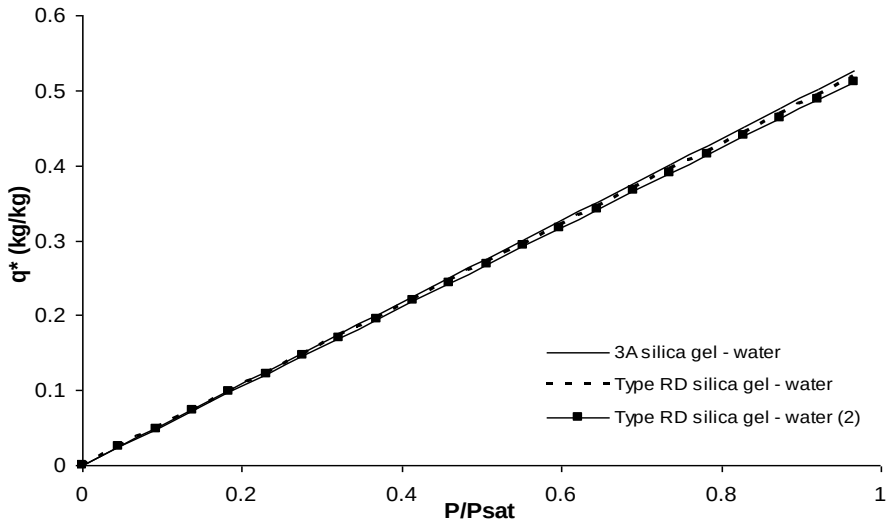

Figure 5.8. Graphical presentation of isotherms for different pairs at 30 °C, based on Henry's equation

Table 5.7. Coefficients for Henry's equation

Pair	Temp. Range (°C)	Pressure Range (kPa)	Adsorbent Type	K_0 (Pa^{-1})	ΔH (kJ/kg)
Silica gel - water	30-60	0.5-6.5	Type 3A	5.2E-12	2380
Silica gel - water	30-60	0.5-6.5	Type RD	5.5E-12	2370
Silica gel - water	30-60	0.5-6.5	Type RD (2)	2E-12	2510

5.3.7. Toth's Equation

Toth's equation is a rarely encountered equation and it is derived from Henry's equation. It is also related with the isosteric heat of adsorption of pair. The equation is given below;

$$q^* = \frac{K_0 \exp(\Delta H_{ads}/RT)P}{\left\{1+\left[K_0/q_m \exp(\Delta H_{ads}/RT)P\right]^t\right\}^{1/t}} \tag{5.18}$$

q*, again, denotes equilibrium adsorbed amount in kg/kg; q_m denotes the monolayer coverage (kg/kg); P is pressure in Pa; T is temperature in K; R is gas constant in kJ/kgK; ΔH_{ads} is isosteric heat of adsorption in kJ/kg; K_0 is a constant in Pa^{-1}; t is dimensionless Toth's constant. Coefficients of Toth's equation for two types of silica gel when it is paired with water are given in Table 5.8. The isotherm plots for these constants are given in Figure 5.9 (Chua et al. 2002).

Table 5.8. Coefficients for Toth's equation

Pair	Adsorbent Type	Temp. Range (°C)	Pressure Range (kPa)	K_0 (Pa^{-1})	ΔH (kJ/kg)	q_m	t
Silica gel - water	Type A	25-65	0.5-7	4.65E-10	2710	0.40	10
Silica gel - water	Type RD	25-65	0.5-7	7.3E-10	2693	0.45	12

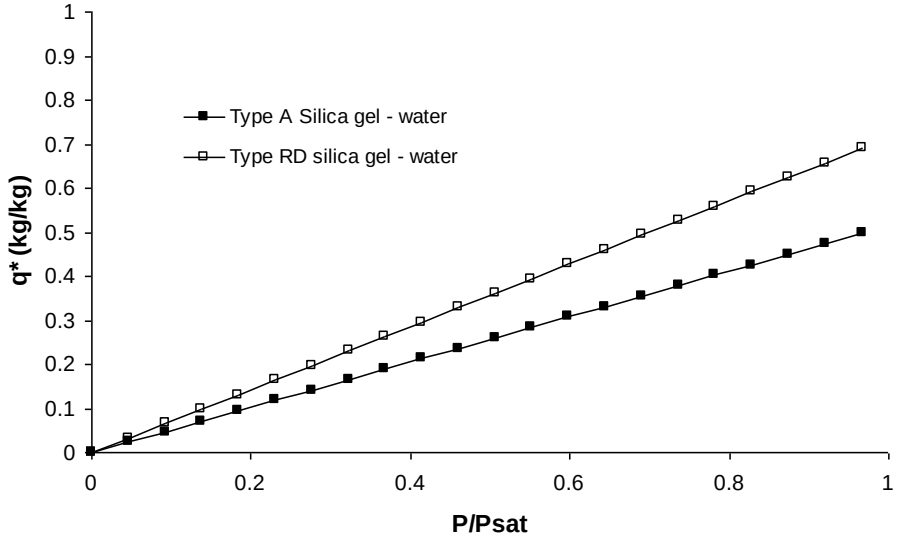

Figure 5.9. Graphical presentation of isotherms for different pairs at 30 °C, based on Toth's equation

5.3.8. Isoster Equation

Isoster equation is applicable for specified pairs with constants given in Table 5.9 (San and Lin 2008; Ülkü 1986; Ülkü et al. 1986). Isotherm plots for isoster equation using these constants are given in Figure 5.10. The equation series are given as;

$$lnP = a(q) + [b(q)/T] \quad (5.19)$$

$$a(q) = a_0 + a_1 q + a_2 q^2 + a_3 q^3 + a_4 q^4 \quad (5.20)$$

$$b(q) = b_0 + b_1 q + b_2 q^2 + b_3 q + {}^3 b_4 q^4 \quad (5.21)$$

where, P is pressure in mbar; T is temperature in K; a and b are functions of q; and P is function of a, b and T.

Table 5.9. Coefficients for isoster equation

Pair	**Adsorbent Type**	**a_0**	**a_1**	**a_2**	**a_3**	**a_4**
Zeolite - water	13X	13.4244	110.854	-731.76	1644.8	0
Zeolite – water	natural zeolite	73.25	-2772	55890	-472600	1437000
Active carbon - methanol	-	20.3305	6.53035	-16.6841	52.3793	0
Pair	**Adsorbent Type**	**b_0**	**b_1**	**b_2**	**b_3**	**b_4**
Zeolite – water	13X	-7373.78	6722.92	5624.47	-3486.7	0
Zeolite - water	natural zeolite	-30860	1277000	24680000	206800000	627900000
Active carbon – methanol	-	-6003.58	6315.16	-26058.7	40537.9	0

4.3.9. Empirical Equation

In literature, an empirical equation is defined (San and Lin 2008) for silica gel – water pair which is;

$$P/P_{sat} = (2.112q)^{[1+0.2843\exp(-10.28q)]}\, x\,(29.91P_{sat})^{[0.2843\exp(-10.28q)]} \quad (5.22)$$

Here, q denotes the adsorbed amount in kg/kg while P is specified pressure and P_{sat} is saturation pressure at specified temperature in atm. This equation is followed by another empirical saturation pressure equation which will be given in Section 5.3.10.

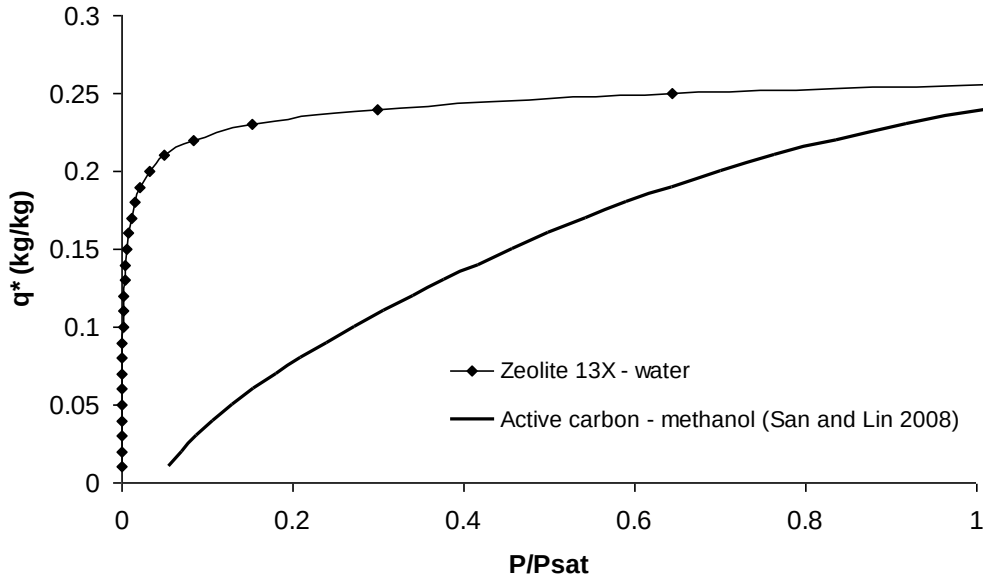

Figure 5.10. Graphical presentation of isotherms for different pairs at 40 °C, based on isoster equation

5.3.10. Mathematical Relations for Determination of Saturation Pressure

The isothermal and isosteric relations for adsorbent – adsorbate pairs used in adsorption heat pumps are given in previous sections. In order to apply the equations, primarily, the saturation pressure and temperature values should be calculated. The saturation pressure as a function of temperature can be found with the Antoine equation relation which is;

$$\ln P_{sat} = A - \frac{B}{T_{sat} + C} \tag{5.23}$$

Here, P_{sat} is the saturation pressure in mmHg; T is temperature in K; A, B and C are component-specific constants. Table 5.10 includes the Antoine constants of water and ethanol (Yang et al. 2006).

Table 5.10. Constants of Antoine equation for three different adsorbates

Adsorbate	A	B	C
Water	18.3036	3816.44	-46.13
Ethanol	18.9119	3803.98	-41.68

A simplified form of Antoine equation may be given as;

$$\ln P_{sat} = a - \frac{b}{T_{sat}} \tag{5.24}$$

Here, P_{sat} is the saturation pressure in Pa; T is temperature in K; a and b are component-specific constants. Table 5.11 includes the constants of common adsorbates used in adsorption heat pumps (Liu and Leong 2006; San and Lin 2008).

Table 5.11. Constants for simplified Antoine equation for three different adsorbates

Adsorbate	a	b
Water	25.1948	5098.26
Methanol	20.8400	4696.00
Ammonia	23.0300	2748.39

An empirical saturation pressure equation and a corresponding equation for silica gel – water pair is defined in literature (San and Lin 2008). The equations are;

$$\ln\left(\frac{P_{sat}}{218.167}\right) = -\frac{z_0}{T}\left(\frac{a_0 + a_1 z_0 + a_2 z_0^{\,3}}{1 + a_3 z_0}\right) \tag{5.24}$$

$$z_0 = 647.27 - T \tag{5.25}$$

Where, P_{sat} is the saturation pressure in Pa; T is temperature in K; z_0 is the function of T; a_1, a_2, and a_3 are equation constants. This saturation relation is only applicable for the empirical equation given (5.22) which is an equilibrium equation for silica gel – water pair.

5.4. Heat of Adsorption

Adsorption is a spontaneous process with loss in the freedom of the adsorbate molecules, resulting a decrease in the free energy and in the entropy of the system and

as a result, it is an exothermic process and while adsorption is going on, heat, called as heat of adsorption, is evolved.

The heat of adsorption indicates the strength of the forces binding adsorbed molecules to the surface of the adsorbent. It depends on temperature, pressure and surface coverage. Heat of adsorption may be defined in three ways.

- Differential Heat of Adsorption (change in integral heat of adsorption with change in loading),
- Integral Heat of Adsorption (total heat released from initial state to final state of adsorbate loading, at constant temperature),
- Isosteric Heat of Adsorption (defined by using adsorption isosters and Clausius-Clapeyron relationship) are three terms which are often used in adsorption.

In physical adsorption, heat of adsorption depends on to the change of the state from adsorptive to adsorbate. The differential molar enthalpy of adsorption can be expressed by differential of enthalpy of adsorptive and adsorbate. The differential heat of adsorption is:

$$\Delta_a h = -\frac{\partial Q}{\partial n_a} + V\frac{\partial P}{\partial n_a} \tag{5.26}$$

Where, $\Delta_a h$ is differential enthalpy in adsorbed phase in J/mol, Q is heat transferred in W/kg_s, n_a is amount of adsorbate, mol/kg_s, V is the volume of the system in m^3, and P is pressure in kPa.

The integral heat of adsorption is obtained by integrating the differential heat of adsorption against amount of adsorbate.

$$\Delta_a H = \int_0^{n_a} \Delta_a h dn_a \tag{5.27}$$

where, $\Delta_a H$ is the integral enthalpy of adsorbed phase in J/kg_g.

The integral heat of adsorption can be calculated by the means of Clausius-Clapeyron relationship at a constant adsorbate loading:

$$\frac{d(\ln P)}{d(-1/T)} = -\frac{\Delta H}{R} \tag{5.28}$$

The difference between differential heat of adsorption and isosteric heat of adsorption is so small, indeed. Thus, these two concepts can be considered as identical.

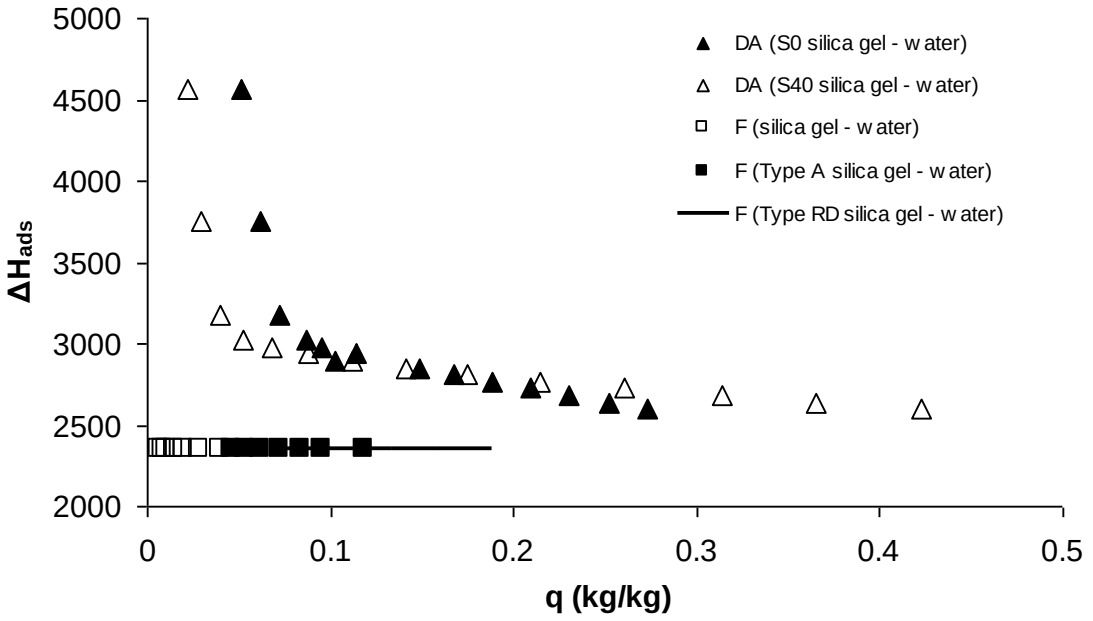

Figure 5.11. Heat of adsorption change with varying adsorbed amount

A numerical study on the change of heat of adsorption with varying adsorbed amount was performed for five different silica gel - water pairs. The calculations are performed according to the Dubinin-Astakhov (DA) and Freundlich (F) equations by using FORTAN software. Figure 5.11 represents the resultant plot for heat of adsorption variation with the change of adsorbed amount (q). The heat of adsorption for three pairs fitting Freundlich equation was found to be constant at 2354 kJ/kg, for all values of q. However, the pairs fitting Dubinin-Astakhov equation had a decrease with increasing adsorption amount. S0 silica gel - water pair has higher heat of adsorption values for the adsorbed amounts lower than 0.1; while S40 silica gel - water pair has higher heat of adsorption values for the adsorbed amounts higher than 0.2.

CHAPTER 6

EFFECTS OF EQUILIBRIUM ON THE PERFORMANCE OF ADSORPTION HEAT PUMPS

The pair used in an adsorption heat pump affects the thermal performance of adsorption air-conditioning device; since the equilibrium behavior of the pair depends on the interaction between the adsorbent and adsorbate. In this chapter, the performed numerical study on the effect of pair on the thermal performance of adsorption chiller is presented.

The processes which occur in an adsorbent bed of an adsorption chiller are isobaric adsorption, isosteric heating, isobaric desorption and isosteric cooling as mentioned before. The heat transfer relations between adsorbent bed and surrounding during processes were presented in Chapter 3. The additional relations are evaporator and condenser capacities and they can be calculated by the following equations;

$$Q_{ev} = m_s (w_{\max} - w_{\min}) \Delta h_{fg(ev)} \tag{6.1}$$

$$Q_{cond} = m_s (w_{\max} - w_{\min}) \Delta h_{fg(cond)} \tag{6.2}$$

6.1. Numerical Study on Effect of Equilibrium on the Performance

A numerical study was performed to investigate the thermal performance change of an adsorption chiller depending on two parameters as the employed pair and the cooling type of adsorbent bed and condenser.

Since the main advantage of using adsorption air-conditioning systems are the possibility of using renewable heat sources such as solar, geothermal and waste heat; the adsorption chillers were designed to be heated with solar energy, in this numerical study.

The temperature of the high temperature heat source should be higher than the maximum bed temperature (i.e. point c, see Fig. 3.5). For example, if the maximum

attainable temperature of a flat plate solar collector was around 90 °C, the maximum temperature of adsorbent bed (T_c) could be nearly 85 °C (Yıldırım et al. 2011).

The minimum adsorbent bed temperature depends on the type of low temperature heat source. The bed and condenser in the chiller might be cooled with air, cooling tower or low temperature heat source reservoir. For example, if the average summer temperature is assumed as 35 °C for Izmir, the minimum temperature of adsorbent bed can be nearly 45 °C; for an air cooled chiller. If the adsorbent bed was cooled with a cooling tower, the minimum bed temperature would be around 35 °C; while it would be around 30 °C in case of cooling with a lower temperature heat source (i.e. with a temperature of 25 °C) such as a river (Yıldırım et al. 2011).

The designed condenser should be cooled by the similar options. The minimum condenser temperatures would be 40, 35 or 30 °C similar to the adsorbent bed. The condenser temperature is important since the high level pressure of cycle depends on this temperature.

Evaporation temperature was another parameter that should be considered for the design of the adsorption chiller. It was assumed that, the water enters to the evaporator heating coil at 12 °C and leaves at 8 °C. Therefore, the evaporation temperature might be around 3 °C.

In this study, the performance analysis was performed for three different adsorption chillers as mentioned below. The COPs and cooling capacities for different pairs were evaluated for summer conditions in İzmir.

In Chiller 1, the adsorbent bed and the condenser were assumed to be cooled with air. Thus, the minimum adsorbent bed temperature and condenser temperature were assumed as 40 °C. Since the high level cycle pressure depends on the condenser temperature, the high level pressure of the cycle obtained for Chiller 1 is 7.37 kPa. In Chiller 2, adsorbent bed and condenser were assumed to be cooled with a cooling tower. Thus, the minimum bed and condenser temperatures that could be achieved are around 35 °C. The adsorbate (water) has a 5.81 kPa saturation pressure as a high level cycle pressure. In Chiller 3, the adsorbent bed and the condenser were cooled with a low temperature heat source such as a river which is around 25 °C temperature, thus the minimum temperature of adsorbent bed and condenser are 30 °C. Therefore the high level cycle pressure is 4.24 kPa. These three adsorption chillers are illustrated schematically in Figure 6.1.

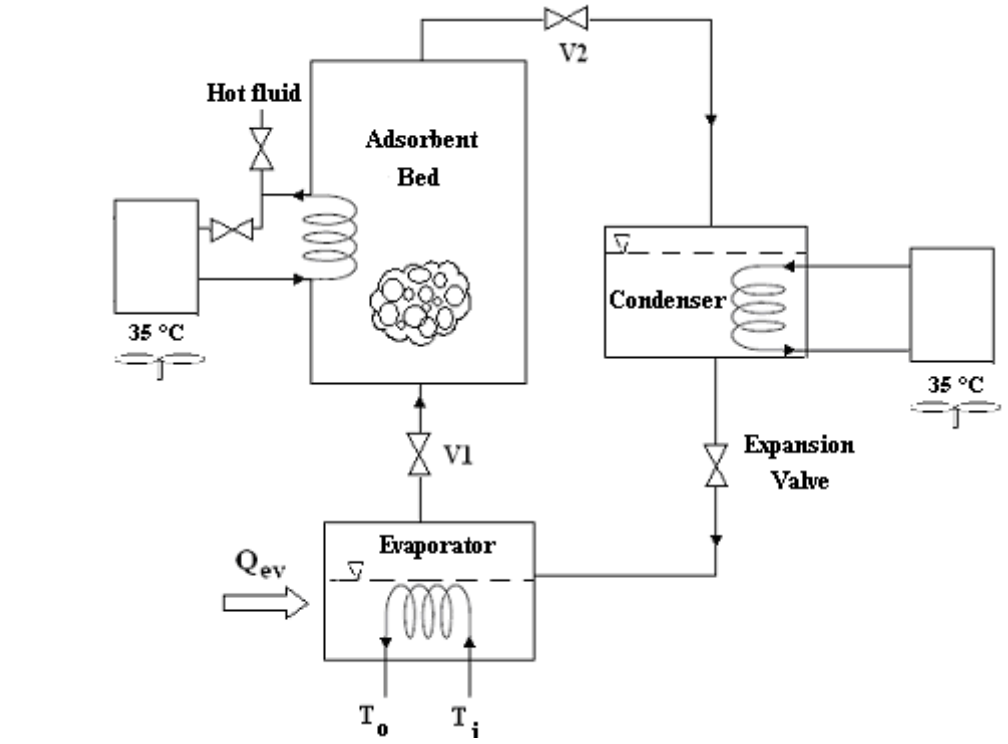
V2
Hot fluid
Adsorbent
Bed
35 °C
Condenser
35 °C
V1
Expansion
Valve
Evaporator
Q_{ev}
T_o
T_i

a

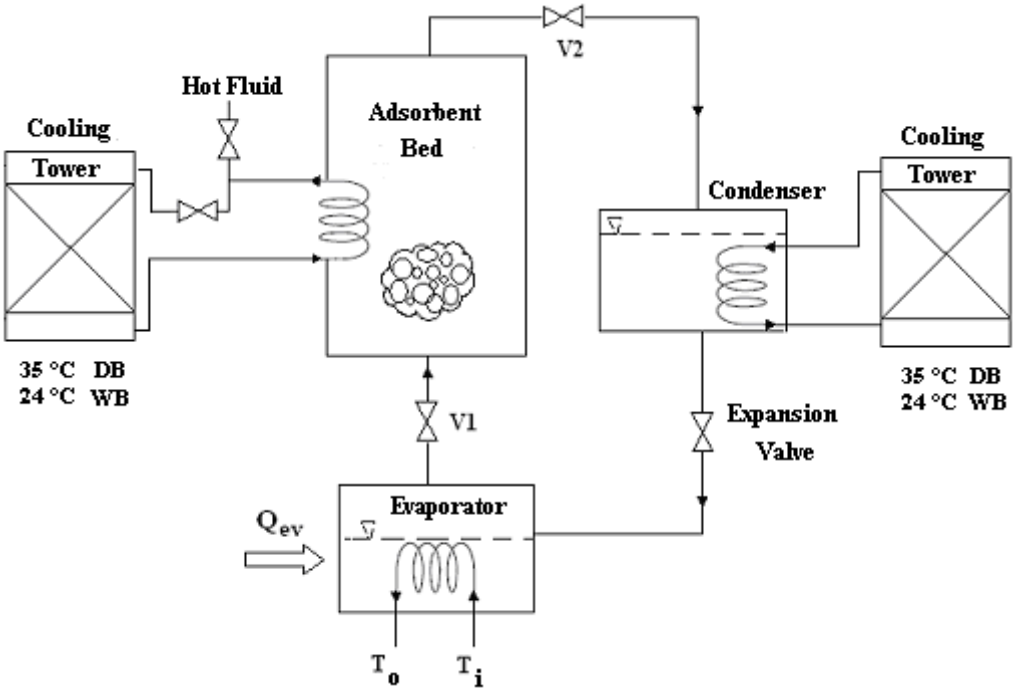
V2
Hot Fluid
Cooling
Tower
Adsorbent
Bed
Cooling
Tower
Condenser
35 °C DB
24 °C WB
35 °C DB
24 °C WB
V1
Expansion
Valve
Evaporator
Q_{ev}
T_o
T_i

b

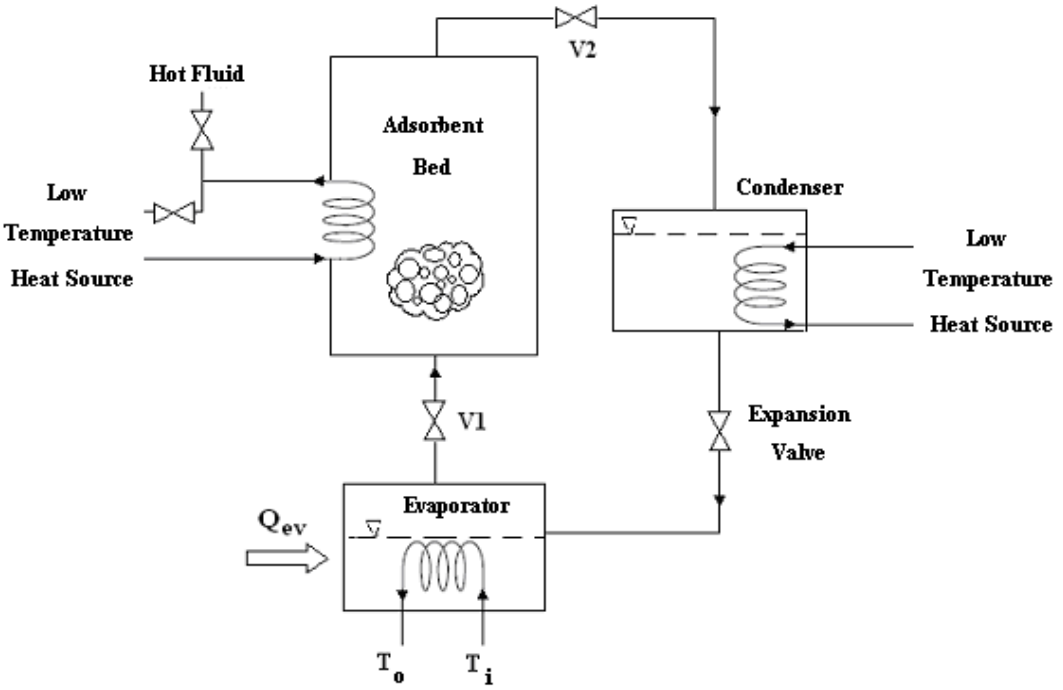

Figure 6.1. Schematical view of designed chillers cooled with air (a), cooling tower (b) and low temperature heat source (c)

The evaporation temperature is another parameter to be considered for the design of an adsorption chiller. If the inlet and exit temperatures of the chilled water are assumed 12 and 8 °C, respectively; the evaporation temperature might be around 3 °C. For evaporation temperature with 3 °C, the low level cycle pressure is 0.767 kPa.

The numerical study was performed using a computer program written by FORTRAN. The heat transfer relations mentioned in previous section, adsorption equilibrium equations, cooling capacity and COP relations were used to determine the performance and capacities depending on the maximum cycle temperature (T_c). The steps for the numerical study is shown as a flow chart in Appendix B.

In three different types of adsorption chillers, silica gel – water and modified silica gel (S0 and S40) – water pairs were studied. Freundlich and Dubinin – Astakhov equations with corresponding coefficients (reported in literature) were used. The studied pairs, equations and their coefficients used in calculations are listed in Table 6.1.

Table 6.1. Coefficients for silica gel – water pairs fitting Dubinin-Astakhov (a) and Freundlich (b) equations

a

	q_0	D	n
S0 – water	0.35	0.000006	1.7
S40 – water	0.68	0.0000156	1.65

b

	k	n
Silica gel 1 – water	0.346	1.6
Silica gel 2 – water	0.355	0.79
Silica gel 3 – water	0.444	1.346
Silica gel 4 – water	0.552	1.6

6.1.1. Results and Discussion of Numerical Study

The results of the numerical study are presented by the graphs. X-axis in all plots is the maximum bed temperature (T_c).

Figure 6.2 and 6.3 show that, Chiller 1 has higher evaporation capacities and COPs at lower temperature ranges when modified silica gel (S40 and S0) – water pairs are used. For the chiller 1 with S40 – water pair, when the maximum temperature of the cycle is 108 °C; the evaporation capacity increases to 300 MJ and COP increases to 0.8. Silica gel 4 (type RD) – water pair has the maximum COP and evaporator capacity values among four different silica gel – water pairs fitting Freundlich equation.

Figure 6.4 and 6.5 are the plots for the second designed chiller. Similar to the first chiller, modified silica gel (S40 and S0) – water pairs have better performances than conventional silica gels. When the maximum temperature of the cycle of Chiller 2 is 95 °C, the evaporation capacity and COP increase to 600 MJ and 0.9, respectively, when S40 – water pair is used.

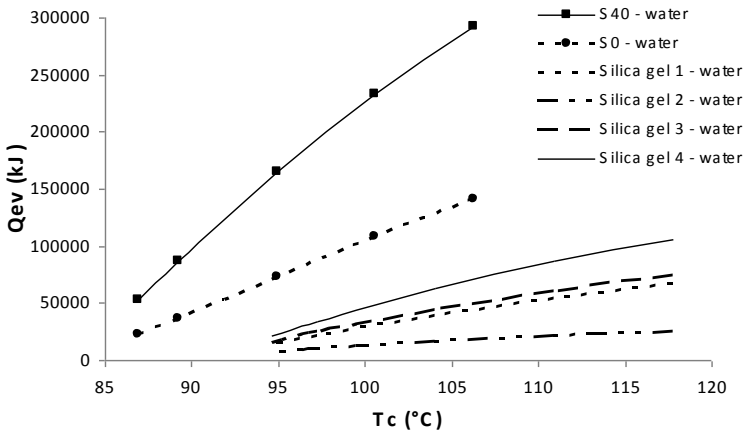

Figure 6.2. Evaporator capacity results of Chiller-1 with six different pairs

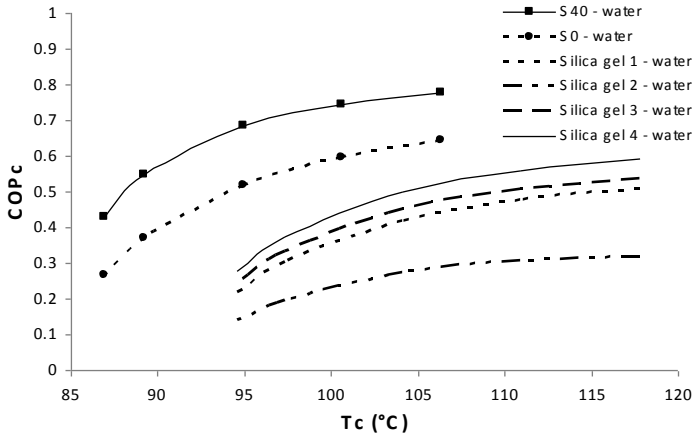

Figure 6.3. COP results of Chiller-1 with six different pairs

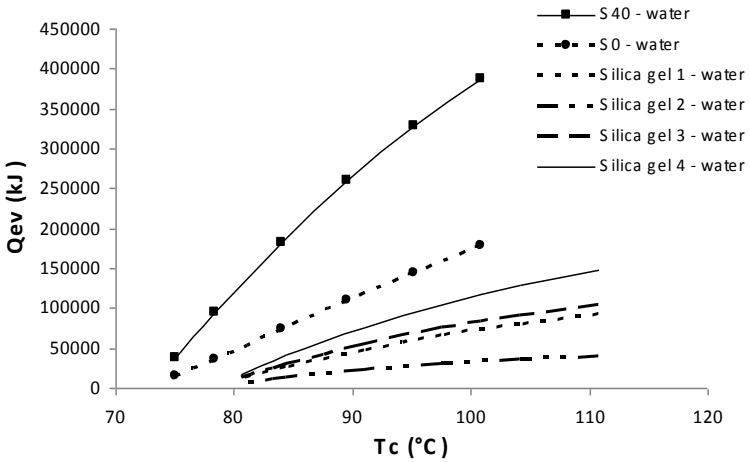

Figure 6.4. Evaporator capacity results of Chiller-2 with six different pairs

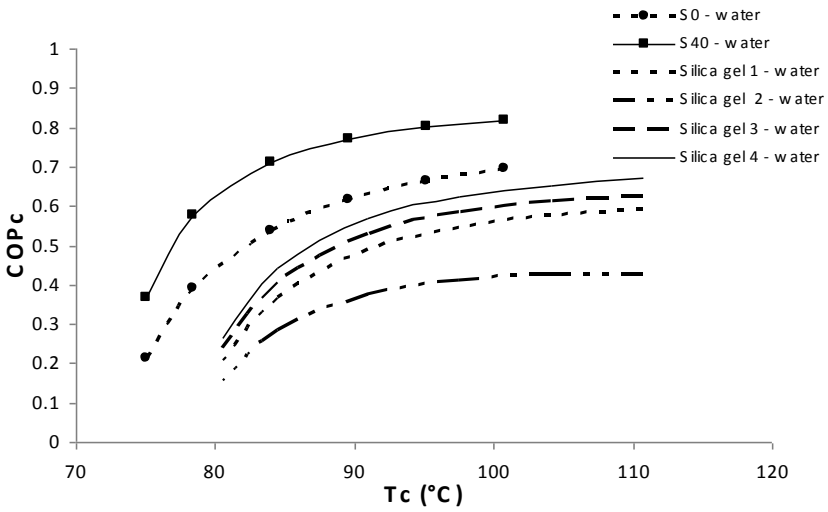

Figure 6.5. COP results graph of Chiller-2 with six different pairs

The results for Chiller 3 are different than other chillers as it can be seen in Figures 6.6 and 6.7. In this chiller, S0 silica gel has a behavior very similar to the conventional silica gels. The temperature ranges were again lower than the conventional ones; however the evaporation capacity and COP values were very close to values of silica gel 4.

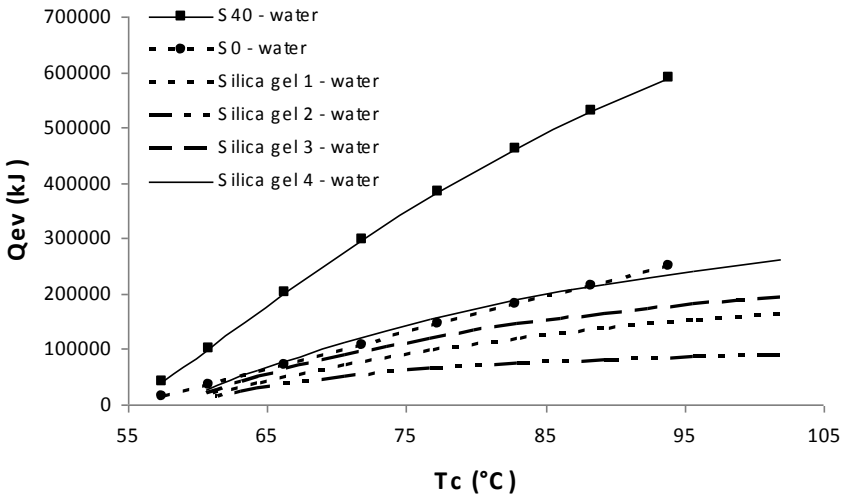

Figure 6.6. Evaporator capacity results of Chiller-3 with six different pairs

Figures 6.8 and 6.9 compare the performances for three designed chillers when S40 – water pair is used. As seen from the figures, Chiller 3 has the lowest operation temperature range while having the highest evaporator capacity and COP values. Chiller 3 can achieve 0.9 COP and 600000 kJ evaporator capacity for 95 °C maximum

bed temperature. Chiller 3 has a better performance compared to Chiller 1 and 2. As the minimum bed and condenser temperatures decrease, the performance of the chiller increases.

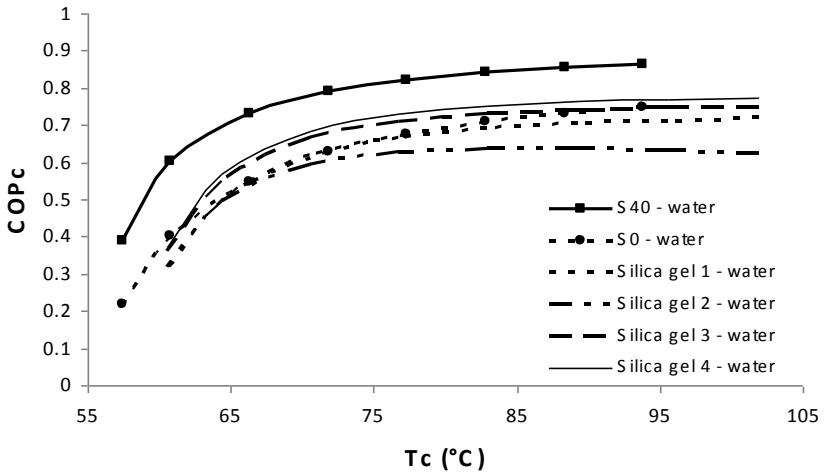

Figure 6.7. COP results of Chiller-3 with six different pairs

Coefficients of performances achieved from three chillers are given in Figure 6.9 as a plot of COP versus maximum bed temperature when S40 –water pair is used. COP quantities for all chillers have a typical behavior, as it can be seen from the plot. The COP value increases with increase of maximum bed temperature; however after a specified temperature it remains constant. For example, the COP of chiller 1, 2 and 3 does not change after 95, 85 and 75 °C.

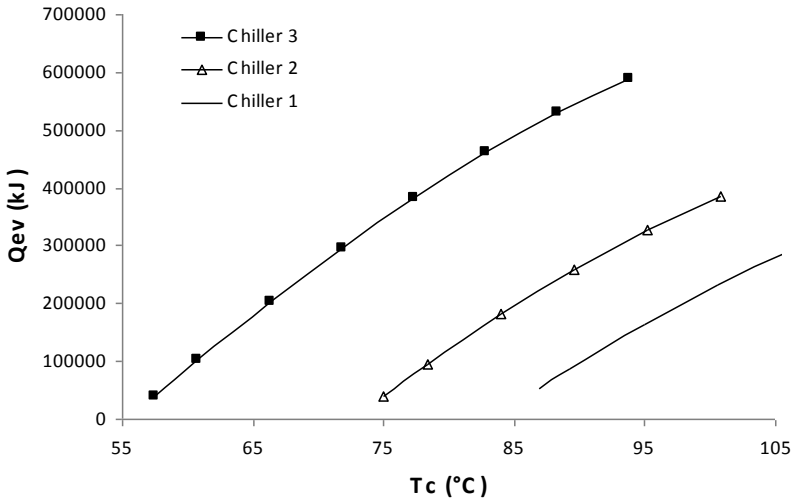

Figure 6.8. Evaporator capacity results comparing chillers using S40 – water pair

This study was performed to investigate the effect of different pairs on the adsorption chiller thermal performance. The effect of cooling type on thermal performance of chillers was also examined. As a result of the study, Chiller 3 using the modified silica gel (S40) – water pair was found to have the best performance along 18 different designs. Chiller 3 has the highest evaporation capacity and efficiency since the adsorbent bed and condenser are cooled by low level temperature source as 25 C. S40 – water pair has the best performance because of its high adsorption capacity.

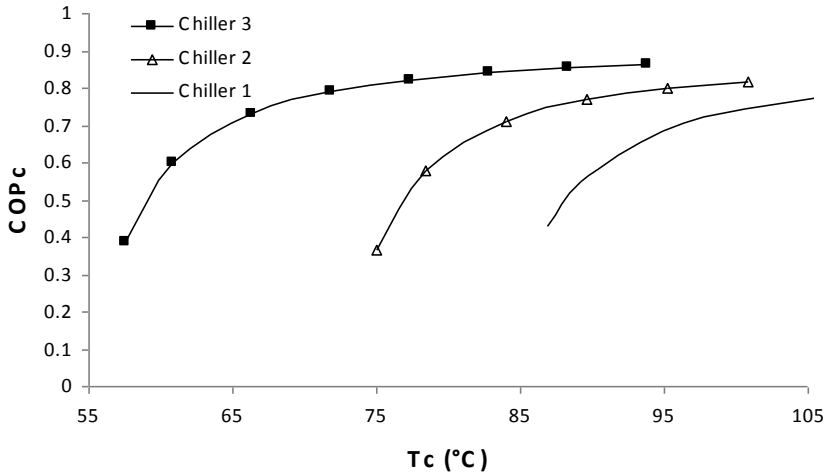

Figure 6.9. COP results comparing chillers using S40 – water pair

CHAPTER 7

EXPERIMENTAL STUDY

The thermo physical properties and equilibrium state of a pair should be well known in order to be able to provide high efficiencies in an adsorption heat pump. The aim of this experimental study was to investigate the adsorption characteristics, such as adsorption capacity, equilibrium behavior, the isotherm type and effective diffusivity of silica gel - water pair which is a commonly used pair in adsorption heat pumps. The methods reported in literature for determination of equilibrium state of adsorbent-adsorbate pair were briefly explained in Chapter 2. In this study, a volumetric method was used. The equipment used in volumetric method has more availability and the construction of the system and methodology of the experiments are more applicable. Gravimetric and micro-calorimetric methods are more complex for construction and performing the experiments.

A volumetric setup was designed and constructed; several experiments were performed, however the obtained results were not very successful. That is why this experimental setup was revised and the second experimental setup was constructed.

The second experimental setup is going to be described in this chapter, briefly. The components of the experimental setup, their functions and the experimental procedure are explained in details. The results of experiments are explained in Chapter 8.

7.1. Components of Experimental Setup

The first experimental setup is illustrated as a picture in Figure 7.1. The apparatus consists of nine components as liquid vessel, vapor vessel, adsorbent vessel, three manual and two solenoid valves, two pressure (vacuum) transducers, pressure scanning and controlling device with a data logging software, vacuum pump, electrical heater and temperature controller.

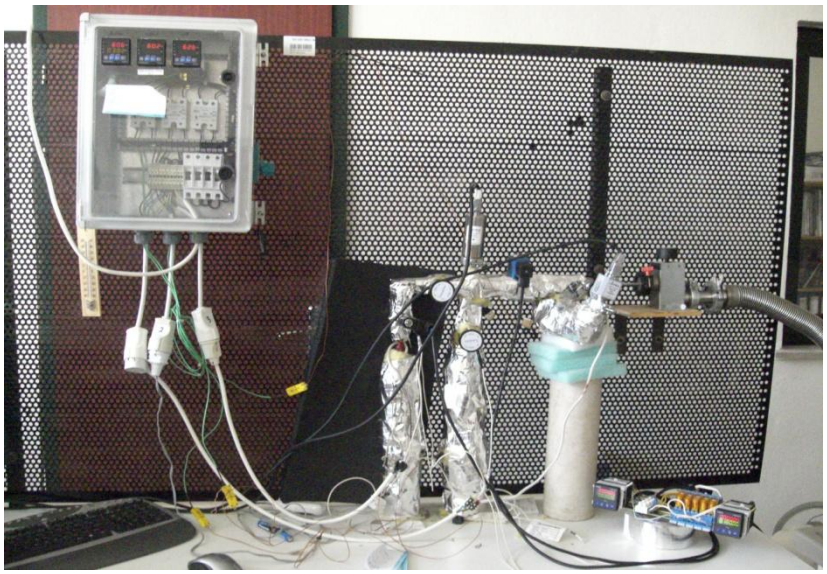

Figure 7.1. Picture of the first experimental setup

An experiment was performed with this setup at 60 °C. Unfortunately, some unexpected errors occurred during the experiments. The solenoid valves were defected over time, therefore the operation of solenoid valves have failed, and the flow of water vapor from one vessel to another became out of control. Since the calculations for adsorbed amount was performed with ideal gas equation by using the obtained water vapor pressure difference at each pulse, the continuous water vapor flow caused the calculated results to be unpredictable. The deterioration of the equipment in the system prevented the experiments to be performed for other temperatures. Thus, the first constructed volumetric setup could not be used. The setup was demounted and a new setup with manual, air-tight valves was constructed.

The components of the second experimental setup were identical with the first one except a few improvements applied. Figure 7.2 is the picture of the second experimental setup with all components and connections. Figure 7.3 is the schematical view of the second experimental apparatus. The main components of the second system are a liquid vessel, a vapor vessel, an adsorbent vessel, three manual valves, a pressure (vacuum) transducer, a pressure scanning and controlling device connected to a data logging software, a vacuum pump, three electrical heaters, temperature controller, a temperature scanning and logging device. The components are described in details below.

- Liquid vessel:

The liquid vessel (Vessel 1, see Fig. 7.3) contains water in liquid phase. It has a cylindrical shape with dimensions of 320 mm length and 50 mm diameter (Swagelok 304 L-500). It has a volume of 500 ml and contains water in liquid phase.

- Vapor vessel:

The vapor vessel (Vessel 2) contains water in vapor phase. It was a sample cylinder (Swagelok 304 L-50) with dimensions of 70 mm length and 35 mm diameter and a volume of 50 ml. The adsorptive was vaporized in the liquid vessel (Vessel 1) and stored in vapor phase in this vessel. A manual valve (V1) was placed between the liquid and vapor vessels.

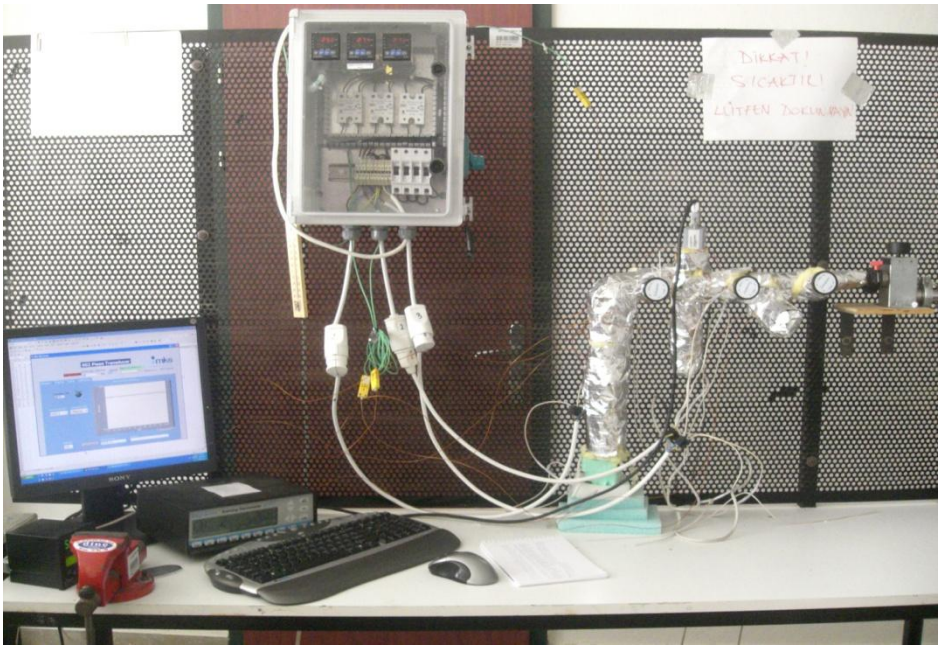

Figure 7.2. Picture of improved experimental setup

- Adsorbent vessel:

This vessel (Vessel 3) was used for the placement of silica gel particles and it was the bed where adsorption takes place. It was a sample cylinder (Swagelok 304 L-50) with dimensions of 70 mm length and 35 mm diameter and it has a volume of 50 ml. Vessel 3 was located horizontally, in order to keep the silica gel particles on a horizontal plane and prevent their accumulation. A valve (V2) was placed between vapor vessel and adsorbent vessel; while another valve (V3) was placed between vacuum pump and adsorbent vessel.

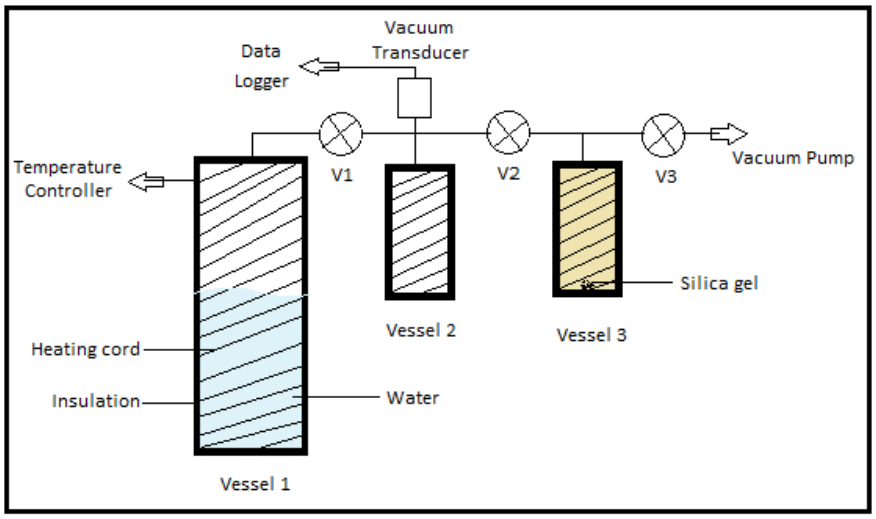

Figure 7.3. Schematical view of improved experimental setup

- Valves:

There were three manual valves (V1, V2 and V3) in the setup in order to manipulate the flow of the water vapor between vessels. The valves were Swagelok Bellows Sealed Valves for ¼" pipes.

- Pressure transducers:

The pressure (vacuum) transducer connected to the vapor vessel was a MKS Series 902P vacuum transducer with a range from 13.332 Pa to 133 kPa, and an accuracy of 1% of reading.

- Pressure logging:

Pressure transducer was connected to a digital scanning and controlling device. The pressure readings were received to MKS Series PDR 900-1 controller. It was connected to the computer having software of MKS Series to collect the data. MKS PDR 900-1 had a display range from 10^{-10} Torr to 1500 Torr (from 0 kPa to 199.98 kPa). The pressures were scanned at adjusted time intervals and logged to a Microsoft Excel worksheet. A picture of pressure logging software is shown in Figure 7.4.

- Vacuum pump:

The system purge and desorption of adsorbent particles were obtained with a vacuum pump. Varian – Turbo-V 70 SH100 vacuum pump with $50 m^3$/hr pumping and 1425 rpm operating speeds was used to evacuate the system, and it had an operating range from 1 atm to 10^{-3} torr.

- Heating elements and temperature controllers:

Three vessels and pipes between components were wrapped around and heated with three flexible electrical heaters. Cole-Parmer Flexible, small-diameter, fiberglass insulated heating cords with 24 inches of length and 562 watts, 120 VAC were used.

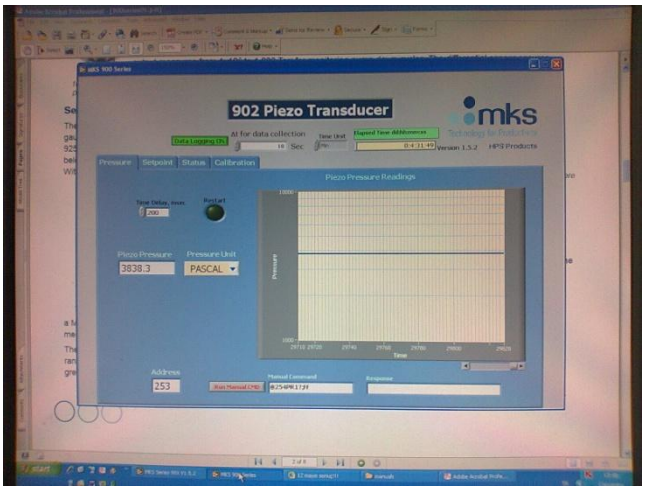

Figure 7.4. Picture of the pressure logging software

The flexible electrical heating cords were connected to a temperature controller panel. Three PID type temperature controllers manufactured by ORDEL and named as PC441 were used in the controller panel to upload the time depending temperature programs and maintain a constant temperature. The temperature distribution at the entire system should have been homogenous and it must be kept constant during the experiment, since the adsorbed amount strongly depends on temperature. The temperature feedback of the controller was supplied by thermocouples. Three Cole-Parmer K-type thermocouples were placed on the outer walls of three vessels. An additional heater fan was used to heat the space around the system to prevent water condensation.

An additional temperature scanning and logging device which was Cole-Parmer Digi-Sense scanning thermometer with twelve channels was used. This device was connected to another computer and Scanlink 2.0 software is used to log the temperature data. The temperature loggings were achieved with three other Cole-Parmer K-type thermocouples. The first thermocouple was used for measuring the temperature of vessel 2, the second thermocouple was used for temperature of vessel 3

and the last one was used for the ambient temperature. The temperatures were scanned for every 10 seconds and logged to a WordPad file by the software.

- Adsorption pair:

The silica gel particles used in experiments were supplied from Merck Co. Some adsorption properties of silica gel particles were examined by Micromeritics ASAP2010. The surface area, pore volume and average pore diameters were investigated using nitrogen as the adsorptive gas. Micromeritics results (structural properties and isotherm plot) are illustrated in Appendix C. The equivalent diameter of supplied silica gel granules varied between 3 - 5 mm. The silica gel particles were exposed to screening process with multi-storey sieves by a shaker. The layers of the sieve were used to separate the silica gel particles with decreasing diameters. In the experiments, 0.3 grams of silica gel particles with diameters between 0.3 and 0.4 mm were used. De-ionized pure water was placed to the liquid vessel.

After the complement of setup construction and electrical connections, the next step was sealing process. In order to obtain adsorption equilibria at different temperatures less than 100 ^{o}C, the experiments should be performed at low pressure. Air leakage may take place in the system during the experiment. The first measure to prevent the leakage was using stainless steel vacuum equipment and wrapping Teflon tapes on the joints of pipes and valves. The vacuum test was applied to the system and the leakage rate was found high for applicability of adsorption experiments. Various types of sealing materials were tried in the system. The test of different methods for leakage prevention took very long time as eight months. The supply of sealing material, sealing and evacuating processes, and leakage test steps were repeated after each failure. Finally, Loctite red gasket was found to be the best insulation material, thus it was applied on every joint. The detection of leakage locations for an evacuated system was considerably difficult. Water bubble check, performed by the compression of air into the system, could give an idea about the leakage location. After detection of leakage points, the sealing materials were applied to these specific points. The results of leakage rate and achieved improvements within the system will be presented in Results and Discussion chapter.

After the sealants were applied to connections and dried, the heating cords were wrapped and the heat insulation was employed. The all system was covered with fiber insulation pads and wrapped with heat resisting tapes. The grey cover around the equipment seen on the pictures (Figure 7.1 and 7.2) is the insulation tape. The heat

insulation was important to provide homogenous temperature along the system and also to prevent condensation of water vapor at the inner surface of the setup.

7.2. Experimental Procedure

The employed method for adsorption experiments was volumetric method, as mentioned before. Here the application of the volumetric method for the experiments is going to be presented.

The first step of experiments was the leakage test. The experiments were performed under low pressures from 5 Pa to 20 kPa. The air leakage possibility from the environment into the system should be taken into account. The next step of the experimental study was the condensation check. The amount of adsorbed water vapor onto silica gel was calculated with the pressure change observed by the decrease of water vapor in the adsorbent bed and water vapor vessel. Ideal gas law was used to determine the amount of adsorption from pressure difference. The difference between the initial and final pressures indicates the amount of water vapor adsorbed onto silica gel. Any condensation within the setup reduces the pressure. Therefore, the pressure difference may involve both adsorbed and condensed amount and it causes inaccurate results for the calculated adsorbed amount. Since it is difficult to predict or calculate condensed amount during the adsorption experiment, the net adsorbed amount of water vapor will not be known.

The condensation may occur on the inner walls of experimental setup, especially on the walls of joints, elbows, or fittings. At the locations close to ambient, if any temperature drop occurs, water may be condensed. The joints near the valves and vacuum transducers were the most probable locations which may cause condensation occurrence.

In order to prevent condensation, the space around setup was heated by an external electrical heater fan. Setting liquid vessel temperature below the experiment temperature may also reduce the possibility of condensation occurrence, since the remaining surfaces of setup had higher temperature than the temperature of liquid vessel.

The observation and calculation of condensation rate during the adsorption experiments were impossible in the designed system. The condensation test was done

to check the condensation rate at the inner surface of setup equipments, before the adsorption experiments, which means before the placement of silica gel into the adsorbent vessel.

The following procedure was followed to determine the rate of condensation before the adsorption experiments:

- The liquid vessel was filled with deionized pure water.
- The liquid vessel valve (V1) was fully closed, while V2 wad opened.
- The remaining portions of the system were heated up to test temperature.
- The whole system was evacuated and purged completely. It should be mentioned again that no silica gel exists in the system.
- After completing vacuum procedure which was about 12 hours, the vacuum (V3) valve was fully closed.
- The pressure recording was started.
- V1 valve was opened for about 10 minutes to let the water to vaporize and flow through the system.
- V1 valve was closed when the pressure was stabilized.
- The recorded pressure data was tabulated or shown by a graph.
- The decrease of vapor pressure indicates the condensation occurrence within the system.
- The condensation test procedure was repeated for different experimental temperatures.

The result of the performed condensation test is given in Results and Discussion chapter. After the completion of condensation test, adsorption experiments were performed. Since the condensation experiments were performed without adsorbent inside the system, silica gel was placed into the system. The sealing step, wrapping the electrical heater around the adsorbent bed and thermal isolation were repeated. After the certainty of lack of leakage and condensation, the adsorption experiment was performed.

Adsorption experiments were performed with the following steps:

- All three valves were closed,
- Temperature and pressure loggings were on,

- Temperature controllers connected to vessel 2 and vessel 3 were set to105 °C desorption temperature and run,
- Vacuum pump was turned on,
- V3 and V2 were opened in turn,
- Evacuating was continued for 24 hours at 105 °C,
- After 24 hours the temperature controllers were set to the experiment temperature; while evacuation continued,
- When the temperature of the system reached to the equilibrium experiment temperature; V2 and V3 were closed in turn,
- Vacuum pump was closed,
- V1 was opened for approximately 5 minutes and then closed,
- Pressure of vessel 2 was checked for approximately 5 minutes, for the observation of condensation,
- If no pressure drop was observed, V2 was opened for approximately 15 minutes, and then closed.

A set of experiment begins with opening V1 and ends up with closing V2; the sets were repeated until the maximum adsorption capacity was achieved. The measured pressure at the end of each set defines the equilibrium pressure. The difference between the amount of water vapor at the beginning and at the end of a set defines the adsorbed amount. The experiments were performed for 35, 45 and 60°C temperatures. Each experiment was repeated three times to validate the achieved results. The experimental results achieved at every step and the comments on the results are going to be discussed in the next chapter.

CHAPTER 8

RESULTS AND DISCUSSION

The silica gel - water adsorption experiments were performed in the volumetric experimental setup which was described in previous chapter. The pressure change with time was logged and plotted. The adsorption equilibrium points were determined according to the adsorbed amounts at the equilibrium pressures. The results of performed studies such as leakage and condensation tests, adsorption experiments and also the diffusivity results are presented with either plots or calculations in this chapter.

8.1. Uncertainty Analysis

Uncertainty analysis deals with assessing the uncertainty in a measurement. The experimental results might be affected by errors due to instrumentation or methodology. The uncertainty of the result of a measurement expresses the lack of exact knowledge for the value of the measured quantity. Uncertainty of a measurement is mostly based on the accuracy and precision of the measuring device.

In this study, the basic equation for calculation of adsorbed amount is evaluated using ideal gas law equation, and it can be shown as;

$$q = \frac{\Delta m_v}{m_s} = \frac{\Delta P_v V}{m_s RT} \cong \frac{P_v V}{m_s RT} \tag{8.1}$$

Table 8.1. Accuracies and uncertainties of measured parameters

Measurement	Device	Accuracy	Uncertainty
Pressure	MKS 902P	1 %	± 0.01
Volume	-	1 %	± 0.01
Mass	Precisa XB 220A	0.0001 %	± 0.000001
Temperature	K-type Thermocouple	0.3 %	± 0.003

As can be seen from the equation, the calculation depends on pressure, volume, mass and temperature parameters. Therefore, the uncertainty analysis should be performed based on the accuracy of devices used to measure the quantities of these

parameters. Table 8.1 shows the accuracy and corresponding uncertainty values of measuring devices used in experiments.

Uncertainty of experimental results can be calculated by the following equations;

$$u_q = \pm\left\{\left[\left(\frac{P}{q}\right)\left(\frac{\partial q}{\partial P}\right)u_P\right]^2 + \left[\left(\frac{V}{q}\right)\left(\frac{\partial q}{\partial V}\right)u_V\right]^2 + \left[\left(\frac{m}{q}\right)\left(\frac{\partial q}{\partial m}\right)u_m\right]^2 + \left[\left(\frac{T}{q}\right)\left(\frac{\partial q}{\partial T}\right)u_T\right]^2\right\}^{1/2} \quad (8.2)$$

$$u_q = \pm\left[\left(\frac{PmRT}{PV}\frac{V}{mRt}u_P\right)^2 + \left(\frac{VmRT}{PV}\frac{P}{mRt}u_V\right)^2 + \left(\frac{mmRT}{PV}\frac{-1}{m^2}\frac{PV}{TR}u_T\right)^2 + \left(\frac{TmRT}{PV}\frac{-1}{T^2}\frac{PV}{mR}u_T\right)^2\right]^{1/2} \quad (8.3)$$

$$u_q = \pm\left\{\left[(1).\pm u_p\right]^2 + \left[(1).\pm u_V\right]^2 + \left[(-1).\pm u_m\right]^2 + \left[-(1).\pm u_T\right]^2\right\}^{1/2} \quad (8.4)$$

Therefore,

$$u_q = \pm\left\{\left[(1).\pm 0.01\right]^2 + \left[(1).\pm 0.01\right]^2 + \left[(-1).\pm 0.000001\right]^2 + \left[(-1).\pm 0.003\right]^2\right\}^{1/2}$$

$$u_q = \pm 0.0144$$

The uncertainty of this experimental study is found 0.0144. The achieved calculations and results should be evaluated considering this uncertainty quantity.

8.2. Isotherm Results

The results section for the experiments can be started with the illustration of leakage rate versus time (Figure 8.1). The time axis is limited with 1200 minutes, since the experiments were ended in around 1100 minutes. The dashed line with a leakage rate of 4.205 Pa/min shows the result of the first vacuum test. The adsorption experiments could not be performed with this leakage rate, thus some further improvements were done to reduce leakage. After improvement, the leakage test was repeated. The line with the leakage rate of 1.316 Pa/min shows the results of the second vacuum test. The achieved leakage rate was again not satisfactory and further measures were applied once more. The line with leakage rate of 0.535 Pa/min was the results of the third and last vacuum test. The value of 0.535 Pa/min was an acceptable leakage rate; therefore, the next step which was condensation test was performed.

The graph of condensation test for 35 and 70 °C is illustrated in Figure 8.2. At the beginning of the experiment (for about 170 minutes), the system was again checked for the leakage (up to point “a” for 35 °C, point “A” for 70 °C). After 170 minutes, V1 valve was opened and water vapor was introduced to the vapor vessel. After stabilization of pressure (point “b” for 35 °C, point “B” for 70 °C), V1 valve was closed, After a period of time, V2 valve was opened (at point “c” for 35 °C, point “C” for 70 °C). A sudden pressure drop occurred because the volume was doubled after opening V2 valve. No pressure drop was observed for both 35 and 70 °C experiments. Therefore, no condensation occurred in the system, which means adsorption experiments could be performed.

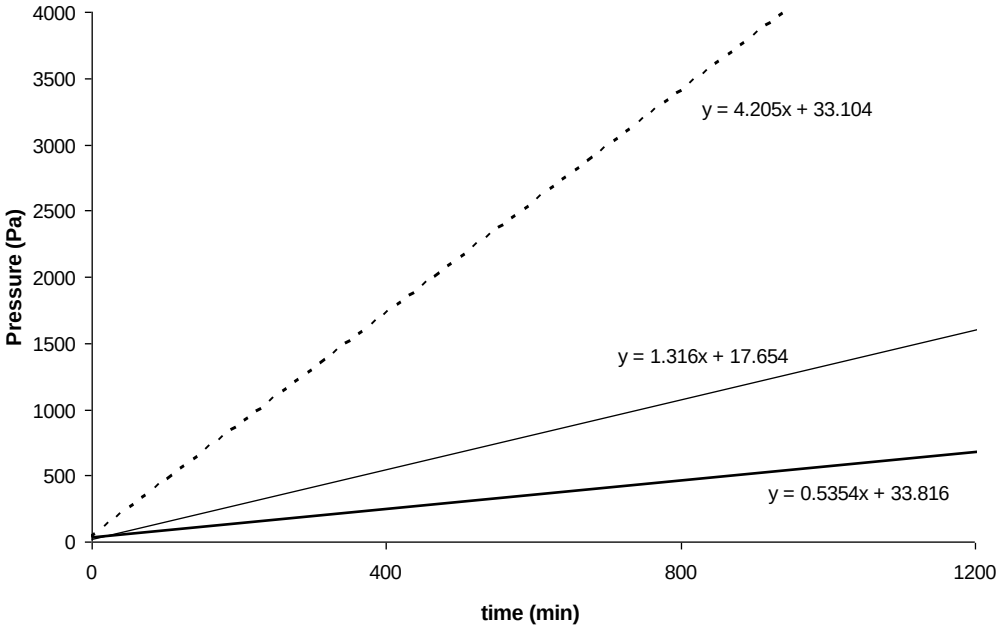

Figure 8.1. Leakage test results

Figure 8.3 indicates the result of experiment performed at 35 °C. It shows the pressure change during the experiment. Every vertical line between low and high pressures represents the new pulses (i.e., introducing new water vapor amount to the adsorbent vessel). Figure 8.4 shows the same graph for a narrow period of 250 minutes. The first eleven pulses can clearly be seen in this figure. The observation of constant pressure indicates the achievement of equilibrium state for each pulse. For the first pulse, the vapor vessel pressure was stable at 3378 Pa, then, V2 valve was opened. Water vapor flowed to the adsorbent bed. By opening of V2 valve, the volume of tank was doubled and the adsorption process was started. The pressure suddenly dropped to

nearly 15 Pa and remained constant at 5.33 Pa which is equilibrium pressure. For the second pulse, after the observation of stable pressure, V2 valve was closed. The V1 valve was opened and the vapor vessel was filled with water vapor. After stabilizing the vapor pressure in the vapor vessel, V1 valve was closed. Any pressure change in the vessel 2 was checked by waiting for 5 minutes. V2 valve was opened when no drop was observed. A pressure drop occurs due to the doubling of volume and the adsorption was started again. The sets (pulses) were repeated for 68 times and experiment ended after 18 hours.

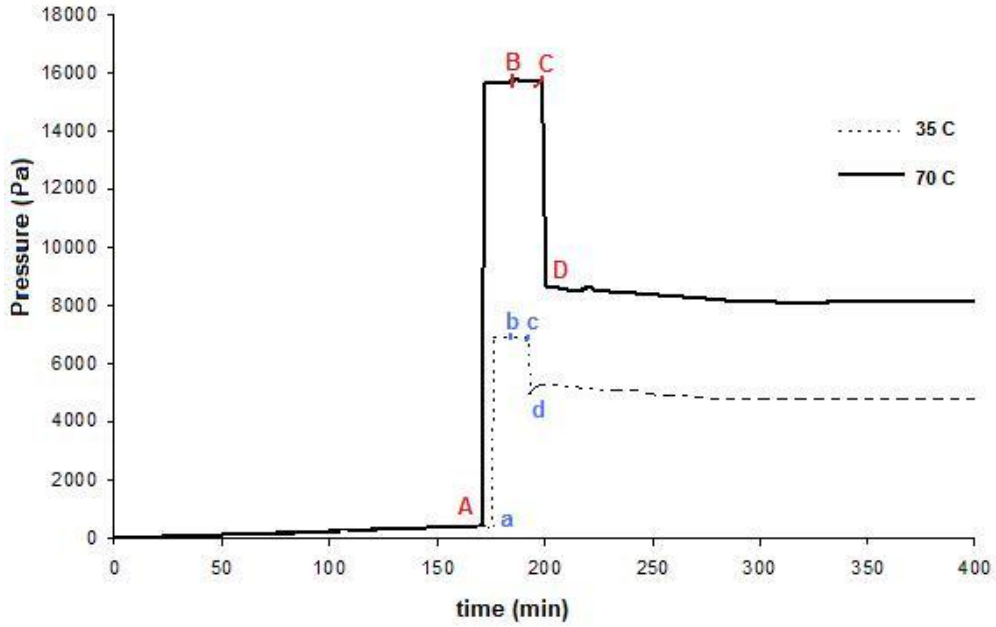

Figure 8.2. Condensation tests performed at 35 and 70 °C

The adsorbed amounts were calculated by using ideal gas law. The method for calculations was as follows;

For the first pulse,

3378 Pa was read for the vapor vessel. After opening V2, the volume was doubled and the pressure dropped to 3378/2=1689 Pa, the final pressure was observed as 5.33 Pa. The following calculation procedure was performed,

$PV = mRT$

V = 50ml+50ml+4ml = 104 ml = 0.104×10^{-3} m^3 (volume of vapor vessel + adsorbent vessel + pipes)

R = 0.461 m^3Pa/gK

T = 308.15 K

$P_{initial}$ = 3378 Pa, P_{eq} = 5.33 Pa, ΔP = 3372.67 Pa, for the first pulse

$$\Delta m_{ads} = \frac{3372.67x0.104x10^{-3}}{0.461x308.15} = 1.230x10^{-3}\,g\,,$$ the first adsorbed amount

$$q_1 = \frac{\Delta m_{ads}}{m_{silicagel}}100 = \frac{1.230x10^{-3}}{0.3}x100 = 0.41\%$$ kg water/kg silica gel, for P_{eq} = 5.33 Pa,

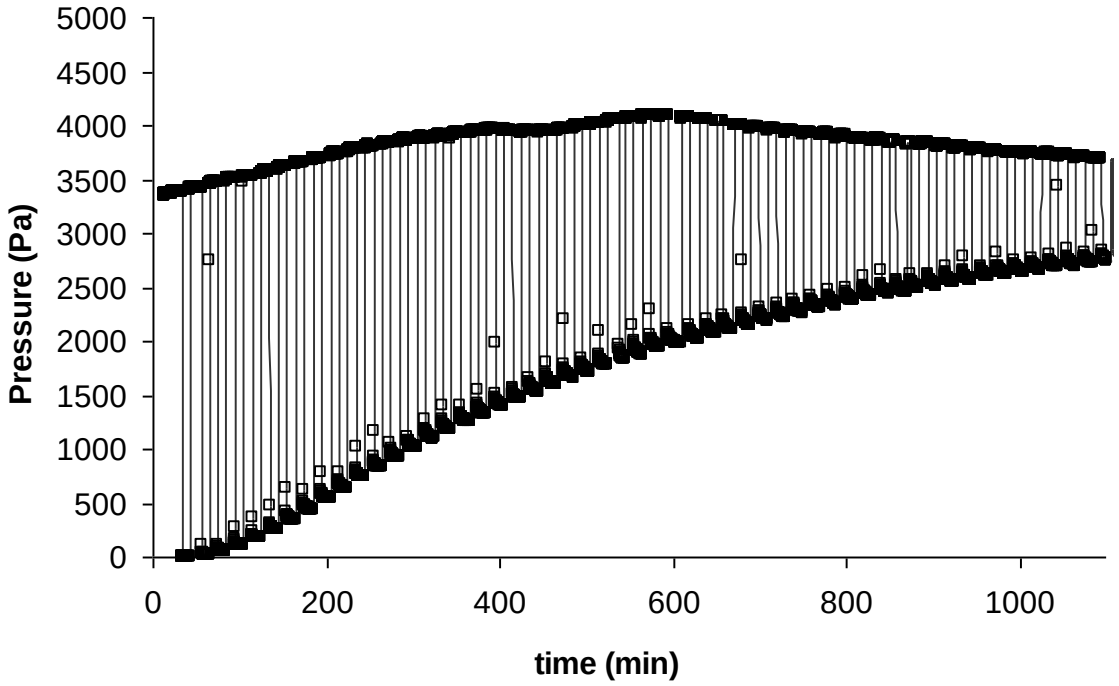

Figure 8.3. Experimental result for the first 35 °C adsorption experiment

For the second pulse the procedure is a little bit different. 5.33 Pa was the equilibrium pressure in adsorbent bed and vapor vessel (which was not adsorbed). Therefore the mass of remaining water vapor is;

$PV = mRT$

V = 50ml+2ml = 52 ml = 0.052x10^{-3} m^3 (volume of adsorbent vessel + pipes)

R = 0.461 m^{3}Pa/gK

T = 308.15 K

$$m_{rem} = \frac{5.33x0.052x10^{-3}}{0.461x308.15} = 1.95x10^{-6}\,g$$

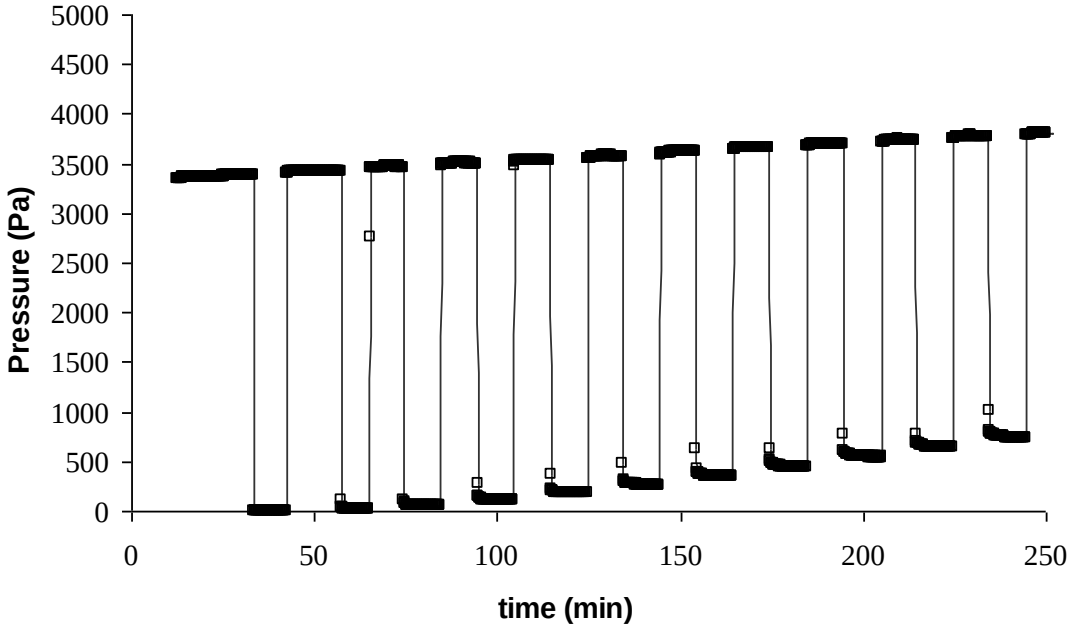

Figure 8.4. Result for adsorption experiments at 35 °C including eleven pulses

This amount existed in the adsorbent vessel and it was not adsorbed. With the second pulse and opening of V1 valve, the observed pressure in the vapor vessel was 3426 Pa,

$PV = mRT$

V = 50ml+2ml = 52 ml = $0.052x10^{-3}$ m^3 (volume of vapor vessel + pipes)

R = 0.461 m^3Pa/gK

T = 308.15 K

$$m_{2nd\ pulse} = \frac{3426x0.052x10^{-3}}{0.461x308.15} = 1.253x10^{-3}\,g,$$

After closing of V1 valve, this amount of vapor existed in the vapor vessel. The total mass of water vapor in adsorbent bed and vapor vessel was:

$$m_{total} = m_{rem} + m_{second} = 1.95x10^{-6} + 1.253x10^{-3} \cong 1.255x10^{-3}\,g$$

After adsorption, the equilibrium pressure achieved for the second pulse was 16 Pa. The total amount of vapor in adsorbent bed and vessel, which was not adsorbed, was:

$$m_{vapor} = \frac{16x0.104x10^{-3}}{0.461x308.15} = 1.169x10^{-5}\,g$$

Hence, the amount of vapor adsorbed by silica gel particles was calculated as:

$$m_{ads,2nd} = m_{total} - m_{vapor} = 1.255x10^{-3} - 1.169x10^{-5} \cong 1.244x10^{-3},$$

Therefore, the total adsorbate concentration for the first and second part for P_{eq} = 16 Pa can be calculated as follows:

$$q_{2nd} = \frac{m_{ads,2nd}}{m_{silicagel}} = \frac{1.244x10^{-3}}{0.3} = 4.14x10^{-3},$$

$$q_2 = (q_1 + q_{2nd}) = (4.10x10^{-3} + 4.14x10^{-3}) + 100 = 0.824\% \text{ kg water/kg silica gel}$$

Similarly, further calculations for 68 pulses were performed and the obtained equilibrium points at equilibrium pressures were plotted.

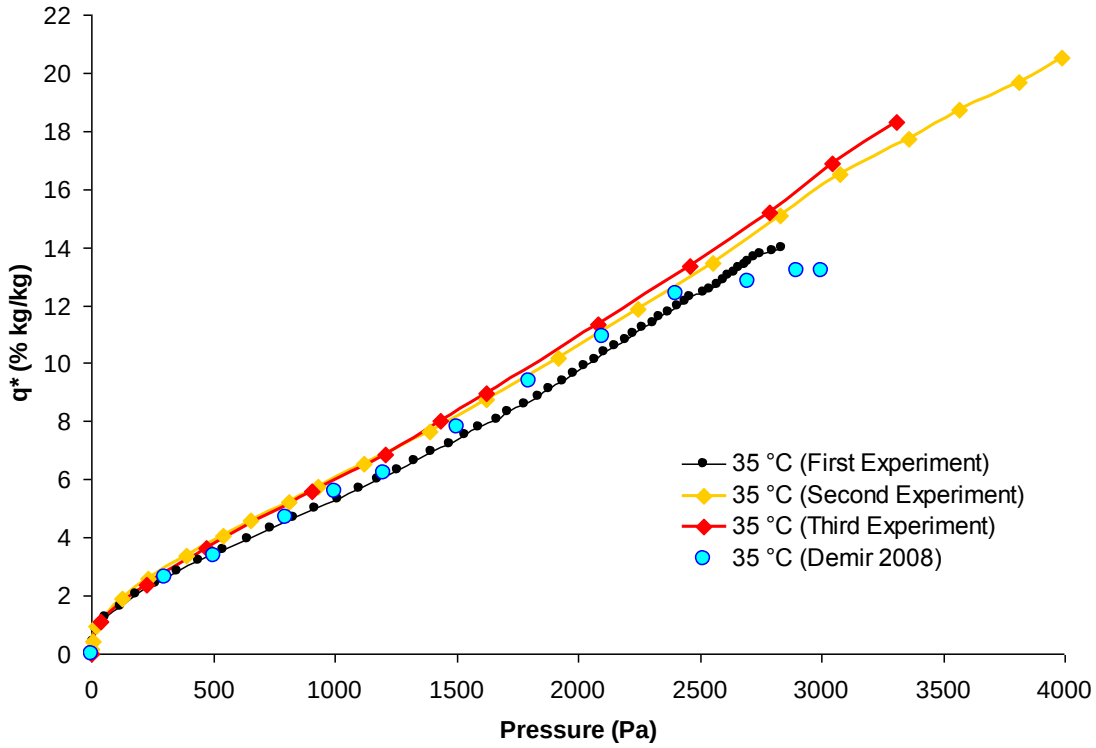

Figure 8.5. Adsorbed amount versus equilibrium pressure plot for 35°C experiments

Two further experiments at 35 °C were performed for the reliability of the experiment. Equilibrium adsorbed amount (i.e., q) versus equilibrium pressures were plotted for three performed experiments at 35 °C. The obtained graphs are observed in Figure 8.5. The figure also involves the comparison between present study and Demir's study, since he studied on the same pair using the same silica gel. The blue points in the figure depict the equilibrium points achieved by Demir (Demir 2008). An excellent agreement between the present results and Demir's study can be observed indicating correctness of the present experimental study.

As it can be seen from the figure, a knee shape is observed for the pressures below 500 Pa. After that, a slight convexity is observed up to 3000 Pa; while an upward trend is observed for the pressures higher than 3 kPa. For 4000 Pa, the maximum adsorbed amount was found around 20 % (kg water vapor/kg silica gel).

After 35 °C, two experiments for 45 °C and two experiments for 60 °C were performed in a similar way. Figure 8.6 illustrates the results for 45 °C temperature. The results of performed experiments could not be compared with Demir's study, since experiment for 45 °C temperature was not available in his study. The results of two performed experiments are in a good agreement with each other. The first experiment was ended at 3600 Pa, while the second experiment was performed until 6000 Pa equilibrium pressure. At 6000 Pa pressure, around 19 % (kg water vapor/kg silica gel) adsorbate concentration was achieved.

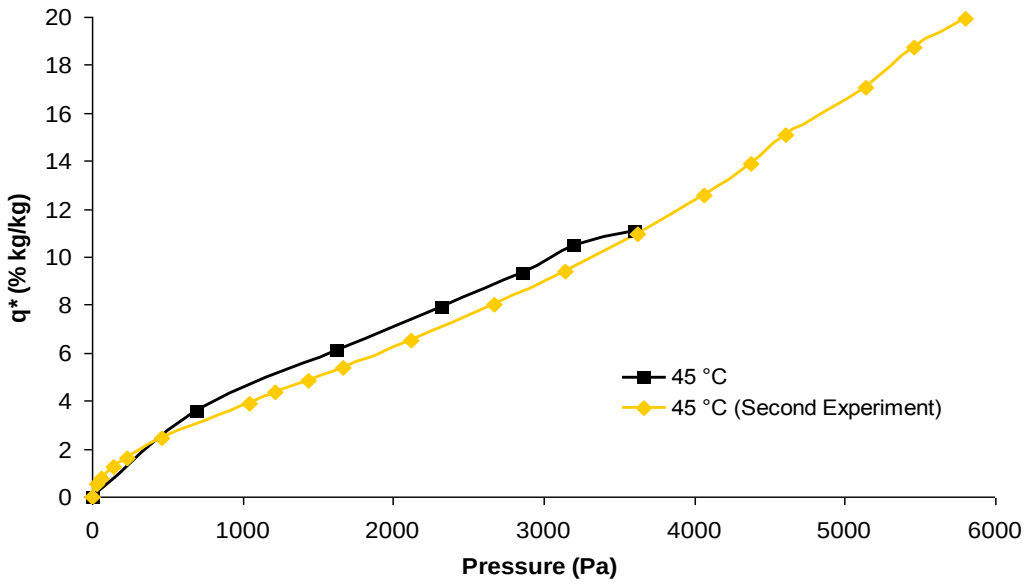

Figure 8.6. Adsorbed amount versus equilibrium pressure plot for 45°C experiments

Figure 8.7 shows the experimental results of 60 °C experiments. As seen, two experiments were performed and the obtained results were compared with the result of Demir's at 60 °C. Two performed experiments are in a good agreement between each other. The first experiment was ended at equilibrium pressure of 5000 Pa while second experiment lasted until equilibrium pressure of 10000 Pa. At 60 °C and 10 kPa equilibrium pressure, around 11 % (kg water vapor/kg silica gel) adsorption capacity was achieved. For the pressures below 2000 Pa, a good agreement between Demir's

and present study was observed. For the region after 2000 Pa, the adsorbed amount increases with pressure in the results of present study, however it becomes constant in the results of Demir's study. The reason of this difference may be due to the difference of particle sizes. Demir performed experiments with particles having 3-5 mm diameters; while in present study the particles have nearly 0.35 mm diameter. The diffusion through the pores might have been affected by the clogged pores for the larger particles; therefore the adsorption capacity would also be affected.

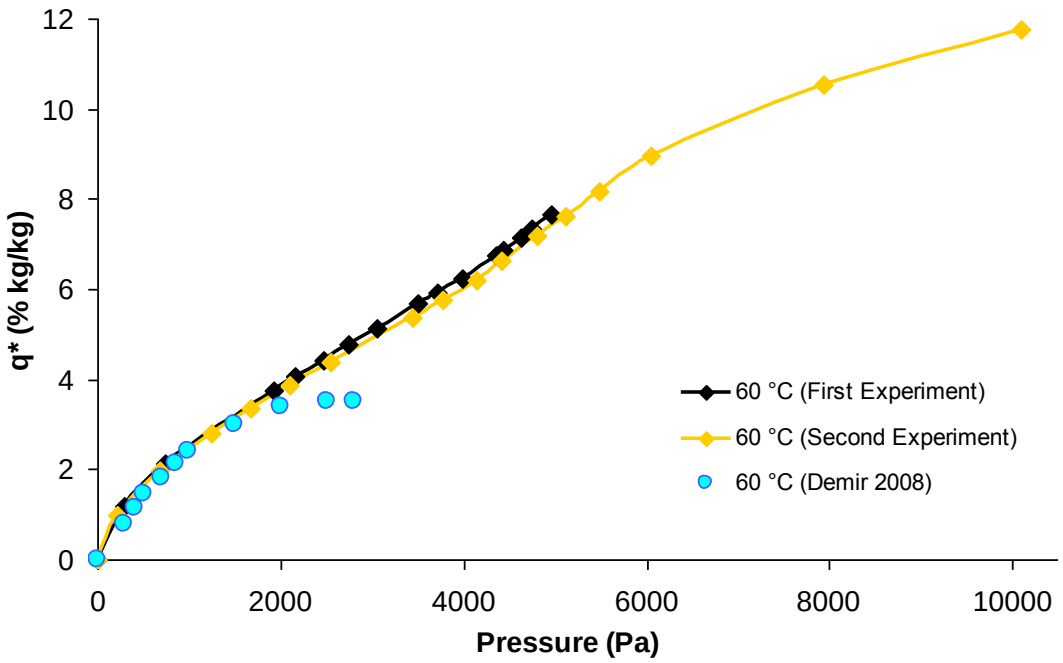

Figure 8.7. Adsorbed amount versus equilibrium pressure plot for 60°C experiments

Isotherms of pairs are plotted as adsorbed amount versus relative pressure and types of isotherms were classified by IUPAC, as mentioned in Chapter 5. In Figure 8.8, the isotherm plots are given for all performed experiments at three different temperatures. They are almost fitting to each other, as expected. As having a knee shape for lower relative pressures and a convexity for further pressures, the isotherm may be classified as Type II isotherm. This isotherm behavior is compatible with water vapor adsorption onto microporous silica gel defined in literature (Gregg and Sing 1982).

The experimental results were properly fitting Freundlich equation with constants k=0.2958 and n=1. Therefore the isotherm equation becomes:

$$q = 0.2958\left(\frac{P}{P_{sat}}\right)^{1} \tag{8.5}$$

The isotherm equation based on adsorbed amount versus relative pressure was plotted and compared with the obtained results. A good agreement between results of isotherm equation and experiments can be seen (see Fig. 8.8).

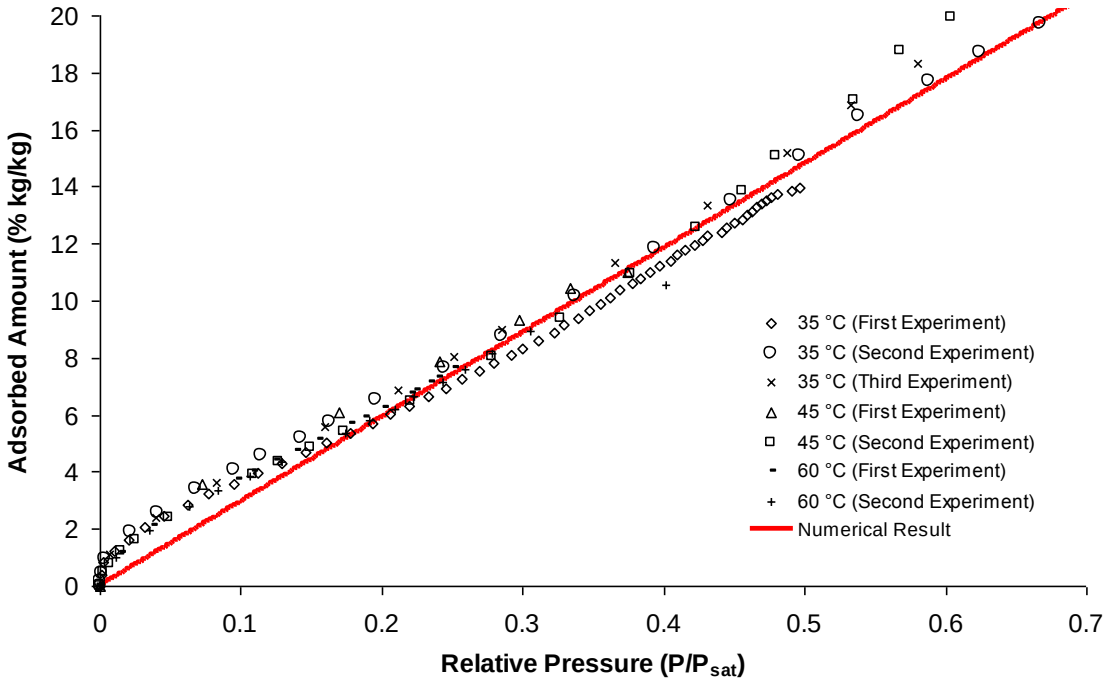

Figure 8.8. Isotherm plot of experimental results

8.3. Effective Diffusivity

The mass transfer of adsorbate flow through the porous adsorbent is performed by diffusion mechanism. Diffusion process involves mechanisms such as micropore diffusion, macropore diffusion and surface diffusion etc.

The effective mass diffusivity describes the rate of diffusion through the pore space of porous media. It involves all diffusion mechanisms. The effective diffusivity can be evaluated using solid diffusion model which is:

$$\frac{\partial q}{\partial t} = \frac{1}{r^2}\frac{\partial}{\partial r}\left(r^2 D_{eff}\frac{\partial q}{\partial r}\right) \tag{8.6}$$

The initial and boundary conditions of Eq. 8.2 can be written as;

$$\text{At } r = 0 \qquad \frac{\partial q}{\partial r} = 0 \tag{8.6.a}$$

$$\text{At } r = r_p \qquad q = q_\infty \tag{8.6.b}$$

$$\text{At } t = 0 \qquad q = 0 \tag{8.6.c}$$

Analytical solution of Equation 8.2 can be defined by Equation 8.3. D_{eff} of an adsorbate into a single particle can be calculated using this equation.

$$\frac{q - q_i}{q_\infty - q_i} = 1 - \frac{6}{\pi^2} \sum_{n=1}^{\infty} \frac{1}{n^2} \exp\left(- \frac{n^2 \pi^2 D_{eff} t}{r_p{}^2} \right) \tag{8.7}$$

The left side of the equation, which is a non-dimensional term, defines the uptake of adsorption process. The uptake curves for each pulses of each experiment were plotted on the same graph, as shown in Figure 8.9. This figure belongs to the second 60 °C experiment having 15 pulses. As seen from the figure, uptakes slightly depend on concentration. As particle adsorbs adsorbate, diffusivity through the pores decreases. Since the curves are very near to each others; the average of uptake curves was used to calculate effective mass diffusivity. As a result, the effective diffusivity of water vapor into a silica gel particle was found as 1.90×10^{-10} m^2/s at 60 °C by using eqn. 8.7. The comparison between the uptake curve based on average of experimental results and the uptake curve based on the calculated effective diffusivity is given in Figure 8.10. The analytical result is found to be compatible with experimental one.

Table 8.2. Calculated effective mass diffusivity results of each experimental temperature

	D_{eff} (m^2/s)
35 °C	1.35 E-10
45 °C	1.54 E-10
60 °C	1.90 E-10

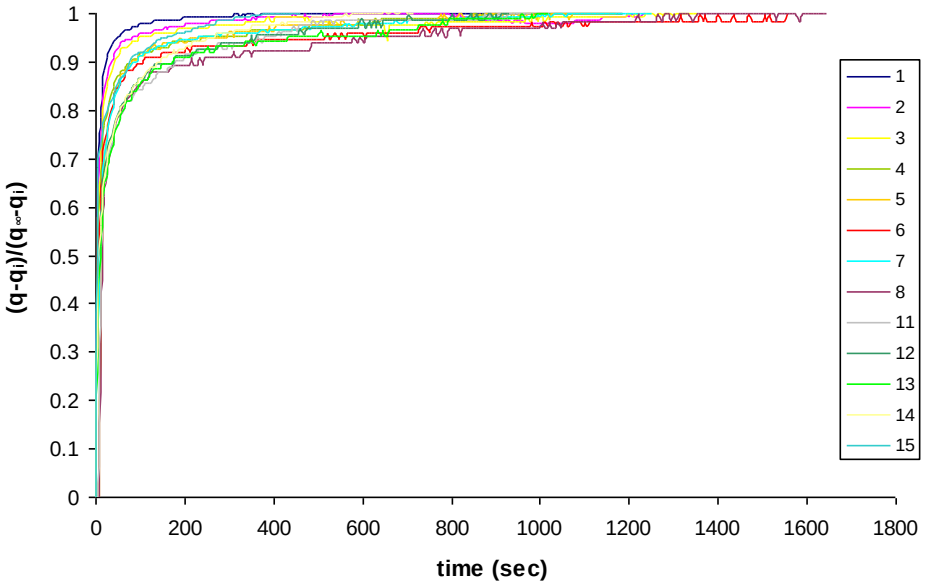

Figure 8.9. Uptake curves for each pulses of the second 60 °C experiment

The average uptake curves for the studied temperatures are given in Figure 8.11. The diffusion rate in the adsorbent particle increases with temperature. This is due to the increase of activation energies of water molecules. The effective diffusivity calculations for the other experimented temperatures were calculated by the same method and the results are listed in Table 8.2. The adsorption capacity of the pair decreases with increase of temperature, while the effective mass diffusivity increases with temperature.

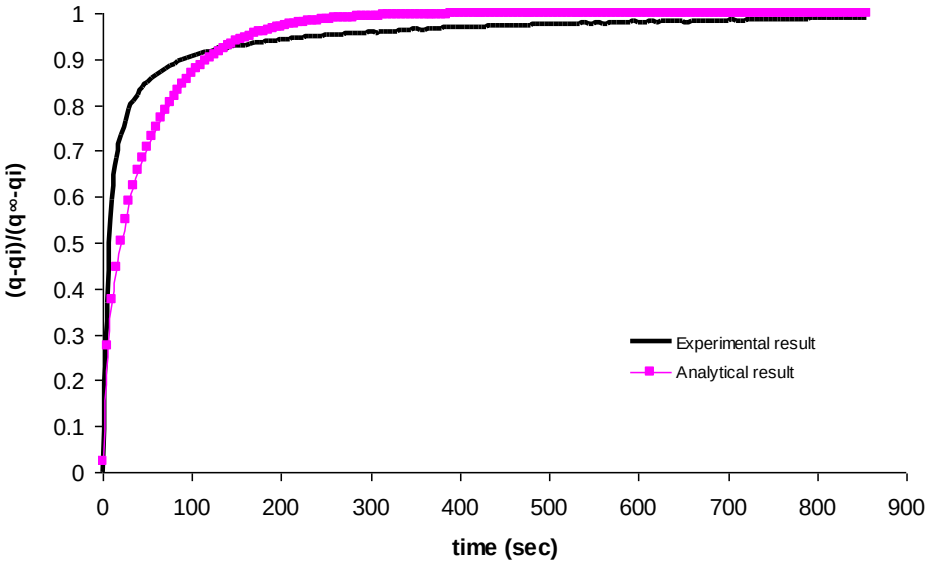

Figure 8.10. Comparison of experimental average uptake curve and analytical result of calculated effective diffusivity

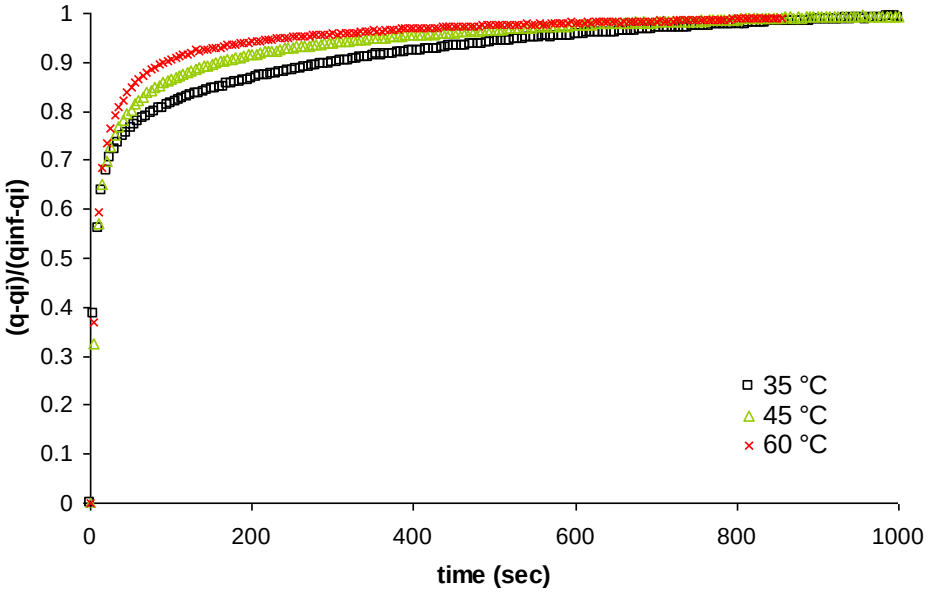

Figure 8.11. Average uptake curves of 35, 45 and 60 °C experiments

CHAPTER 9

CONCLUSIONS

Adsorption heat pumps gained importance due to the growing energy demand. In this study, the importance of adsorption heat pump, its working principle and advantages are explained in detail. Since the main principle of these systems is based on adsorption phenomena, the adsorbent-adsorbate pairs used in the system have also great importance. The most common pairs used in the adsorption heat pumps and novel materials being studied and reported in literature were reviewed.

In order to select a suitable pair for an adsorption heat pump, the requirements for adsorbent and adsorbate and their affinity to each other should be well known. The structural and thermophysical properties, such as surface area, pore structure and dimensions, thermal conductivity of the most common adsorbents, such as silica gel, zeolite, and active carbon, were investigated and presented. The studies on novel promising adsorbents which have very high adsorption capacities were also searched and discussed. Physical properties for commonly used adsorbates such as water, methanol, and ammonia were also given. The interaction between an adsorbent and adsorbate is the most important issue for the pair selection of an adsorption heat pump. After discussion on the properties of adsorbents and adsorbates, separately, the equilibrium behaviors of the common pairs were also studied. Maximum adsorption capacity, isotherm type and the heat of adsorption of the pairs reported in literature were given in details.

The remarks which might be concluded in accordance with the performed investigations on adsorption pair can be listed as;

- The selection of a suitable pair is significant for the achievement of high performance adsorption heat pump,
- The structure, thermophysical properties, equilibrium behavior of a desired adsorbent-adsorbate pair should be investigated for the specific temperature and pressure ranges, since the decision on the pair depends on the temperature and pressure conditions of the adsorption air-conditioning system,

- The adsorption equilibrium determination of the pair should be investigated before the design of system.

The review on the reported studies in literature shows that among different adsorbent-adsorbate pairs (silica gel - water, active carbon - ammonia, active carbon - methanol, zeolite - methanol and zeolite – water) the pair of silica gel - water was widely used. The silica gel –water pair has advantage of lower desorption temperature enabling operation with a low heat source such as solar, geothermal energy and/or waste heat.

There are several equations defining equilibrium state of adsorbent-adsorbate pairs. Freundlich, Dubinin – Astakhov, Dubinin – Radushkevich, Lagmuir, Henry's and Toth's equations are a few examples of proposed equations. Freundlich, Henry's and Toth's equations are the most probable fitting equations for silica gel – water pair.

The determination methods of adsorption equilibrium were investigated and presented as a literature survey chapter. Gravimetry, calorimetry and volumetry are the methods used for determination of adsorption equilibrium. Details about the methods were discussed and several reported studies in literature were reviewed. The literature survey showed that the volumetric method was the most common one in order to determine adsorption equilibrium of adsorbent-adsorbate pairs.

A numerical study was performed to investigate the effect of six different silica gel – water pairs on the performance of adsorption heat pump. Three different chillers using six different pairs were numerically studied and their performances were evaluated, and results were presented.

The following remarks may be concluded in accordance with the performed numerical study for three different adsorption chillers with six different pairs;

- The performance and cooling capacity of the chiller depends both on the pair and the type adsorbent bed and condenser cooling,
- A higher performance and a higher cooling capacity are achieved by using pair with higher adsorption capacities,
- As the temperature of heat source which cools condenser and adsorbent bed of the chiller decreases, both the performance and cooling capacity increases,
- Finally, the performance of the chiller increases with increasing maximum bed temperature, but it remains constant after a specified point.

An experimental work was also performed to determine adsorption equilibrium for silica gel-water. The volumetric method was chosen. An experimental setup was designed and constructed based on the volumetric method. There were serious difficulties with maintaining vacuum in the setup. Many designs and sealants were examined and finally a setup with very small leakage rate was achieved.

The experiments were performed for 35, 45 and 60 °C isotherm temperatures. The experimental procedure and obtained results were presented.

The remarks that could be concluded in accordance with the results of adsorption experimental study are;

- Silica gel - water pair used in experiments are found to be compatible with Type II isotherm (based on IUPAC classification),
- The maximum achieved adsorption capacities were around 21%, 19% and 11% kg water vapor/kg silica gel, for 35, 45 and 60 °C; respectively.
- These adsorption capacity values are lower than the capacities of silica gel (i.e. type RD silica gel) - water pairs reported in literature.
- The experimented pair may not be proper to be used in an adsorption heat pump due to its low adsorption capacity.
- Therefore a much better silica gel having capacities more than 25-30% for 30-35 °C might be used for the application of an adsorption heat pump.
- Effective mass diffusivity was found based on these experimental studies. D_{eff} were found as 1.35×10^{-10}, 1.54×10^{-10} and 1.90×10^{-10} m^2/s for 35, 45 and 60 °C; respectively.

REFERENCES

Afonso, M. and V. Silveira (2005). "Characterization of equilibrium conditions of adsorbed silica gel - water bed according to Dubinin - Astakhov and Freundlich." *Thermal Engineering **4***(1): 3-7.

Al-Ghouti, M. A., I. Yousef, R. Ahmad, A. M. Ghrair and A. A. Al-Maaitah (2010). "Characterization of diethyl ether adsorption on activated carbon using a novel adsorption refrigerator." *Chemical Engineering Journal **162(1)***: 234-241.

Aristov, Y., G. Restuccia, G. Cacciola and V. N. Parmon (2002). "A family of new working materials for solid sorption air conditioning." *Applied Thermal Engineering **22***: 191-204.

Aristov, Y. I. and L. G. Gordeeva (2009). "“Salt in a porous matrix” adsorbents: Design of the phase composition and sorption properties." *Kinetics and Catalysis **50(1)***: 65-72.

Bauer, J., R. Herrmann, W. Mittelbach and W. Schwieger (2009). "Zeolite/aluminum composite adsorbents for application in adsorption refrigeration." *International Journal of Energy Research **33***(13): 1233-1249.

BenAmar, N., L. M. Sun and F. Meunier (1996). "Numerical analysis of adsorptive temperature wave regenerative heat pump." *Applied Thermal Engineering **16(**5)*: 405-418.

Boubakri, A. (1985). Determination des caracteristiques thermodynamiques du couple carbon actif AC 35 - methanol et etude de son application a la refrigeration soliare. *Physics.* Paris, Pierre and Marie Curie University. **Doctor of philosophy**.

Cal, M. P., S. M. Larson and R. M. J. (1994). "Experimental and modeled results describing the adsorption of acetone and benzene onto activated carbon fibers." *Environmental Progress **13(**1)*: 36-30.

Chahbani, M. H., J. Labidi and J. Paris (2004). "Modeling of adsorption heat pumps with heat regeneration." *Applied Thermal Engineering **24(**2-3)*: 431-447.

Choudhury, B., P. K. Chatterjee and J. P. Sarkar (2010). "Review paper on solar-powered air-conditioning through adsorption route" *Renewable & Sustainable Energy Reviews **14(**8)*: 2189-2195.

Chua, H. T., K. C. Ng, A. Chakraborty, N. M. Oo and M. A. Othman (2002). "Adsorption Characteristics of Silica Gel + Water Systems" *Journal of Chemical & Engineering Data **47(**5)*: 1177-1181.

Çengel, Y. and M. A. Boles (2002). Thermodynamics: An engineering approach, McGraw Hill.

Daou, K., R. Wang, G. Yang and Z. Xia (2008). "Theoretical comparison of the refrigerating performances of a $CaCl_2$ impregnated composite adsorbent to those of the host silica gel." *International Journal of Thermal Sciences* ***47****(1)*: 68-75.

Dawoud, B. and Y. Aristov (2003). "Experimental study on the kinetics of water vapor sorption on selective water sorbents, silica gel and alumina under typical operating conditions of sorption heat pumps" *International Journal of Heat and Mass Transfer* ***46***: 273-281.

Dellero, T., D. Sarmeo and P. Touzain (1999). "A chemical heat pump using carbon fibers as additive. Part I: enhancement of thermal conduction" *Applied Thermal Engineering* ***19****(9)*: 991-1000.

Demir, H. (2008). An experimental and theoretical study on the improvement of adsorption heat pump performance. *Chemical Engineering*. İzmir, İzmir Institute of Technology. **Doctor of philosophy**.

Demir, H., M. Mobedi and S. Ülkü (2006). Adsorption heat pump: a clean and environmental friendly technology. *International Green Energy Conference. Oshawa, Canada, IGEC***:** 602-613.

Demir, H., M. Mobedi and S. Ülkü (2008). "A review on adsorption heat pump: problems and solutions" *Renewable & Sustainable Energy Reviews* ***12***: 2381-2403.

El-Sharkawy, I., B. Saha, S. Koyama, J. He, K. Ng and C. Yap (2008). "Experimental investigation on activated carbon–ethanol pair for solar powered adsorption cooling applications" *International Journal of Refrigeration* ***31****(8)*: 1407-1413.

El-Sharkawy, I. I., K. Kuwahara, B. B. Saha, S. Koyama and K. C. Ng (2006). "Experimental investigation of activated carbon fibers/ethanol pairs for adsorption cooling system application" *Applied Thermal Engineering* ***26****(8-9)*: 859-865.

Elnekave, M. (2008). "Adsorption heat pumps for providing coupled heating and cooling effects in olive oil mills*"* *International Journal of Energy Research* ***32****(6)*: 559-568.

Gottardi, G. and E. Galli (1985). Natural zeolites. New York, Springer-Verlag.

Gregg, S. J. and K. S. W. Sing (1982). Adsorption surface area and porosity. London, Academic Press.

Grisel, R. J. H., S. F. Smeding and R. de Boer (2010). "Waste heat driven silica gel/water adsorption cooling in trigeneration" *Applied Thermal Engineering* ***30****(8-9)*: 1039-1046.

Hamamoto, Y., K. C. A. Alam, B. B. Saha, S. Koyama, A. Akisawa and T. Kashiwagi (2006). "Study on adsorption refrigeration cycle utilizing activated carbon fibers. Part1: Adsorption characteristics" *International Journal of Refrigeration-Revue Internationale Du Froid* ***29****(2)*: 305-314.

Hassan, H. Z., A. A. Mohamad and R. Bennacer (2011). "Simulation of an adsorption solar cooling system" *Energy **36**(1)*: 530-537.

Henninger, S. K., F. Jeremias, J. Ehranmann and C. Janiak (2011). The potential of PCPs/MOFs for the use in adsorption heat pump processes. *Sources/Sinks alternative to the outside air for heat pump and air-conditioning techniques*, Padua, Italy, 415-424.

Kakiuchi, H., M. Iwade, S. Shimooka, K. Ooshima, M. Yamazaki and T. Takewaki "Novel zeolite adsorbents and their application for AHP and desiccant system" *IEA-Annex 17 Meeting*, Beijing, 2004

Keller, J. and R. Staudt (2005). Gas adsorption equilibria. New York, Springer.

Kor, O. (2010). Enhancement of jet shear layer mixing and surface heat transfer by means of acoustic disturbances. *Mechanical Engineering*. İzmir, İzmir Institute of Technology. **Master of Science**.

Kubota, M., T. Ueda, R. Fujisawa, J. Kobayashi, F. Watanabe, N. Kobayashi and M. Hasatani (2008). "Cooling output performance of a prototype adsorption heat pump with fin-type silica gel tube module" *Applied Thermal Engineering **28**(2-3)*: 87-93.

Li, C. H., R. Z. Wang and Y. Z. Lu (2002). "Investigation of a novel combined cycle of solar powered adsorption-ejection refrigeration system" *Renewable Energy **26**(4)*: 611-622.

Li, X., Z. Li, Q. Xia and H. Xi (2007). "Effects of pore sizes of porous silica gels on desorption activation energy of water vapor" *Applied Thermal Engineering **27**(5-6)*: 869-876.

Liu, Y. and K. C. Leong (2006). "Numerical study of a novel cascading adsorption cycle" *International Journal of Refrigeration-Revue Internationale Du Froid **29**(2)*: 250-259.

Liu, Y. and K. C. Leong (2008). "Numerical modeling of a zeolite/water adsorption cooling system with non-constant condensing pressure" *International Communications in Heat and Mass Transfer **35**(5)*: 618-622.

Luo, H., Y. Dai, R. Wang, J. Wu, Y. Xu and J. Shen (2006). "Experimental investigation of a solar adsorption chiller used for grain depot cooling" *Applied Thermal Engineering **26**(11-12)*: 1218-1225.

Makimoto, N., B. Hu and S. Koyama (2011). A study on thermophysical characteristics of activated carbon powder/ethanol pair in adsorber. *Sources/Sinks alternative to the outside air for heat pump and air-conditioning techniques*, Padua, Italy.

Makni, F., M. Clausse and F. Meunier (2011). Development of a 3D simulation tool for design improvement of adsorbers dedicated to solar air-conditioning systems. *Sources/sinks alternative to the outside air for heat pump and air-conditioning techniques*, Padua, Italy.

Mbaye, M., Z. Aidoun, V. Valkov, A. Legault (1998). “Analysis of chemical heat pumps: basic concepts and numerical model descriptions”. *Applied Thermal Engineering* ***18***: 131-146.

Ng, K., H. Chua, C. Y. Chung, L. C. H., T. Kashiwagi, A. Akisawa and B. B. Saba (2001). "Experimental investigation of the silica gel - water adsorption isotherm characteristics". *Applied Thermal Engineering* ***21***: 1631-1642.

Nunez, T., W. Mittelbach and H. M. Henning (2007). "Development of an adsorption chiller and heat pump for domestic heating and air-conditioning applications" *Applied Thermal Engineering* ***27****(13)*: 2205-2212.

Özkan, F., S. Ülkü (2005). “The effect of HCl treatment on water vapor adsorption characteristics of clinoptilolite rich natural zeolite”. *Microporous and Mesoporous Materials* ***77***: 47-53

Perry, R. H. and D. W. Green (2008). Perry's Chemical Engineering Handbook, McGraw-Hill.

Restuccia, G., A. Freni, S. Vasta and Y. Aristov (2004). “Selective water sorbent for solid sorption chiller: experimental results and modeling” *International Journal of Refrigeration-Revue Internationale Du Froid* ***27****(3)*: 284-293.

Rouquerol, F., J. Rouquerol and K. Sing (1999). Adsorption by powders and porous solids. London, Academic Press.

Saha, B., A. Chakraborty, S. Koyama and Y. Aristov (2009). "A new generation cooling device employing $CaCl_2$-in-silica gel–water system" *International Journal of Heat and Mass Transfer* ***52****(1-2)*: 516-524.

Saha, B. B., K. Habib, I. I. El-Sharkawy and S. Koyama (2009). "Adsorption characteristics and heat of adsorption measurements of R-134a on activated carbon" *International Journal of Refrigeration-Revue Internationale Du Froid* ***32****(7)*: 1563-1569.

San, J. Y. and H. C. Hsu (2009). "Performance of a multi-bed adsorption heat pump using SWS-1L composite adsorbent and water as the working pair" *Applied Thermal Engineering* ***29****(8-9)*: 1606-1613.

San, J. Y. and W. M. Lin (2008). "Comparison among three adsorption pairs for using as the working substances in a multi-bed adsorption heat pump" *Applied Thermal Engineering* ***28****(8-9)*: 988-997.

Solmuş, İ., C. Yamalı, B. Kaftanoğlu, D. Baker and A. Çağlar (2010). "Adsorption properties of a natural zeolite–water pair for use in adsorption cooling cycles." *Applied Energy* ***87****(6)*: 2062-2067.

Srivastava, N. C. and I. W. Eames (1998). "A review of adsorbents and adsorbates in solid - vapour adsorption heat pump systems" *Applied Thermal Engineering* ***18***: 707-714.

Sumathy, K. and Z. F. Li (1999). "Experiments with solar-powered adsorption ice-maker" *Renewable Energy* ***16****(1-4)*: 704-707.

Sumathy, K., K. H. Yeung and L. Yong (2003). "Technology development in the solar adsorption refrigeration systems" *Progress in Energy and Combustion Science* ***29****(4)*: 301-327.

Suzuki, M. (1990). Adsorption engineering. Amsterdam, Elsevier Science.

Tamainot-Telto, Z. and R. Critoph (2001). "Monolithic active carbon for sorption refrigeration and heat pump applications" *Applied Thermal Engineering* ***21***: 37-52.

Tamainot-Telto, Z., S. J. Metcalf, R. E. Critoph, Y. Zhong and R. Thorpe (2009). "Carbon–ammonia pairs for adsorption refrigeration applications: ice making, air conditioning and heat pumping" *International Journal of Refrigeration* ***32*** *(6)*: 1212-1229.

Ülkü, S. (1986). "Adsorption heat pumps" *Journal of Heat Recovery Systems* ***6***: 277-284.

Ülkü. S. (1986). "Natural Zeolites in Energy Storage and Heat Pumps", *Studies in Surface Science and Catalysis,* **28**: New Developments in Zeolite Science and Technology: 1047-1054

Ülkü, S., Kıvrak, Z., Mobedi, M. (1986). "Air Drying in Packed Bed Absorbers", Drying 86, Hemisphere Pub. Corp. Washington, 807-812

Ülkü, S. (1987). Solar adsorption heat pumps. Solar energy utilization: fundamentals and applications. H. Yüncü, E. Paykoç and Y. Yener. Netherlands, Martinus Nijkoff Publishers.

Ülkü, S. (1991). Heat and mass transfer in adsorbent beds. Convective heat and mass transfer in porous media. S. Kakaç, B. Kılkış, A. F. Kulakçı and F. Arınç. London, Kluwer Academic Pubs. **196:** 695-724.

Ülkü, S. and M. Mobedi (1989). Adsorption in energy storage. Proceedings of NATO Advanced Study Institute on Energy Storage Systems. **167:** 487-507.

Ülkü, S., Balköse D., Çağa, T., Özkan, F., Ulutan, S. (1998). "A study of adsorption of water vapour on wool under static and dynamic conditions" *Adsorption* ***4***: 63-73.

Wang, D. C., J. Y. Wu, H. G. Shan and R. Z. Wang (2005). "Experimental study on the dynamic characteristics of adsorption heat pumps driven by intermittent heat source at heating mode" *Applied Thermal Engineering* ***25****(5-6)*: 927-940.

Wang, D. C., J. Y. Wu, Z. Z. Xia, H. Zhai, R. Z. Wang and W. D. Dou (2005). "Study of a novel silica gel-water adsorption chiller. Part II: Experimental study" *International Journal of Refrigeration-Revue Internationale Du Froid* ***28****(7)*: 1084-1091.

Wang, D. C. and J. P. Zhang (2009). "Design and performance prediction of an adsorption heat pump with multi-cooling tubes" *Energy Conversion and Management* ***50****(5)*: 1157-1162.

Wang, L., R. Wang and R. Oliveira (2009). "A review on adsorption working pairs for refrigeration" *Renewable and Sustainable Energy Reviews* ***13****(3)*: 518-534.

Wang, R. and R. Oliveira (2006). "Adsorption refrigeration—An efficient way to make good use of waste heat and solar energy" *Progress in Energy and Combustion Science **32**(4)*: 424-458.

Wang, R. Z., T. S. Ge, C. J. Chen, Q. Ma and Z. Q. Xiong (2009). "Solar sorption cooling systems for residential applications: Options and guidelines" *International Journal of Refrigeration **32**(4)*: 638-660.

Wang, R. Z., M. Li, Y. X. Xu and J. Y. Wu (2000). "An energy efficient hybrid system of solar powered water heater and adsorption ice maker" *Solar Energy **68**(2)*: 189-195.

Wang, R. Z., J. Y. Wu, Y. X. Xu, Y. Teng and W. Shi (1998). "Experiment on a continuous heat regenerative adsorption refrigerator using spiral plate heat exchanger as adsorbers" *Applied Thermal Engineering **18**(1-2)*: 13-23.

Wang, R. Z., J. Y. Wu, Y. X. Xu and W. Wang (2001). "Performance researches and improvements on heat regenerative adsorption refrigerator and heat pump" *Energy Conversion and Management **42**(2)*: 233-249.

Wang, X. and H. Chua (2007). "Two bed silica gel - water adsorption chillers: An effectual lumped parameter model" *International Journal of Refrigeration **30***: 1417-1426.

Wongsuwan, W., S. Kumar, P. Neveu and F. Meunier (2001). "A review of chemical heat pump technology and applications" *Applied Thermal Engineering **21**(15)*: 1489-1519.

Xia, Z. Z., C. J. Chen, J. K. Kiplagat, R. Z. Wang and J. Q. Hu (2008). "Adsorption Equilibrium of Water on Silica Gel" *Journal of Chemical & Engineering Data **53**(10)*: 2462-2465.

Xia, Z. Z., R. Z. Wang, D. C. Wang, Y. L. Liu, J. Y. Wu and C. Chen (2009). "Development and comparison of two-bed silica gel-water adsorption chillers driven by low-grade heat source" *International Journal of Thermal Sciences **48**(5)*: 1017-1025.

Yang, R. T. (2003). Adsorbents: fundamentals and applications. New Jersey, John Wiley and Sons.

Yang, Y., J. Jia, Q. Li and Z. Guan (2006). "Experimental investigation of the governing parameters in the electrospinning of polyethylene oxide solution" *IEEE Transactions on Dielectrics and Electrical Insulation **13**(3)*: 580-585.

Yaping, Z. and Z. Li (1996). "Experimental study on high pressure adsorption of hydrogen on active carbon" Science in China Series B **39**: 598-607.

Yıldırım, Z. E., Mobedi, M., Ülkü, S. (2010). A review on proper working pairs for solar adsorption heat pumps. *Solar Future Conference*, İstanbul, Turkey

Yıldırım, İliş, G. G., Z. E., Mobedi, M., Ülkü, S. (2011). Adsorpsiyonlu Chillerlerde kullanılabilecek adsorbent-adsorbat özellikleri ve çevrim performanslarının incelenmesi. X. Ulusal Tesisat Mühendisliği Kongresi, İzmir, Türkiye

Zhong, Y. and R. E. Critoph (2005). "Review of trends in solid sorption refrigeration and heat pumping technology" Proceedings of the Institution of Mechanical Engineers, Part E. *Journal of Process Mechanical Engineering* **219**(3): 285-300.

APPENDIX A

ISOTHERM PLOTS FOR DIFFERENT EQUILIBRIUM EQUATIONS REPORTED IN LITERATURE

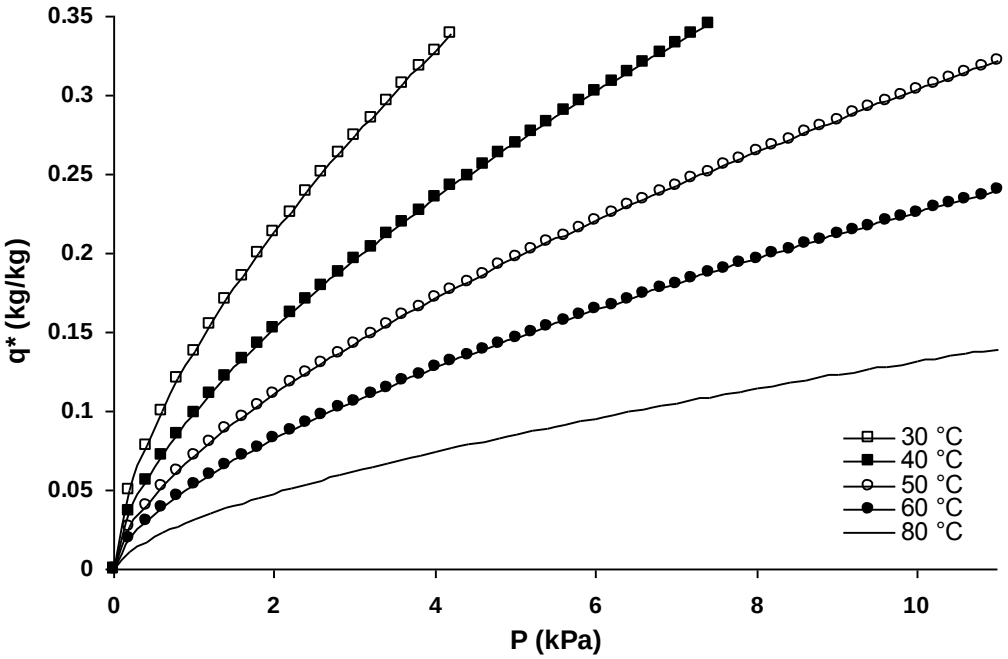

Figure A.1. Freundlich Equation isotherms for silica gel – water pair with coefficients k=0.346, n=1.6

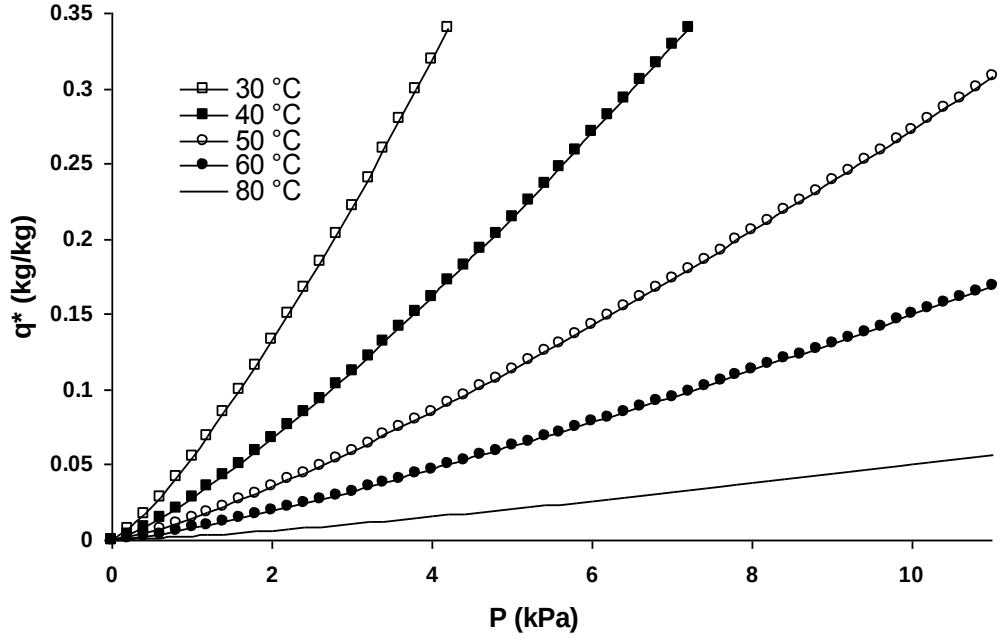

Figure A.2. Freundlich Equation isotherms for silica gel – water pair with coefficients k=0.355, n=0.79

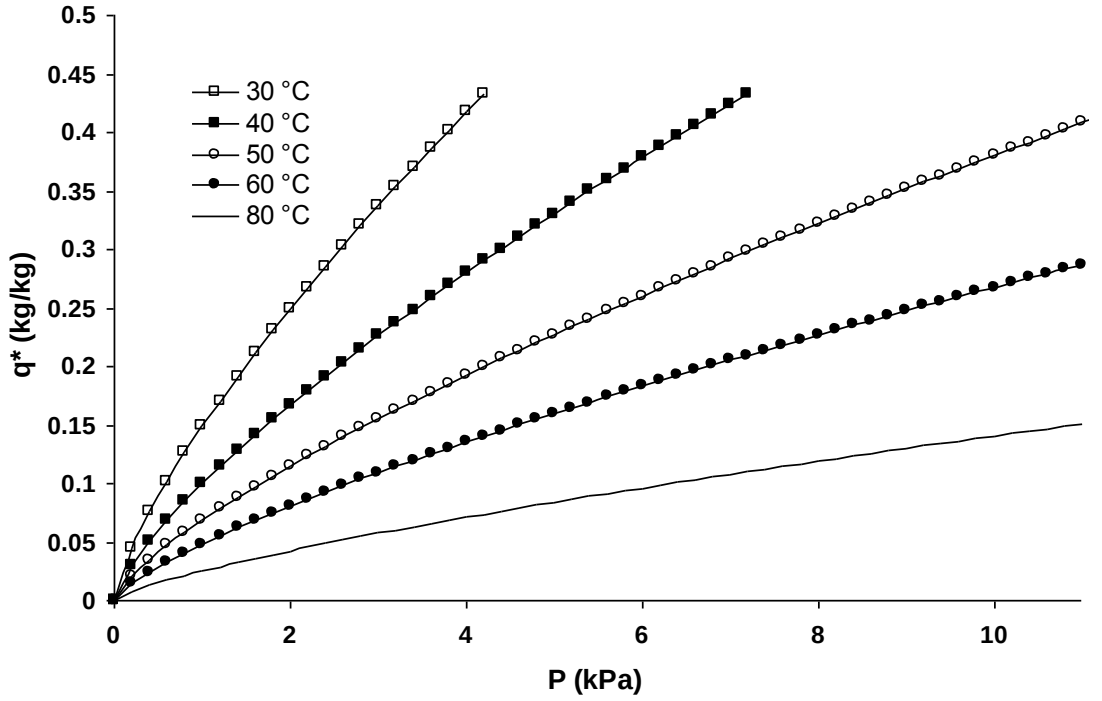

Figure A.3. Freundlich Equation isotherms for silica gel – water pair with coefficients k=0.444, n=1.346

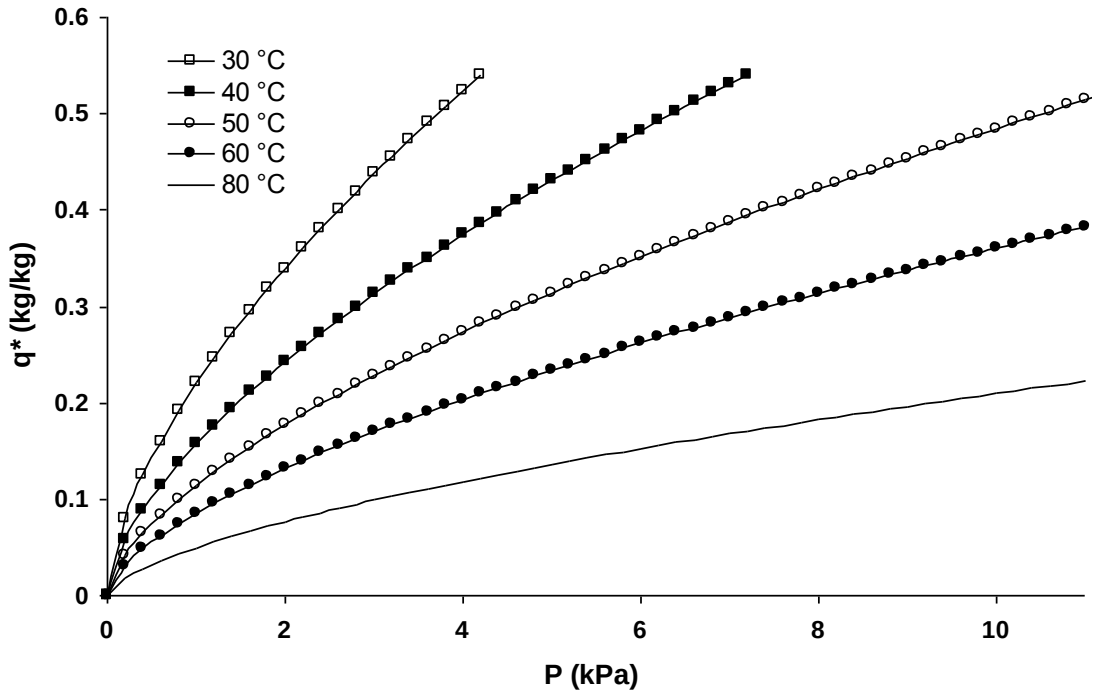

Figure A.4. Freundlich Equation isotherms for silica gel – water pair with coefficients k=0.552, n=1.6

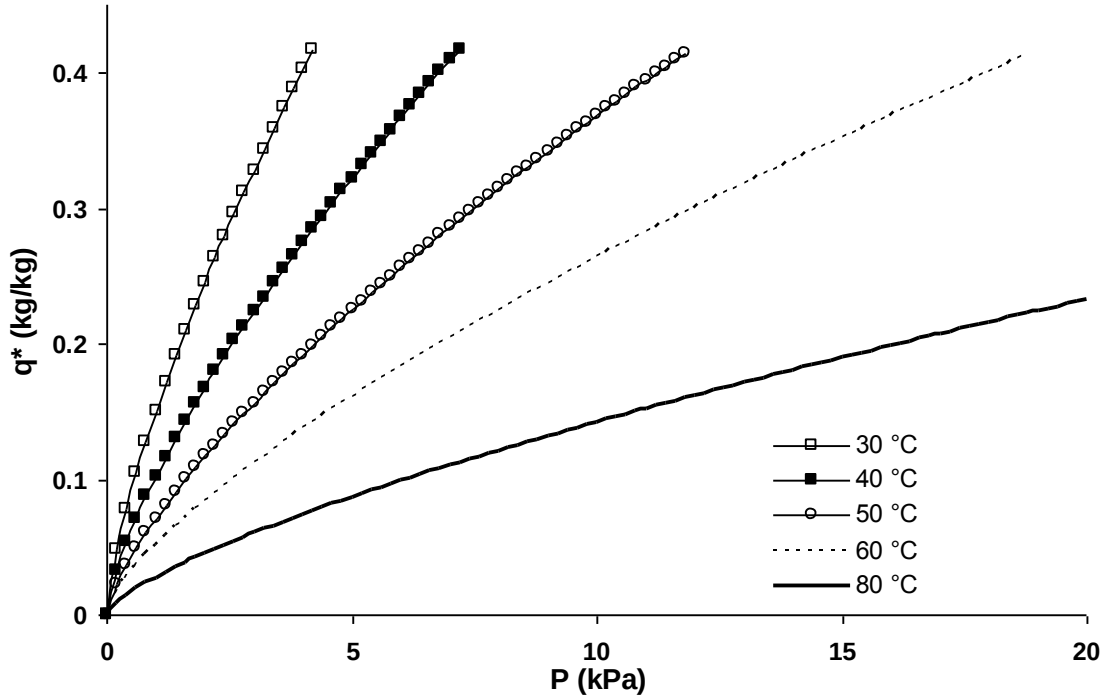

Figure A.5. Modified Freundlich Equation isotherms for silica gel – water pair

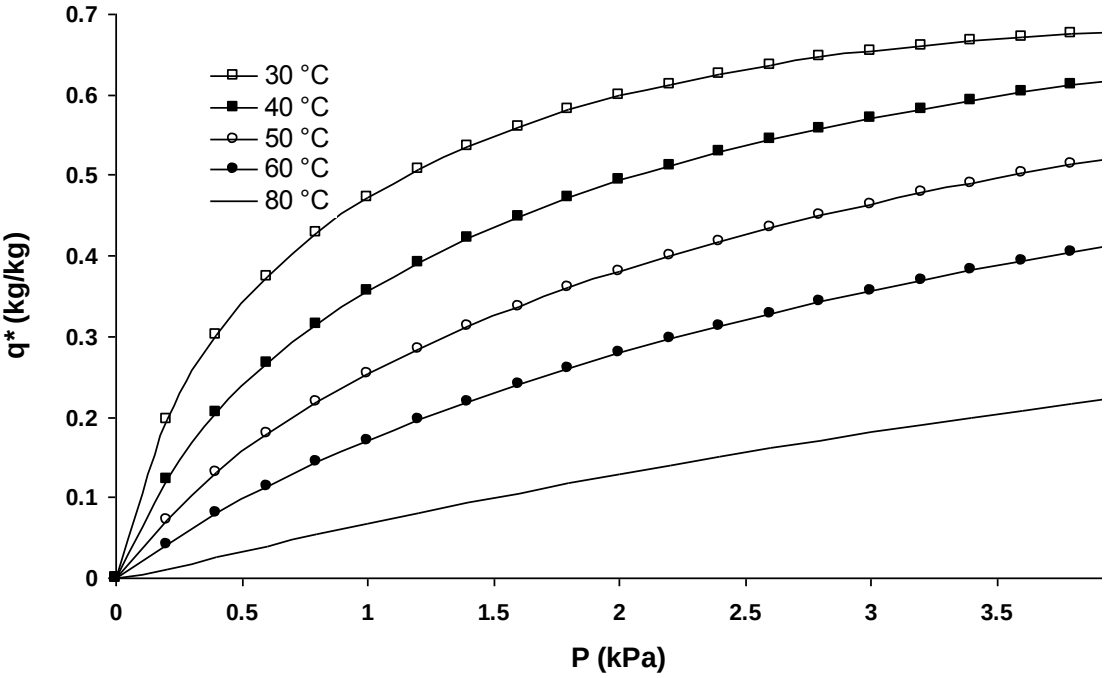

Figure A.6. Dubinin - Astakhov Equation isotherms for silica gel – water pair with coefficients q_0=0.68, D=1.56E-5, n=1.65

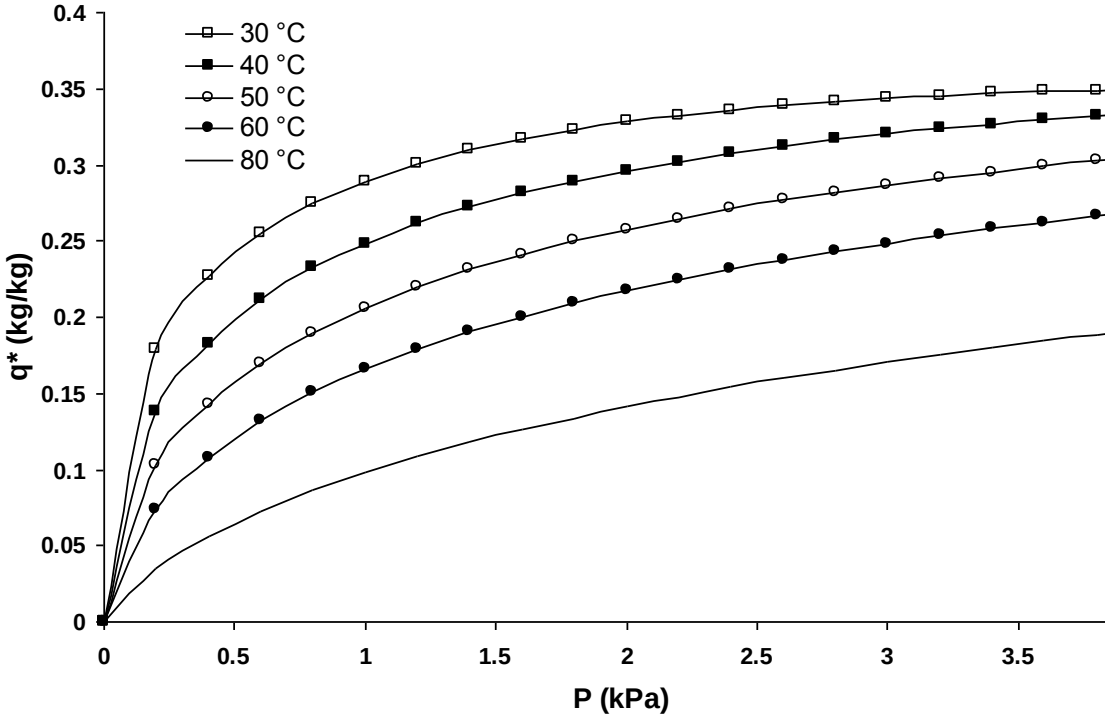

Figure A.7. Dubinin - Astakhov Equation isotherms for silica gel – water pair with coefficients q_0=0.35, D=6E-6, n=1.65

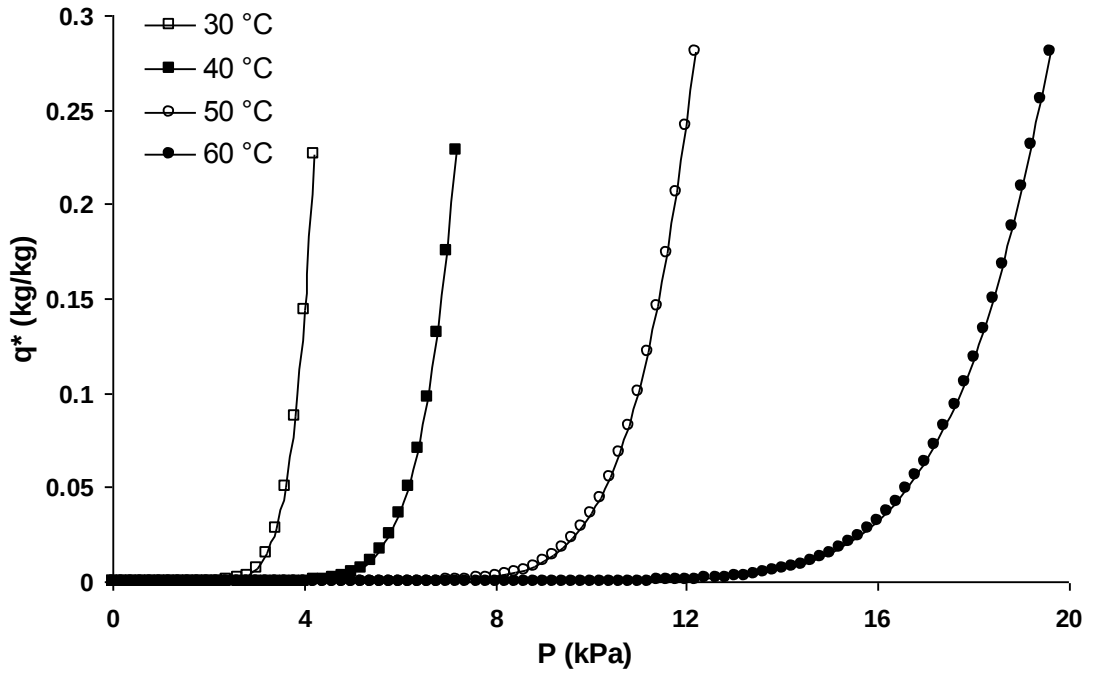

Figure A.8. Dubinin - Astakhov Equation isotherms for silica gel – water pair with coefficients q_0=0.301, D=0.0226, n=1.08

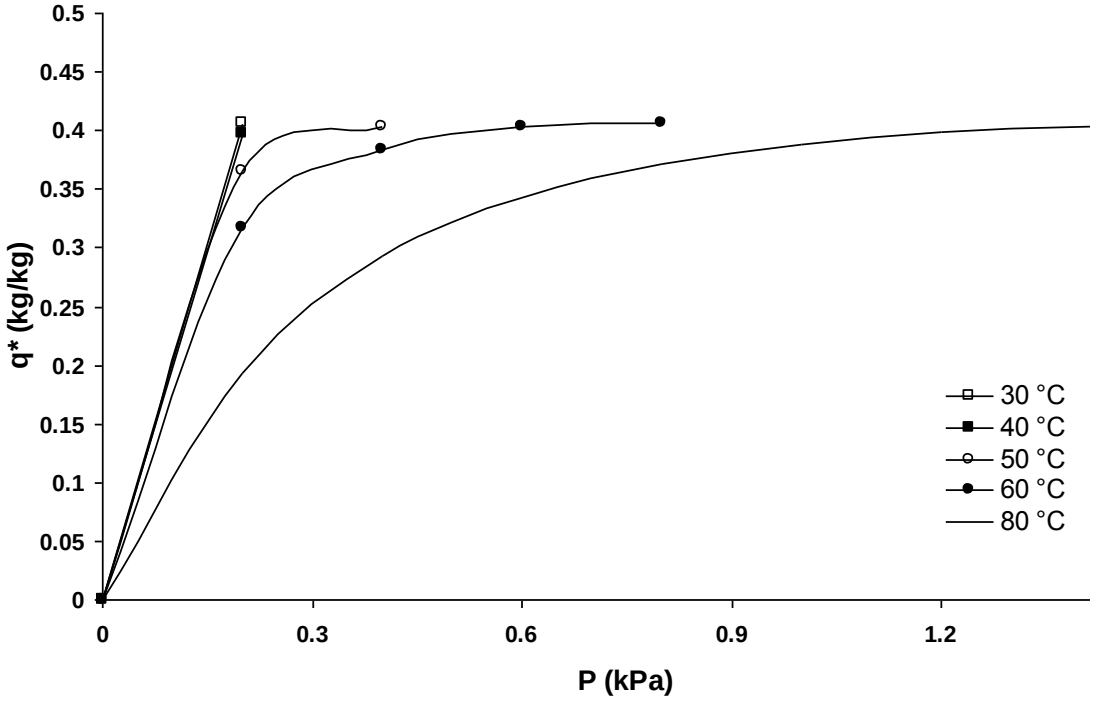

Figure A.9. Dubinin - Astakhov Equation isotherms for active carbon - methanol pair with coefficients q_0=0.407, D=3.22E-7, n=2.195

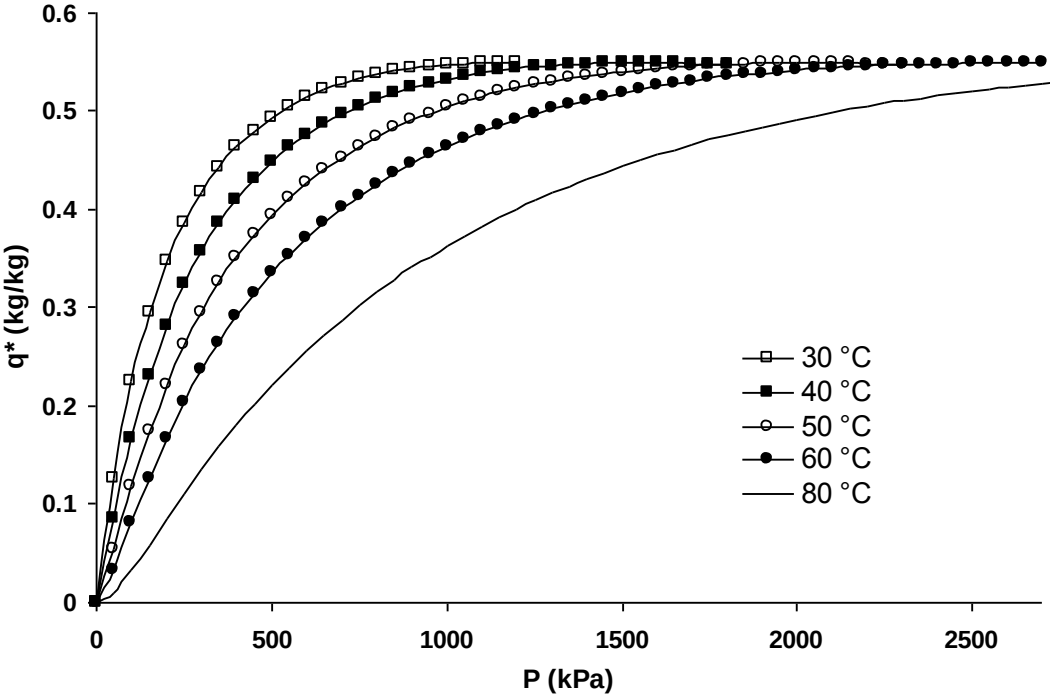

Figure A.10. Dubinin - Astakhov Equation isotherms for active carbon - ammonia pair with coefficients q_0=0.549, D=1.617E-6, n=2

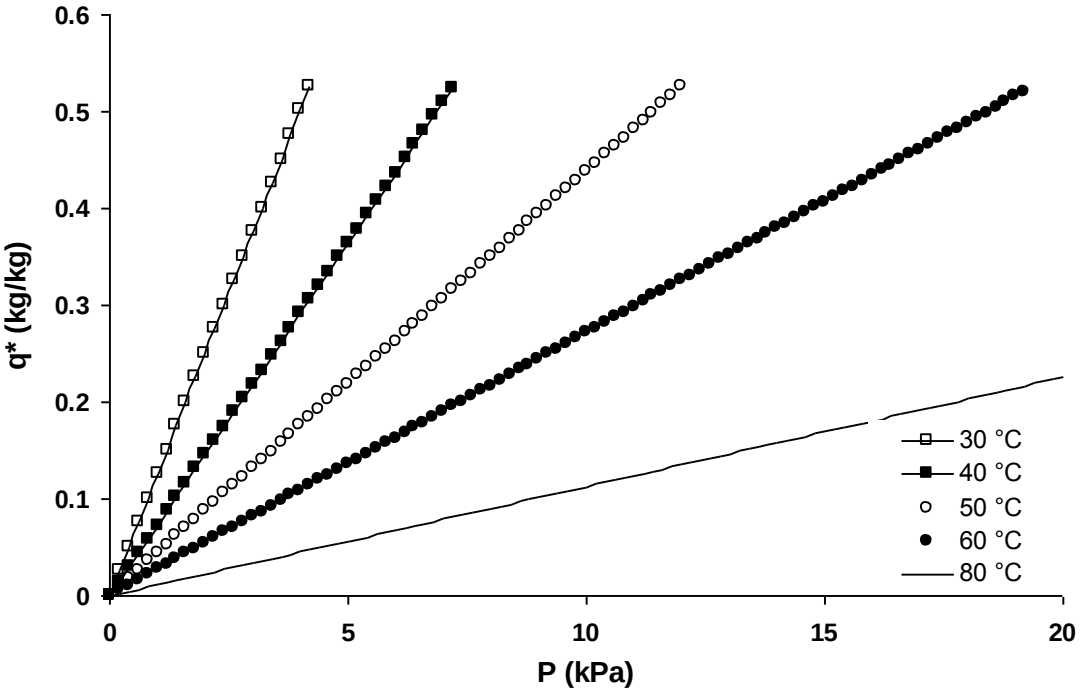

Figure A.11. Henry's Equation isotherms for Type 3A silica gel - water pair

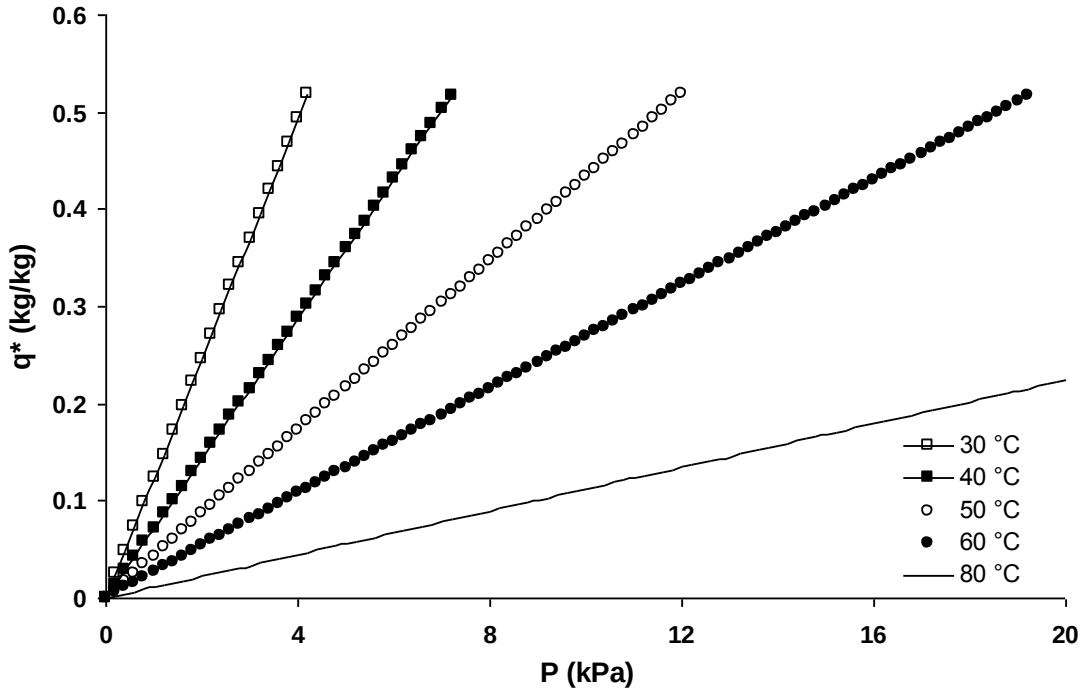

Figure A.12. Henry's Equation isotherms for Type RD silica gel - water pair

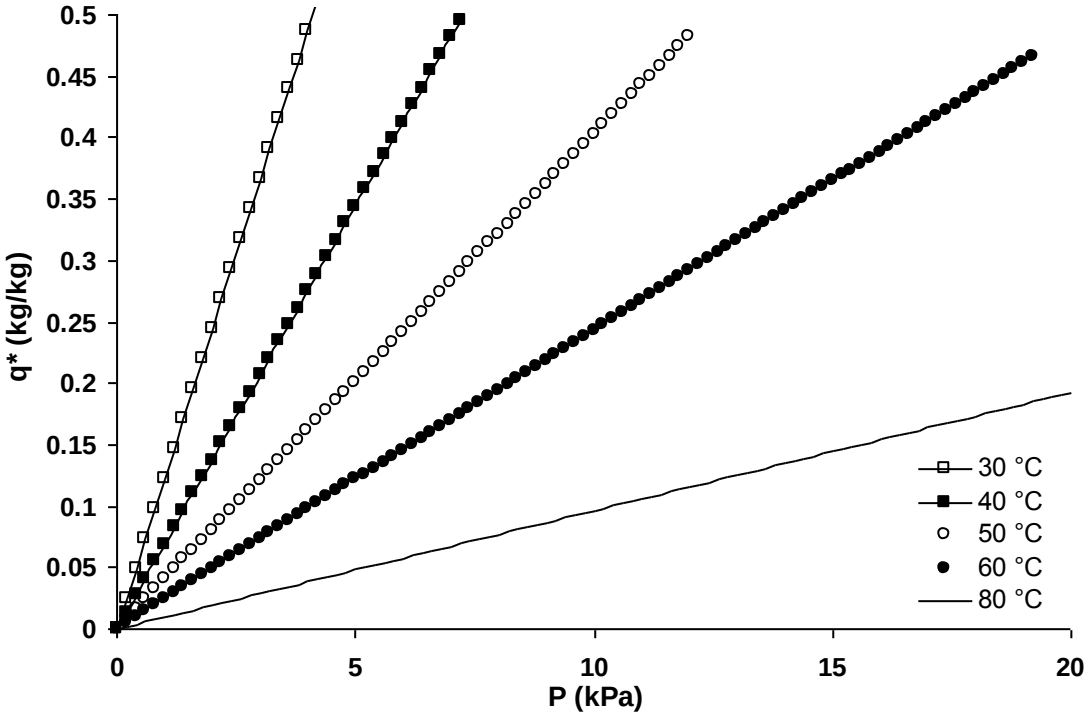

Figure A.13. Henry's Equation isotherms for Type RD silica gel (2) - water pair

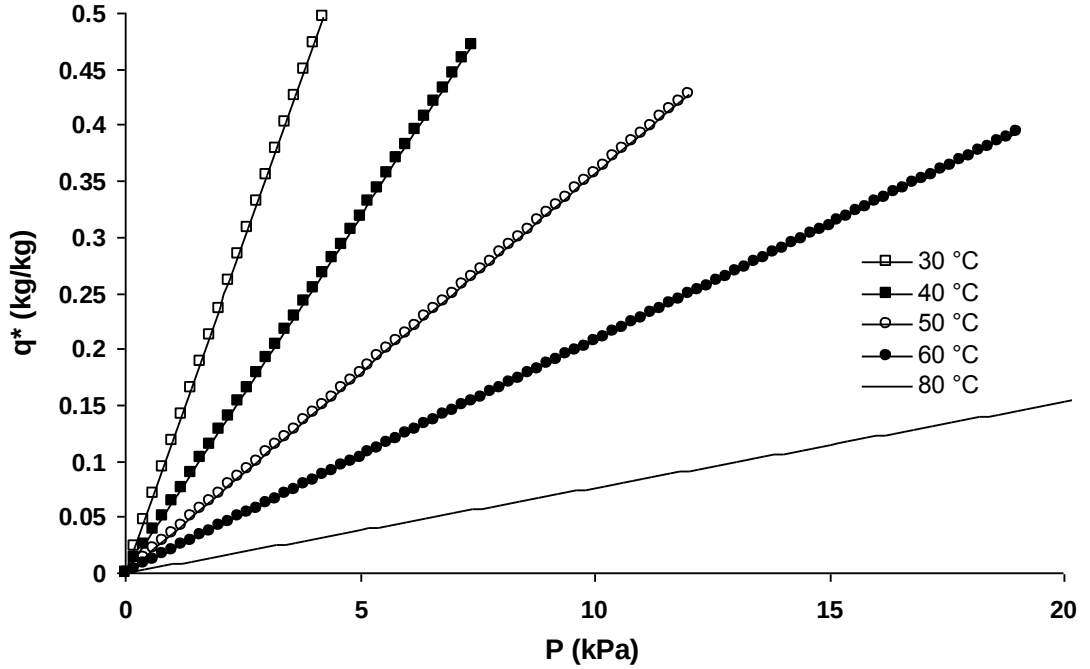

Figure A.14. Toth's Equation isotherms for Type A silica gel - water pair

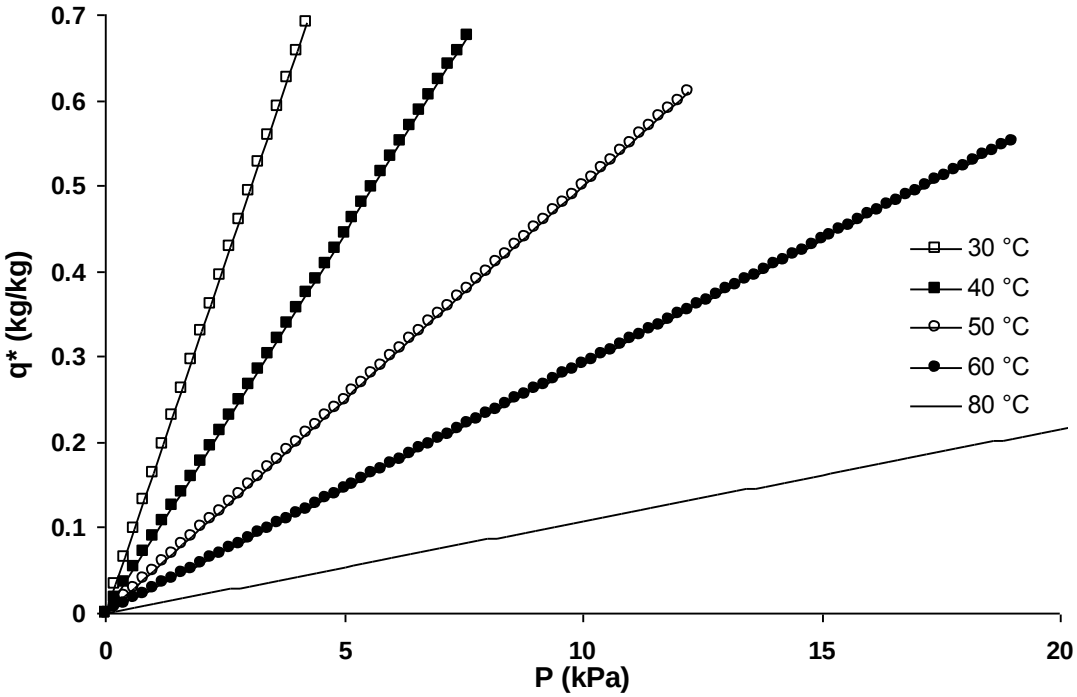

Figure A.15. Toth's Equation isotherms for Type RD silica gel - water pair

APPENDIX B

NUMERICAL STUDY FLOW CHART

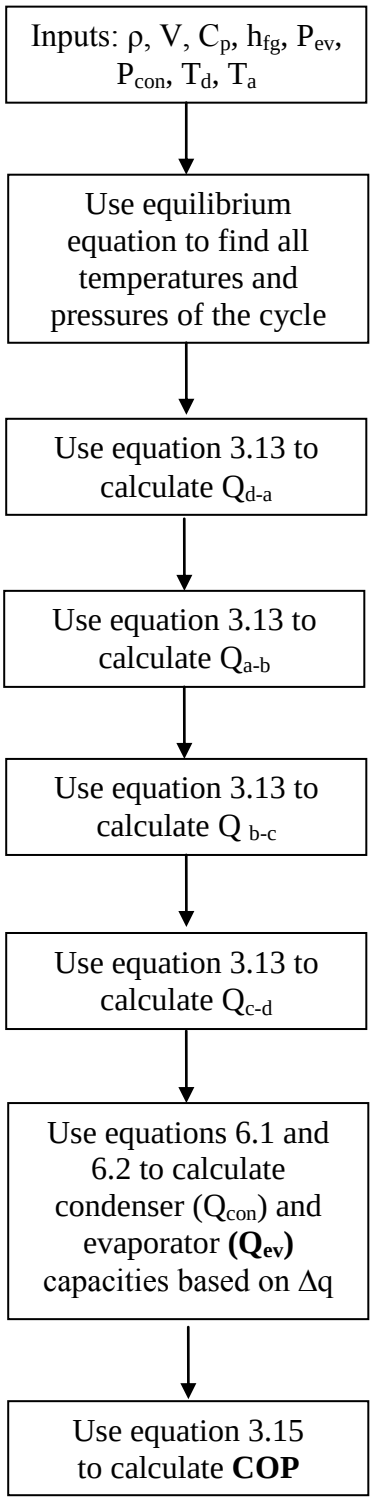

Figure B.1. Flow chart of the numerical study on effect of equilibrium on the performance of adsorption chiller

APPENDIX C

MICROMERITICS ASAP 2010 SILICA GEL TEST RESULTS

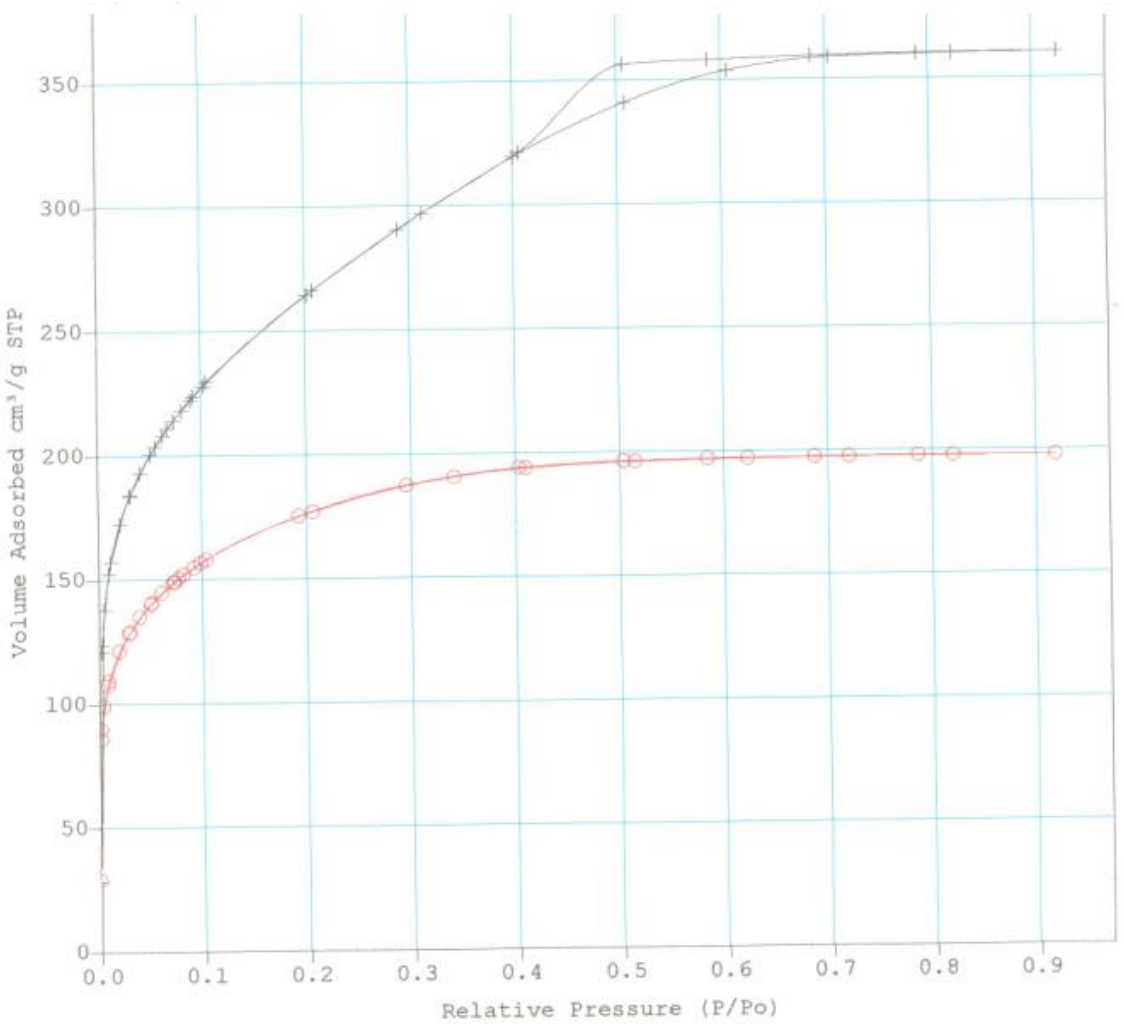

Figure C.1. Nitrogen adsorption onto silica gel isotherm plot
(red curve: silica gel used in experimental study, black curve: BASF silica gel)

Sample Id: Silicagel (beyaz), (EY), 25.01
Operator Id: Nesrin Tatlidil
Submitter Id: Elvan Yildirim
File Name: C:\ASAP2010\DATA\2011\001-460.SMP

Started: 25.01.11 13:12:08 Analysis Adsorptive: N2
Completed: 26.01.11 15:54:02 Analysis Bath: 77.39 K
Report Time: 28.01.11 08:50:21 Thermal Correction: No
Sample Weight: 0.3096 g Smoothed Pressures: No
Warm Freespace: 19.6002 cm³ Cold Freespace: 57.7970 cm³
Equil. Interval: 45 secs Low Pressure Dose: 25.00 cm³/g STP

Summary Report

Area

Single Point Surface Area at P/Po 0.34189229 :	545.4453	m²/g
Langmuir Surface Area:	852.2591	m²/g
Micropore Area:	421.4080	m²/g
BJH Adsorption Cumulative Surface Area of pores between 17.000000 and 3000.000000 A Diameter:	97.0582	m²/g
BJH Desorption Cumulative Surface Area of pores between 17.000000 and 3000.000000 A Diameter:	122.3972	m²/g

Volume

Single Point Total Pore Volume of pores less than 254.7208 A Diameter at P/Po 0.91949987:	0.305803	cm³/g
Micropore Volume:	0.083644	cm³/g
BJH Adsorption Cumulative Pore Volume of pores between 17.000000 and 3000.000000 A Diameter:	0.053708	cm³/g
BJH Desorption Cumulative Pore Volume of pores between 17.000000 and 3000.000000 A Diameter:	0.073307	cm³/g

Pore Size

Average Pore Diameter (4V/A by LANGMUIR):	14.3526	A
BJH Adsorption Average Pore Diameter (4V/A):	22.1342	A
BJH Desorption Average Pore Diameter (4V/A):	23.9569	A

Horvath-Kawazoe

Maximum Pore Volume at Relative Pressure 0.103994250:	0.244003	cm³/g
Median Pore Diameter:	8.2131	A

Dubinin-Astakhov Data

Micropore Surface Area (Astakhov):	618.292723	m²/g
Limiting Micropore Volume:	0.301515	cm³/g